Project

WIDE AREA DIFFERENTIAL GPS

Study in the Context of AGNES

Collaboration between the

AIUB and the

Swiss Federal Office of Topography

Gerhard Beutler, Stefan Schaer, and Markus Rothacher

Astronomical Institute of the University of Bern

Sidlerstrasse 5

3012 Bern

Printing Office, University of Bern

Bern, September 17, 1999

Contents

List of Figures

List of Tables

1. Introduction

AGNES stands for *Automated GPS-Network Switzerland*. The network serves several purposes, in particular monitoring and maintenance of the Swiss first order network (*Landesvermessung*), navigation, and research (*GPS meteorology, geodynamics, etc.*). Here, we address aspects of *wide-area differential GPS (WADGPS) including* real-time positioning with meter- to centimeter-accuracy using GPS code and/or carrier phase observations stemming from the reference stations of AGNES.

The *planned sites* of AGNES are shown in Figure 1. Data from Andermatt and Locarno were not available to us in the context of this study. This is made up by the fact data from the Station Sierre (Siders) were available for the purpose of this study.

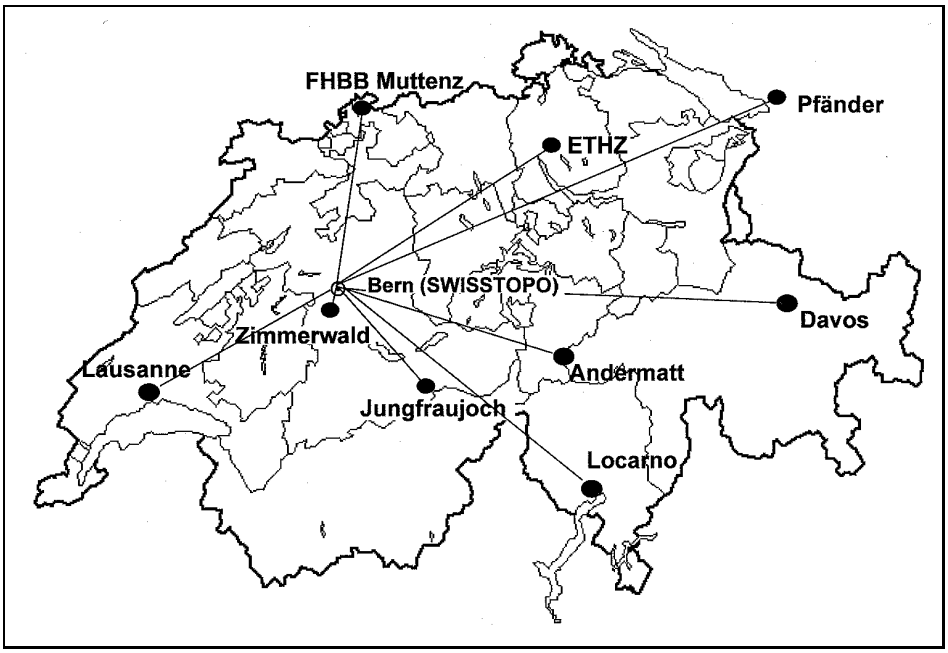

Figure 1: The Reference Stations of the AGNES Network 1999

The site characteristics are specified in Table 1. One may recognize that the equipment within AGNES is rather homogeneous. The user equipment may of course be noticeably different.

Tables 2 and 3 give the distances in kilometers between the sites considered. Note that the distances with respect to the fundamental station Zimmerwald are contained in the first line, and that the distances to the "user equipment" are contained in Table 3. Baselines that could never be observed simultaneously with the data available for this study are marked with "—".

Site	**4-Char ID**	**Number**	**Receiver/Antenna**
Lausanne	EPF2	805	Trimble SSI/DORNE MARGOLIN T
Sierre	SIER	756	Trimble SSI/DORNE MARGOLIN T
Zimmerwald	ZIMM	751	Trimble SSI/DORNE MARGOLIN T
FHBB Muttenz	FHBB	752	Trimble SSI/DORNE MARGOLIN T
Jungfraujoch	JUJO	754	Trimble SSI/DORNE MARGOLIN T
ETH Zürich	ETHZ	753	Trimble SSI/DORNE MARGOLIN T
Andermatt	ANDR	—	Trimble SSI/DORNE MARGOLIN T
Locarno	—	—	Trimble SSI/DORNE MARGOLIN T
Pfänder	PFAN	757	Trimble SSI/TR GEOD L1/L2 GP
Davos	DAVO	802	Trimble SSI/DORNE MARGOLIN T
Bern ExWi	DACH	801	Trimble SSI/???
Thun	THUN	803	Trimble SSI/TR GEOD L1/L2 GP
Wichtrach	WICH	804	Trimble SSI/???

Table 1: AGNES and other Station Characteristics

Name	EPF2	SIER	FHBB	JUJO	ETHZ	PFAN	DAVO
ZIMM	79	65	74	54	99	190	182
EPF2		—	139	109	178	—	253
SIER			138	44	144	218	—
FHBB				113	67	162	186
JUJO					104	174	145
ETHZ						97	121
PFAN							—

Table 2: Distances between AGNES Sites

Name	DACH	THUN	WICH
ZIMM	6	17	10
EPF2	81	84	86
SIER	—	—	—
FHBB	69	86	77
JUJO	59	37	45
ETHZ	96	100	94
PFAN	—	—	—
DAVO	183	171	173
DACH		22	13
THUN			10

Table 3: Distances between AGNES Sites and User Sites (cont)

As we can see in Table 2, the distances between the AGNES reference sites range between 54 km and 254 km. For a user working somewhere in the AGNES-area (*i.e., in Switzerland*) this means that he has to cope with distances to the next AGNES reference station of the order of 20 km to perhaps 50 km (less favorable situations may occur also). This means in particular that high accuracy applications using short data spans (seconds to a few minutes) requiring ambiguity resolution in real-time are a *non-trivial affair*. The use of the AGNES for *rapid static positioning* or even *"on-the-fly" (horrible imagination to sit on a fly)* ambiguity resolution techniques is in the focus of our interest in this study.

Special attention has to be paid to the distribution of the stations as a function of height. Table 4 shows that the AGNES sites cover a range of more than 3000 m and that the distribution is far from equidistant. This aspect will be of particular interest in Chapter 7.

Station	Height (m)
FHBB	378
EPF2	459
ETHZ	595
SIER	602
ZIMM	956
PFAN	1090
JUJO	3635

Table 4: Ellipsoidal Station Heights (ITRF-96) in the AGNES

The "test users" in the area of Bern (Bern ExWi, Thun, Wichtrach) were just lucky to be close to Zimmerwald and Jungfraujoch.

One obvious, and to some extent trivial, concept for precise relative positioning in a particular area of AGNES is to download the data from the nearest AGNES reference station and to perform relative positioning *w.r.t.* this site. The quality of results undoubtedly will heavily depend on the distance from the receiver. For distances $<$ 10 km this strategy might be the best possible.

From the *purist's point of view* it would be best to process all user data simultaneously with the data from the reference receivers to produce a correct network solution. No better solution is possible — provided the problem is correctly parameterized. This purist solution is of course also labor-intensive for the operator of the AGNES.

These considerations are the motivation to look for methods to combine the GPS observations from all AGNES reference sites with the goal to generate an *artificial reference receiver with artificial observations close to the user*, which allow the user to position his receiver relative to this *virtual* receiver. One may (must) hope that the systematic errors are greatly reduced in the AGNES network.

It will therefore be an important step to compare a pure baseline solution (to the closest site) with a correct network solution including the user and *all* GPS reference

sites.

We will address the following systematic errors (biases) in the GPS-observable:

- Errors in satellite orbits,
- unmodeled ionosphere refraction corrections,
- unmodeled troposphere corrections,
- antenna phase center variations, and
- multipath effects.

The effects will be studied in varying "depth" — according to their impact on real time positioning *resp.* rapid static positioning. By "rapid static positioning" we understand positioning with data spans of, let us say, 1-5 minutes. Ambiguity resolution using short data spans is a central issue for real-time positioning *and* rapid static applications. The issue will be addressed in Chapter 6.

It is our *a priori* belief, that ionospheric refraction is the central effect for the class of users we are dealing with. We show that it is possible to generate tropospheric corrections in a simple way by analyzing the AGNES reference sites in (near) real time.

We believe that orbits are well taken care of by the IGS (*e.g.*, by the CODE Analysis Center). Even at present there are good predicted orbits available. The situation is expected to improve substantially as soon as the IGS will switch from daily to hourly data download and processing strategies.

Tropospheric refraction is a critical issue, in particular in a country like Switzerland with height differences of up to a few kilometers. Also, in an Alpine area, there are substantially different climate zones (we mention, *e.g., Jura, Mittelland, Wallis, Alpensüdseite, Engadin*). In view of these facts and of the average distances of the AGNES sites there is hardly hope that this effect may be very well interpolated. The issue will have to be addressed in detail.

Let us conclude this introduction with an overview of the subsequent chapters of this report:

- **Chapter 2:** We briefly discuss the (rather sparse) open literature available for our purpose. We also introduce work performed previously at AIUB which may be of interest in our context.
- **Chapter 3:** We develop the theory of how to correctly combine observations from different receivers, *assuming that the relative geometry between all reference stations and all satellites and the atmosphere over each site is perfectly known.* We address the combination of code and phase measurements separately.
- **Chapter 4:** We present the computer program **CLKEST** which was developed in the context of this *AGNES*-study and of *LEO*-projects. **CLKEST** processes Bernese zero difference code- and phase-files, computes for each epoch satellite and receiver clock errors using code, clock difference corrections pertaining

to subsequent epochs using phase, and it generates epoch and satellite specific ionosphere corrections using the $L4$ linear combination of the phase observations. **CLKEST** gives an impression of what is achievable today using arrays of permanently operating GPS receivers.

- **Chapter 5:** We first introduce the data analyzed in this report. We then process the observations in the best possible "standard" way using the Bernese GPS Software, Version 4.1. This includes ionosphere modeling and optimal use of material from the IGS, in particular from the CODE Analysis Center of the IGS. The two basic results of this chapter are: (a) establishment of a "ground truth" (coordinates, ambiguities) for all baselines, (b) a discussion of the impact of systematic errors for the standard network solution to be produced in near real time using the data from the AGNES sites.

- **Chapter 6:** We discuss the impact of biases on the results of a user of AGNES products. We assume short data spans and resolved ambiguities.

- **Chapter 7:** We develop ideas and methods to interpolate the tropospheric zenith estimates stemming from the network processing program. Then, we deal with the central aspect of resolving ambiguities in an environment of moderate/high ionospheric activity.

- **Chapter 8:** We summarize our investigations, draw the conclusions, and recommend further work.

2. Brief Overview of Existing Work

Today, quite a few active Control Networks for high-accuracy differential positioning and navigation have been deployed. Let us mention, *e.g.*, that the Geodetic Survey Division (GSD) from *Energy, Mines and Resources, Canada* was building up the *Canadian Active Control System (CACS)* already at the end of the 1980s and early 1990s. It consists of 12 stations. It is the declared goal of the CACS to give access to best possible realization of the ITRF.

According to [*Kouba and Popelar*, 1994] access to the reference frame is provided using three strategies:

- By processing the user data at GSD using the best possible correct methods (actually, it would be best to incorporate the user data into the daily Canadian processing).
- By using the CACS/IGS orbits and observations from one of the stations with double differencing software.
- By using the CACS/IGS orbits and satellite clocks in connection with single point positioning techniques.

The first two methods promise sub-cm accuracy, the third gives an accuracy which is limited by the code accuracy of the user equipment. It is very simple in application.

All three techniques mentioned by [*Kouba and Popelar*, 1994] are worth being considered today for AGNES-like networks. Of course we would translate CACS/IGS orbits (and clocks) by L+T/CODE/IGS orbits (and clocks). It should be pointed out in particular, that there cannot be a better method than the above mentioned strategy (1). Translated into the philosophy of the Bernese processing environment this would mean that *L+T* would operate as a computing center for such requests.

It would also be rather easy to come up with a solution of the third kind meeting the needs of many real time applications. This latter strategy is of course equivalent for the user to accept the reference station coordinates and to work in the double difference mode using the CODE-RINEX file from one of the reference receivers or using an artificial, combined file (see next Chapter).

Let us now review the issue, what kind of processing strategies of the second kind are possible *which go beyond making available the RINEX file plus coordinates of the nearest AGNES station*. The goal is to reduce the noise and to eliminate station/receiver-specific systematic errors (biases) using all reference receivers of the AGNES-network, leaving, however, the actual processing to the user. The *virtual reference station concept* is a candidate technique for this purpose.

It is fair to state that *Lambert Wanninger* is one of the (if not *the*) protagonist(s) of the *virtual reference station concept*. He produced quite a few papers related to that topic. We refer, among other, to [*Wanninger*, 1995], [*Wanninger*, 1996], [*Wanninger*, 1997], and [*Wanninger and Böhme*, 1998]. Let us briefly review here his latest 1998-paper as an example.

[*Wanninger and Böhme*, 1998] actually proposes to generate a RINEX-file using the data of $n \geq 3$ reference receivers with separations of the order of about 40km. The test area of his 1998-paper is essentially flat (at least when compared to Swiss standards).

Wanninger produces observations for each satellite based on approximate coordinates of a user in the area. It is his declared goal to minimize the systematic errors for the area of the user. According to our understanding, Wanninger proceeds in the following way:

- Processing is performed epoch by epoch. Each epoch is treated independently.
- In essence the baseline residuals referring to one epoch are fitted as a linear function of the coordinates longitude λ and latitude ϕ of the reference receivers. Height is not considered as a parameter in Wanninger's analysis (flatland geodesy).
- The residual-fitting procedure is performed on the double difference level. It is unclear whether Wanninger is using a network approach (with correct mathematical correlations) or a baseline-specific approach to compute the residuals. We believe that the latter is the case.
- According to our understanding each frequency (at least L1 and L3) are treated independently. It is not clearly specified *how* the individual carriers are treated to guarantee consistency of L1 and L2 (which have to be stored in the RINEX-file) and L3. There can be no doubt, however, that this can be done in a correct way.
- The result of the procedure is a RINEX-file with Code (L1 and L2) and phase (L1 and L2) observations for each epoch.

It is not clearly stated, how the zero difference observations are generated. It is on the other hand possible, to do that in a correct way, provided coordinates are available for the reference receiver.

Wanninger is not the only author developing such concepts. We refer, *e.g.*, to [*Wübbena et al.*, 1996]. The basic ideas are similar, the difference lies in technicalities, how corrections (extracted from a correct network solution) are transmitted to the user.

Let us also mention the recent article [*Van der Marel and De Jong*, 1999] describing the *active GPS reference system for the Netherlands*, where the *virtual GPS reference stations concept* is shortly, but very clearly described. We believe that this concept is correct to the extent possible. Let us quote a few statements from this paper:

Virtual reference station data is computed using the following procedure. First a network adjustment with GPS data from all reference stations is done. This results in adjusted GPS observations and atmospheric parameters. After the adjustment all data is consistent. Following the adjustment several corrections are applied to the GPS data:

- *A geometric correction (re-location) of the code and phase data to make the user's software believe that the station is at a different location (...)*
- *A correction for the antenna phase center (...) is applied.*
- *Atmospheric corrections are applied.*

The procedure assumes that the user has to specify his antenna and receiver type in addition to his approximate position. We agree in essence with this procedure and will outline in the next section the theory *how* such a combination has to be done technically.

For applications of the "AGNES-type" the ionosphere will play a crucial role. This was recognized by the authors of this report already at a very early stage (see, *e.g.*, [*Beutler et al.*, 1989]). Some of our analysis will rely on techniques developed in this "old" article.

Let us also point out that the average ionospheric refraction may well be taken into account (eliminated) using ionosphere modeling and prediction procedures as developed and described in [*Schaer*, 1999]. We will make extensive use of such techniques in this report.

Epilogue: At a very late state of our investigation we obtained the latest paper [*Wanninger*, 1999] concerning the virtual reference station concept directly from Lambert Wanninger. The paper, to appear in *Zeitschrift für Vermessungswesen* in fall 1999, is well written and we agree with most of his conclusions (although not necessarily with all of his methods).

3. Theory

When constructing artificial observations for a virtual reference receiver with given coordinates one has to make the distinction between

- Creating artificial observations from the ensemble of n receivers under the assumption that there are no biases in the observations of the reference receivers, and
- modeling and application of systematic errors (biases) which are usually not dealt with in commercial-type software.

In section 3.1 we review the phase and code observation equations. These equations are the basis for all our considerations.

Sections 3.2 and 3.3 deal with the first of the above mentioned aspects, where the GPS phase and code observation equations are dealt with separately in sections 3.2 *resp.* 3.3.

The second aspect is addressed in section 3.4, where we address individual error sources from the theoretical point of view. It is our goal to model all satellite- and epoch-specific biases as a function of the (ellipsoidal) coordinates λ and β of the reference stations of the network.

3.1 Recollection of the Observation Equations

Let us briefly review the phase and code observation equations for a single receiver and a single satellite.

The C/A- and/or the P- or Y-code p_{il}^j, as registered by receiver i at receiver time t_{il} from satellite j, is defined as follows:

$$p_{il}^j \doteq c \cdot (t_{il} - \tau_l^j) \tag{3.1}$$

where

t_{il} is the arrival time, or observation time, of a signal as measured by the clock of the receiver i,

τ_l^j is the transmission time of the same signal, measured in the time frame of the satellite j.

All GPS receivers of a reference network are scheduled to observe simultaneously in such a way that the observation time is a full second. It makes thus sense to speak of an (receiver independent) observation epoch for the entire ensemble of GPS receivers and to denote it by t_l.

The *pseudorange* p_{il}^j is related to the *slant range* ρ_i^j at time t_{il} and to the delays due to the Earth's atmosphere. The slant range is the geometrical distance between receiver at observation time t_{il} and the position of the satellite at time τ_l^j:

$$p_{il}^j = \rho_{il}^j - c \cdot \Delta t_l^j + c \cdot \Delta t_{il} + \Delta\rho_{il,ion}^j + \Delta\rho_{il,trop}^j + \epsilon_{cod,il}^j \tag{3.2}$$

where

c is the speed of light,

$\rho_{il}^j \doteq |\boldsymbol{r}(\tau_l^j) - \boldsymbol{R}(t_{il})|$, $\boldsymbol{r}(\tau_l^j)$ being the satellite position at transmission time, $\boldsymbol{R}(t_{il})$ being the position of receiver i at time t_{il},

Δt_l^j is the error of the satellite clock *w.r.t.* GPS-time,

Δt_{il} is the error of the receiver clock *w.r.t.* GPS-time.

$\Delta\rho_{il,trop}^j$ is the delay of the signal due to the neutral atmosphere,

$\Delta\rho_{il,ion}^j$ is the delay of the signal due to the ionosphere, and

$\epsilon_{cod,il}^j$ is the error of the code observation.

At time t_{il} not only the code, but the phase ϕ_{il}^j of the received signal is recorded, as well. We recall that the essential difference of phase *vs.* code is (a) a much higher precision (rms error of about *one millimeter*), and (b) an *unknown number* N_i^j of entire cycles of carrier phase. As the receiver keeps track of the integer number of cycles as a function of time, *only one initial phase ambiguity parameter* N_i^j *is required per satellite pass* (provided that the receiver never looses lock during the pass). An additional difference between code and phase concerns the sign of ionospheric refraction: A signal delay corresponds to a phase advance. This leads us to the following *phase observation equation*:

$$\phi_{il}^j = \rho_{il}^j - \Delta\rho_{il,ion}^j + \Delta\rho_{il,trop}^j - c\cdot\Delta t_l^j + c\cdot\Delta t_{il} + \lambda\cdot N_i^j + \epsilon_{\phi,il}^j \tag{3.3}$$

where N_i^j is the initial phase ambiguity parameter for satellite j and receiver i, λ is the wavelength of the carrier, and $\epsilon_{\phi,il}^j$ is the phase measurement error.

Two equations of type (3.2) and (3.3) are available for the two carriers with wavelengths $\lambda_1 \approx 19$ cm and $\lambda_2 \approx 24$ cm.

3.2 Code Observations for a Virtual Reference Receiver

Let us make the following **assumptions**:

- At a particular epoch t_l, for a particular satellite j, and for a selected wavelength (original carriers or linear combinations thereof) we have *code observations (pseudoranges)* of type (3.2) from n receivers available. Thus we have the following observation equations:

$$\boxed{\begin{aligned} p_{il}^j \;=\; & \rho_{il}^j + \Delta\rho_{il,ion}^j + \Delta\rho_{il,trop}^j - c\cdot\Delta t_l^j + c\cdot\Delta t_{il} + \epsilon_{cod,il}^j \\ & i = 1, 2, \ldots, n \end{aligned}} \tag{3.4}$$

  For our applications we include code multipath errors into the error terms $\epsilon_{cod,il}^j$. This actually means that the error heavily depends on the zenith distance of the

observation. Depending on the particular receiver and on the linear combination analyzed, the rms of the code errors are of the order of a few decimeters to about 2 meters.

- We "perfectly" know receiver and satellite positions. This means that we know all terms ρ_{il}^j.
- Tropospheric zenith delays have been estimated previously with cm-accuracy using double-difference phase data of the reference receivers. Assuming that we know the mapping function, this implies that, in view of the rms of the observation, we perfectly know the tropospheric refraction terms $\Delta\rho_{il,trop}^j$. Alternatively we might even use synthetic tropospheric corrections based, *e.g.*, based on the Saastamoinen model and mapping function for that purpose. In view of the code noise the procedure might be sufficient (except for extreme conditions).
- Ionospheric refraction was established using the methods developed by [*Schaer*, 1999]. We assume to know all the terms $\Delta\rho_{il,ion}^j$, which is probably justified in view of the code rms error. If the ionosphere-free linear combination is analyzed, this term is not present in the observation equations and the assumption is not necessary.
- We want to develop observation equations for a *virtual receiver* with given coordinates $\boldsymbol{R}_0(t)$ in the Earth-fixed reference frame. The atmospheric properties of the atmosphere above the virtual receiver shall follow from the ionosphere model and from the troposphere zenith delays reduced to the height of the virtual receiver. Attention: here we should use orthometric heights.

After this preparatory work it is relatively easy to transform each of the above equations (3.4) into an observation equation for one and the same virtual reference receiver. We simply add the term

$$\xi_{il0}^j \doteq \rho_{0l}^j + \Delta\rho_{0l,ion}^j + \Delta\rho_{0l,trop}^j - \rho_{il}^j - \Delta\rho_{il,ion}^j - \Delta\rho_{il,trop}^j \tag{3.5}$$

on both sides of eqns. (3.4), define a new pseudorange observation as

$$\tilde{p}_{il}^j \doteq p_{il}^j + \xi_{il0}^j \tag{3.6}$$

and we obtain a first set of observation equations for our virtual reference receiver:

$$\boxed{\begin{aligned} \tilde{p}_{il}^j \;=\; & +\rho_{0l}^j + \Delta\rho_{0l,ion}^j + \Delta\rho_{0l,trop}^j \\ & -c\cdot\Delta t_l^j + c\cdot\Delta t_{il} + \epsilon_{cod,il}^j \\ & i = 1, 2, \ldots, n \end{aligned}} \tag{3.7}$$

Eqns. (3.7) may be interpreted as a system of n scalar equations with $3 + n + 1$ unknowns, the coordinates of the virtual reference station, (where, according to our assumptions, we might even consider them as known), the n clock corrections of the receiver, and the satellite clock correction. The system is of course singular.

The situation changes, when combining all systems of type (3.7) referring to epoch t_l for all satellites $j = 1, 2, \ldots, m$ observed by our n receivers.

Assuming for the moment for the sake of the simplicity of the argument, that all satellites are observing the same m satellites, we have $N = n \cdot m$ equations, but only $U = n + m + 3$ unknowns. (for $n = 10$ sites and $m = 8$ satellites we have $N = 80$ equations and $U = 21$ unknowns, and thus a degree of freedom of $f \doteq N - U = 59$).

It thus seems obvious, that the system of all condition equations referring to one epoch is regular. Unfortunately this is not true: all condition equations contain the difference between a satellite- and and a receiver clock. Despite the degree of freedom the system still is *singular*. The situation is cured once and for all, if we assume that one clock, this may be either a satellite or a receiver clock, as known. It would be logical to select for this purpose one of the hydrogen masers in the network (several of them are available in the IGS network), but any of the receiver clocks would serve the same purpose. In global networks, where one can be sure that all satellites are visible simultaneously, it would also be possible to select a satellite clock as reference (*e.g.*, that of PRN 15, today the only GPS satellite without S/A).

We use the following observation equations to determine all satellite and receiver clock errors (plus the position of the virtual receiver) with an accuracy which is in essence only limited by the rms error of the code observations and the degree of freedom of the system:

$$\boxed{\begin{array}{rcl} \tilde{p}^j_{il} & = & +\rho^j_{0l} + \Delta\rho^j_{0l,ion} + \Delta\rho^j_{0l,trop} \\ & & -c \cdot \Delta t^j_l + c \cdot \Delta t_{il} + \epsilon^j_{cod,il} \\ & & i = 1, 2, \ldots, n,\ j = 1, 2, \ldots, m \end{array}} \tag{3.8}$$

Eqns. (3.8) are the basic observation equations for creating artificial observations at epoch t_l for a virtual reference receiver with known coordinates and known atmosphere above it.

Let us mention that it is *not* necessary to assume that each site observes each satellite. Depending on the size of the network and on the horizon masks of individual stations, this assumption might significantly reduce the number of available satellites. Our task to create artificial observations for our virtual receiver becomes really easy, in this case, however: We just may introduce as clock error Δt_{ol} of our receiver the term

$$\Delta t_{0l} \doteq \frac{1}{n} \cdot \sum_{i=1}^{n} \Delta t_{il} \tag{3.9}$$

and introduce as artificial pseudorange for satellite j the mean value of all individual observations

$$\tilde{p}^j_{0l} \doteq \frac{1}{n} \cdot \sum_{i=1}^{n} \tilde{p}^j_{il} \tag{3.10}$$

The $n \cdot m$ equations of type (3.7) are then reduced to the following m observation equations

$$\boxed{\begin{array}{rcl} \tilde{p}^j_{0l} & = & \rho^j_{0l} + \Delta\rho^j_{0l,ion} + \Delta\rho^j_{0l,trop} - c \cdot \Delta t^j_l + c \cdot \Delta t_{0l} + \epsilon^j_{cod,0l} \\ & & j = 1, 2, \ldots, m \end{array}} \tag{3.11}$$

where only the receiver position, the clock error, and the satellite clock errors have to be considered as unknowns. It is interesting to note that the error $\epsilon^j_{cod,0l}$ is formed as the mean value of the individual errors $\epsilon^j_{cod,il},\ i = 1, 2, \ldots, n$. Its rms error is thus a factor of $\sqrt{n}$ smaller than the rms error of each of the individual code observations. This means, *e.g.*, that with an AGNES-type network it is possible to reduce the receiver noise by a factor of about 3. This property is important for code observations *and* it is in essence preserved in the more general case, when we allow for a general observation scenario.

How to proceed in the general case (differing observation scenarios at different sites)? Mathematical correctness asks us to solve the system of equations (3.8) (with the understanding that different receivers may observe different satellites), to arbitrarily define a receiver clock, and to generate m observations for all m satellites. The definition of the clock of the virtual receiver is somewhat arbitrary. Below we define the artificial observations in such a way that the clock term of the artificial receiver is set to zero:

$$\boxed{\tilde{p}^j_{0l} \doteq \frac{1}{n_j} \cdot \sum_{i=1}^{n_j} \left[\tilde{p}^j_{il} - c \cdot \Delta t_{il}\right]} \tag{3.12}$$

where the sum has to be formed over all n_j receivers actually having observed satellite j. With this definition the observation equation for the user is identical with eqns. (3.11).

Let us point out that this procedure is the best possible, provided all our assumptions are correct. It is, however, not completely equivalent to a correct network solution. It remains to be seen whether the differences are relevant.

3.3 Phase Observations for a Virtual Reference Receiver

The phase zero-difference observation equations (3.3) are of a very similar structure as the corresponding code observation equations (3.2). It should thus be possible to proceed in a very similar way as in the case of the code equations for producing phase observations of a virtual reference receiver.

Unfortunately, the ambiguity term $\lambda \cdot N^j_i$ changes the situation considerably. When forming mean values of the type (3.12) we would destroy the integer nature of the ambiguities N^j_i. It would thus never be possible for a user of data from our artificial receiver to resolve ambiguities on the double-difference level. This situation is of course *not* acceptable.

It is also clear, on the other hand, that *if* the ambiguities could be successfully resolved to their integer values, we actually were in a situation analogous to the code equations simply by introducing quasi-observations of the following type:

$$\phi^{*j}_{il} \doteq \phi^j_{il} - \lambda \cdot N^j_i \tag{3.13}$$

Unfortunately, the proposed procedure is purely academic (which is not bad, necessarily) because it is not possible to resolve ambiguities on the zero-difference level. (This statement is true independent on the software or differencing-level used).

It is possible, on the other hand, to resolve ambiguities on the double-difference level. A double-difference observation is defined as follows:

$$\nabla\Delta\phi_{ii_1}^{jj_1} \doteq \left(\phi_i^j - \phi_{i_1}^j\right) - \left(\phi_i^{j1} - \phi_{i_1}^{j1}\right) \tag{3.14}$$

The two terms in (...) on the right hand side are conventionally called a *single-differences* (it would be better to call it a between-station difference). When forming the double-difference observation equations starting from the zero-difference observation equations one immediately sees that all clock terms are canceled. The ambiguity term, however, remains. This is actually only true apart from the fact that the receiver clock error also resides in the geometry terms $\rho_{\cdots}^{\cdots}$. In order not to overload the formalism we assume that the receiver clocks are already synchronized to within 1μs to GPS-time.

The corresponding double-difference observation equation thus reads as follows:

$$\nabla\Delta\phi_{ii_1}^{jj_1} = \nabla\Delta\rho_{ii_1}^{jj_1} + \Delta\left\{\nabla\Delta\rho_{ii_1}^{jj_1}\right\}_{trop} - \Delta\left\{\nabla\Delta\rho_{ii_1}^{jj_1}\right\}_{ion} + \lambda\cdot\nabla\Delta N_{ii_1}^{jj_1} + \nabla\Delta\epsilon_{ii_1}^{jj_1} \tag{3.15}$$

Let us now assume that all ambiguities were successfully resolved. The ambiguity term on the right hand side of eqn. (3.15) is thus known and may be incorporated into the observation, in the same sense as we did it above (see eqn. (3.13)) in the case of zero difference observations:

$$\nabla\Delta\phi_{ii_1}^{*jj_1} \doteq \nabla\Delta\phi_{ii_1}^{jj_1} - \lambda\cdot\nabla\Delta N_{ii_1}^{jj_1} \tag{3.16}$$

We thus obtain a very simple double-difference equation involving stations i, i_1 and satellites j and j_1:

$$\nabla\Delta\phi_{ii_1}^{*jj_1} = \nabla\Delta\rho_{ii_1}^{jj_1} + \Delta\left\{\nabla\Delta\rho_{ii_1}^{jj_1}\right\}_{trop} - \Delta\left\{\nabla\Delta\rho_{ii_1}^{jj_1}\right\}_{ion} + \nabla\Delta\epsilon_{ii_1}^{jj_1} \tag{3.17}$$

It is important to state that these observation equations are unambiguous.

At this point it becomes our task to transform equations (3.17) referring to stations i and i_1 and satellites j and j_1 into four zero-difference equations referring to the receiver-station pairs $i-j$, $i-j_1$, i_1-j, and i_1-j_1.

In principle this may be done easily for each of the double differences. The difficulty resides in the danger that inconsistencies might be introduced when transforming *all* double-differences pertaining to one and the same epoch. We have to make sure that our zero-differences will result in the identical double-differences when again forming double-differences.

Let us summarize the situation in the following way: Assuming that all double-differences could be resolved, we have at one particular epoch, where n receivers and m satellites were used to form the double-differences,

$$(n-1)\cdot(m-1) = n\cdot m - (n+m-1) \tag{3.18}$$

unbiased double differences of type (3.16). *How do we construct $n\cdot m$ zero-difference observations from these double differences which may then be used for double-difference processing software together with data from the user receiver?* The challenge is to transfer the satellite clocks with mm-accuracy to the resulting file.

Let us introduce the following (one dimensional) arrays:

$\boldsymbol{\phi}$ is the matrix of observed phase measurements,

$\boldsymbol{\phi}^*$ is the array of all (constructed) zero-difference observations, and

$\boldsymbol{\nabla\Delta\phi}^*$ is the array of all (used) zero-difference observations.

There is a linear relationship between the two arrays:

$$\boldsymbol{\nabla\Delta\phi}^* = \boldsymbol{A} \cdot \boldsymbol{\phi} \tag{3.19}$$

The concrete form of matrix $\boldsymbol{A}$ depends on the way the double-differences were formed. Each of the $(n-1)\cdot(m-1)$ lines contains exactly four non-zero elements, two equal to $+1$, two equal to -1.

The system of equations (3.19) must now be regularized by adding $n+m-1$ condition equations. This process is by no means unique. We have to make sure, however, that our double differences are not damaged *and* that the satellite clock information is preserved in the zero differences. Let us add the following condition equations:

$$\begin{array}{lcll} \phi_{i1}^{j*} & \doteq & r_{i1}^{j} & j = 1,2,\ldots,m \\ \phi_{i}^{j_1*} - \phi_{i_1}^{j_1*} & \doteq & r_{i}^{j_1} - r_{i_1}^{j_1} & i = 1,2,\ldots,n \quad i \neq i_1, \end{array} \tag{3.20}$$

where the r_i^j on the right hand side have to be constructed in a way to contain the correct range term and the correct satellite and receiver clock terms.

In the proposed scheme we set up m zero-difference and $n-1$ "classical" single-difference observations to regularize the system of eqns. (3.19).

Using for abbreviation the notation

$$\boldsymbol{\nabla\Delta\tilde{\phi}}^{*T} \doteq \left(\boldsymbol{\nabla\Delta\phi}^{*\boldsymbol{T}}, r_{i1}^1, r_{i1}^2, \ldots, r_{i1}^m, r_1^{j_1} - r_{i_1}^{j_1}, r_2^{j_1} - r_{i_1}^{j_1}, \ldots, r_n^{j_1} - r_{i_1}^{j_1}\right) \tag{3.21}$$

we obtain the following non-singular relationship between the zero- and double-difference equations:

$$\boldsymbol{\nabla\Delta\tilde{\phi}}^* = \tilde{\boldsymbol{A}} \cdot \boldsymbol{\phi}^* \tag{3.22}$$

As opposed to eqns. (3.19) the system of equations (3.22) is regular and may be inverted:

$$\boldsymbol{\phi}^* = \tilde{\boldsymbol{A}}^{-1} \cdot \boldsymbol{\nabla\Delta\tilde{\phi}}^* \tag{3.23}$$

Our constructed phase zero-difference equations may now be used exactly like the code zero-difference equations to form the pseudo-observations for the virtual reference receiver.

In practice we may directly use the phase observations $r_i^j \doteq \phi_i^j$ for the purpose of regularizing the relationship (3.19). The satellite clock information is fully preserved in the constructed phases.

If the code observations, prior to combination, are modified in exactly the same way (using the transformation (3.23)) we even establish full consistency of code and phase observations.

The procedure outlined above is a bit laborious. This does not pose a problem for post-processing applications. Whether the matrix inversion required at each epoch

is suitable for real-time applications remains to be proven. The procedure is correct to the extent possible and it leads to a zero-difference set of observations which is absolutely free from cycle-slips on the double difference level.

Theoretically, the noise of the phase equations is reduced by the $\sqrt{n}$-law as in the case of the code equations. The aspect is probably not of vital importance in the case of phase (except for the reduction of multipath). In view of this consideration it may be sufficient to build up the phase observations of the virtual receiver by using the observations of only one receiver. All systematic biases (troposphere, ionosphere, antenna phase center transformation, *e.t.c.*) might be corrected and the transfer to the new location performed easily. The drawback is, however, that the transmitted phase observations will be contaminated by all the problems (cycle slips, outliers) of the selected reference receiver (and one may not hope for a reduction of multipath).

3.4 Epoch- and Satellite-Specific Biases as a Function of the Receiver Coordinates

Let us start our consideration with stating a few principles:

- From a scientific point of view it would be preferable to make available all biases separately to the user. He would then be fully aware of the kind and size of corrections applied. This may not be possible for real-time applications. It should be possible, on the other hand, to transmit the sum of all corrections for each epoch and each satellite.

- It is absolutely mandatory to archive the original (may be screened) observations for all reference receivers *and* at least for one realization of the virtual receiver. If this virtual receiver has identical coordinates as one of the reference receivers, a zero baseline formed by the two corresponding receivers (one real, one virtual) gives an impression of the maximum (bad) effect the bias-removal might have. The procedure allows to improve the procedure steadily.

- It is quite clear (optimists would say: it cannot be completely ruled out) that for short baselines ($<$ 10 km (?)) it is the best strategy to use the *unaltered observations* of the closest reference receiver (except for antenna phase center and multipath effects). Experience will tell where the "break-even" point lies.

- Physical modeling is always better than empirical corrections. There is a certain danger that observation noise is magnified in the second case. We therefore recommend, *e.g.*, to remove the deterministic part of the ionosphere *before* modeling the (residual part of the) ionosphere. Also, instead of using broadcast orbits one should use IGS predicted orbits, in particular if they are based on short turn-around times (let us say 12 hours of less). Similar statements hold for tropospheric refraction: it may be assumed that good real-time estimates for tropospheric zenith delay corrections are available in real-time from a correct double-difference network solution.

Let us now make a few remarks from the theory point of view concerning the following error sources:

- Antenna phase center variations,
- GPS satellite orbits,
- tropospheric refraction,
- multipath, and
- ionospheric refraction.

Antenna Phase Center Variations

The receivers of a centrally controlled reference network should all be equipped with the same antenna type. Using the same receiver type is recommended but not mandatory. The same antenna type guarantees the best possible performance in a network of the size of AGNES (a few hundred km in diameter).

The user is allowed to have any type of antenna (provided the type is known to the network operator). The difference between the user- and the AGNES- antenna type is applied to each generated observation according to the known zenith distance and azimuth of the observation at the very end of the process.

This correction does not require any estimation procedure. It is straight forward, and it is an established fact that such a procedure is successful.

GPS Satellite Orbits

It is nonsense to remove orbit errors on the epoch-by-epoch basis. Orbit errors have time characteristics of a few hours, typically. It is recommended to use the best possible orbit available in real-time. Should — for reasons unclear to us — the orbit quality be insufficient, we recommend to use the AGNES (and other recent) observation data of the previous (maybe 12) hours in a batch process to improve the orbits (maybe once per hour). Only a reduced set of orbit parameters has to be dealt with in this orbit improvement procedure. Experiences gained when processing the Alaska campaigns in the 1980s indicate that an along track-error (orbit element u_0) might be sufficient to remove that largest portion of the orbit error.

We recommend in any case to run such a solution regularly in near real-time. Substantial corrections to the a priori orbit indicate satellite specific problems. It is up to the network operator either to recommend the user not to use a specific satellite or to actually apply the correction. Because such a computation has not to be performed on an epoch-by-epoch basis, computation time (CPU) is not critical.

Tropospheric Refraction

As we all know "the weather takes place" in the lowest (to be generous) five kilometers above each stations. In view of the station separation in the AGNES it does *not* make sense from a physical point of view to make the attempt to estimate *satellite- and epoch-specific* biases. It makes sense, however, to establish tropospheric zenith

corrections with a high (maybe quarter of an hour) time resolution. The estimates should be continuous.

Such corrections may be established in a similar way as the orbit corrections (if possible in the same process). The estimated values may be used (extrapolated for the next, let us say, 15-30 minutes). It might be possible to solve for troposphere gradients in such a process. (Although the correction probably is not significant for 99% of all applications).

Multipath

This error source is critical for code observations, it cannot be neglected for phase observations, either. We view it as a major benefit of using a network of the AGNES-type in the sense of sections 3.2 and 3.3 to create observations of an artificial receiver, that not only the noise, but also multipath is reduced by the $\sqrt{n}$-law (assuming that epoch-specific multipath referring to the same satellite is not correlated for observations made from different sites).

It is well known that multipath effects may be "easily" detected by correlating residuals of baseline- or (what would even be better for that purpose) single-point positioning processing from subsequent days (shifted by four minutes). It might be worthwhile to set up multipath maps for each of the AGNES sites. These effects should be removed (and not applied again (!)) from code and phase data of the individual AGNES receivers. Establishment and analysis of such maps might be the topic for a diploma thesis). The results might be useful for improving the overall performance of the network.

Ionospheric Refraction

After having successfully ruled out all other error sources, we are left with ionospheric refraction as the only candidate for an epoch- and satellite-specific error model which has to be established in real-time.

It is sufficient for our discussions to adopt the single-layer ionosphere model. Figure 2 illustrates the observation scenario for one pair receiver-satellite.

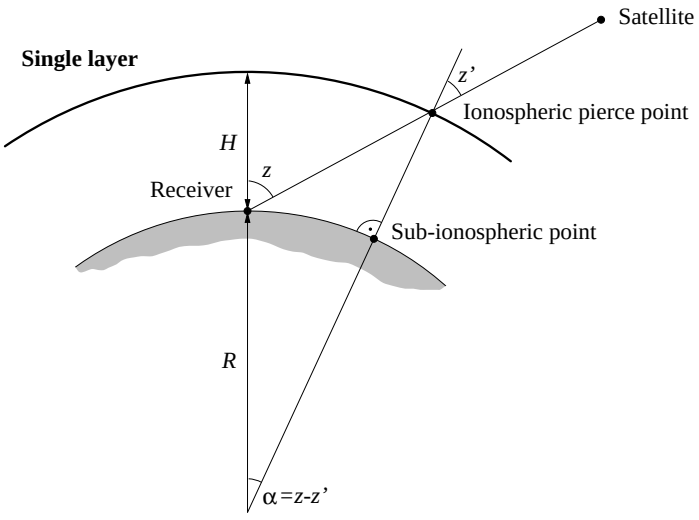

Figure 2: Single Layer Model for the Earth's Ionosphere

Let us point to a few facts:

- Ionospheric refraction is completely removed when forming the ionosphere-free linear combination. This statement is not really helpful because an AGNES-user *has to use* at some point $L1$ and $L2$ observations (or linear combinations other than the ionosphere-free combination).

- The use of ionosphere models, as established by [*Schaer*, 1999] are very useful and must be recommended. Their usefulness increases with the length of the data span: If this data span is long compared to the typical short period variations (*e.g., traveling ionospheric disturbances*) the model does *substantially improve the ambiguity resolution performance*. We refer to chapters 6 and 7 for more information. The network operator is recommended to establish corrections relative to a predicted ionosphere, which may established in a similar way as orbits and troposphere.

- It would make sense to make ionosphere files available for those users who have scientific software packages. When generating the data for the virtual receiver, the entire effect (ionosphere model plus differential corrections) has to be applied to the (ionosphere-free) observations.

- For data spans shorter than, let us say half an hour, and for baselines longer than, let us say, 10 km, short-period variations are often preventing the user from resolving the double-difference ambiguities to integers. It is exactly for this type of applications that an epoch- and satellite-specific ionosphere model must be established and tested.

- Figure 2 clearly shows why the model must be satellite-specific: In the single layer in a height of about $H = 450$ km the tracks of individual satellites may be separated by more than to 2000 km, whereas the tracks in the single layer referring to the same satellite, but to different AGNES sites are in essence separated by distances comparable to the distances of the network.

- Epoch-specific modeling might be replaced by *high time resolution modeling — what would reduce the danger of blowing up noise.*

- Figure 2 also illustrates that success and failure of ionosphere modeling in the sense addressed above heavily depend on the actual characteristics of the ionosphere *and* on the size of the ground tracking network. If the spacing of stations is such that even for the same satellite there is no correlation in the electron content, the model must fail. If the spacing is too fine a model is not required.

- In a network of about ten sites covering an area like Switzerland, a linear model as a function of λ and β is probably the only model that makes sense. Three parameters have to established (using, in the best case, ten observations). A

quadratic model would already have six parameters where we would see the danger of blowing up noise or even blunders. The situation might be improved, if more than one epoch would be combined to extract one set of model parameters. If one-second data is available it would undoubtedly make sense to combine ten to sixty epochs.

4. First Analysis using Program CLKEST

In the current *Version 4.1* of the *Bernese GPS Software* the double difference still is *the* observable promising highest accuracy. Undifferenced processing is possible in

- program **CODSPP**, which is traditionally used to remove the receiver clock errors (on the microsecond level) from GPS code and phase single difference files,
- program **GPSEST**, which may be used for satellite and receiver clock estimates using code or phase-smoothed code observations,
- program **GPSEST**, which may also be used to process zero-difference code and phase observations (without allowing for the resolution of the phase ambiguity parameters).

The latter two options are generalizations implemented by Tim Springer in the context of his Ph.D. Thesis (to be completed in 1999). These developments are most encouraging. It may be viewed as a disadvantage, however, that preprocessing is done on the *single file basis* using the *Melbourne-Wübbena* linear combination. This technique makes it very difficult (a) to clean phase on the *one cycle level*, and (b) to assign detected problems to the correct satellite / station / carrier / observation type combination.

All Bernese (pre-)processing programs are based on the (conservative) assumptions that neither receiver positions nor satellite orbits are accurately known in the moment of (pre-)processing. It is of course important that a general purpose processing software is capable of coping with the worst possible situation.

In the age of a growing number of permanent GPS networks (let us mention, *e.g.*, the *IGS*, the *EUREF*, and the *AGNES* networks) it seems advisable to develop novel processing strategies complementing the existing Bernese strategies.

These considerations, plus the necessity to develop *efficient* processing tools for spaceborne applications of the GPS led to the development of the test program **CLKEST** which might eventually replace the programs

- **CODSPP**,
- **SNGDIF**,
- **MAUPRP**,

at least when processing data from permanent GPS arrays. **CLKEST** should be able to produce clean phase and code files of best possible quality containing the (*epoch specific*) receiver clock estimates. It may also be used to generate clock files of good quality. If these estimates are based on code only, the quality is on the few nanoseconds level. If phase is involved, a few hundreds of a nanosecond seem achievable. After suitable generalization the program might also be used as an "interpolation" tool between the 5 min-epochs, for which precise satellite clocks are available from the CODE "routine" processing.

4.1 Program Description

CLKEST analyzes, epoch by epoch, all observations (phase and code) of all receivers of a permanent GPS array. The program assumes that geodetic-type dual frequency receivers are available (although it might also be used for processing single frequency data). It uses exactly the same models as program **GPSEST**. Subroutines *GETSTA, GETORB, GOBSEP, GFRQEP, and TOPSTA* guarantee compatibility on a high level. Currently, the $L3$ and (if required) the $L4$ observables are analyzed.

Three types of analyses are performed:

- *Epoch-specific clock estimates* using code observations,
- *epoch-specific clock difference estimates* using phase observations, and
- *establishment of satellite and epoch(-difference) specific ionosphere models* for regional networks as a linear function of latitude and longitude of the receivers' coordinates using all $L4$ phase observations of all stations available for a particular epoch difference.

The first two procedures are used to clean the code and phase files and (possibly) to generate a satellite and receiver clock file, the third may be used to extract site-specific ionosphere corrections for a "virtual receiver". Examples may be found in the next section.

Table 5 shows the option/input file of program **CLKEST**. The options are arranged in four groups, namely *general processing options, code processing options, phase processing options*, and *ionosphere processing options*. Most options are self-explanatory. We may therefore confine ourselves to a few remarks.

As we have seen in Chapter 3 we have to fix one clock for each epoch. Either a satellite clock or a receiver clock may be used. If a file number $n_f > 0$ is specified, the clock of the receiver in the indicated file is kept fixed at each epoch (third option in the "general processing options" block). If this file number is $n_f = 0$, the clock of one of the satellites is kept fixed (the first satellite in the list of epoch-specific satellites is chosen). This option makes sense (it is probably the best choice) if a precise clock file, *e.g.*, from the *CODE Analysis Center* is used as a priori clock information.

The program assumes, that a Bernese clock file is available. This file may be based on actual estimates or it may be derived from broadcast clocks. All satellite clock estimates are performed relative to the a priori satellite clocks. As opposed to the normal Bernese processing mode satellite clocks are interpolated between the clock reference epochs. This is done by the subroutine *GTSCLM*, a modified version of subroutine *GTSCLK*.

It is a strength of the program that data of all receivers of an array are processed together. If a particular satellite was only observed by two stations we are, so to speak, back to the baseline-specific processing mode: If problems occur, we are not sure where the problem actually occurred. This is why we may specify (separately for phase and code) the minimum number of stations for a particular satellite to be included in the epoch-specific processing. This aspect should not matter when dealing

with a global tracking network of a certain density. For regional networks the aspect needs to be considered if satellites rise or set. The maximum zenith distance may also be used to influence this aspect in regional networks.

```
CLKEST: OPTION INPUT FILE                                    24-APR-99 01:10
-------------------------------------------------------------------------------
PROCESS ALL OBSERVATIONS (PHASE AND CODE) TO DETECT OUTLIERS (CODE),
CYCLE SLIPS (PHASE) AND TO ANALYZE IONOSPHERIC BEHAVIOUR
-------------------------------------------------------------------------------
1. GENERAL PROCESSING OPTIONS                                ******* UNITS
   -------------------------
SAMPLING OF INPUT DATA                              --> :       1 ---
LINEAR COMBINATION TO BE USED (L1, L2, L3)          --> :       3 ---
REFERENCE CLOCK IN FILE # (0: SATELLITE CLOCK USED)--> :       1 ---
ONE SAT HAS TO BE OBSERVED BY MIN. # OF STATIONS    --> :       3 ---
TROPOSPHERE USING EXTERNAL FILE (2, ELSE 1)         --> :       1 ---
MAXIMUM ZENITH DISTANCE                             --> :      82 DEGREES
2. CODE PROCESSING                                           ******* UNITS
   ---------------
MAX. CLOCK RESIDUAL TOLERATED                       --> :      5. M
MAX. RMS TOLERATED FOR SUCCESSFUL CLOCK ESTIMATION  --> :      4. M
MAX. # OF ITERATIONS, IF RMS EXCEEDED               --> :      10 ---
3. PHASE PROCESSING FOR CLOCK DIFFERENCE ESTIMATION          *******
   ----------------------------------------------
MAX TOLERATED TERM ''OBS-COMP''                     --> :    10.0 M
MAX TOLERATED RESIDUAL                              --> :    0.05 M
MAX TOLERATED RMS FOR CLOCK ESTIMATION              --> :    0.02 M
MAX. # OF ITERATIONS IF RMS EXCEEDED                --> :       1 ---
4. IONOSPHERE PROCESSING                                     *******
   ---------------------
DEGREE OF MODEL (SKIP IF NEGATIVE)                  --> :       1 ---
ONE SAT HAS TO BE AVAILABLE AT MIN. # OF STATIONS   --> :       2 ---
STORE ORIG. ESTIMATES (1) OR ACCUMULATED ESTS (2)   --> :       2 ---
CORRECT TO ZENITH? (YES=1)                          --> :       0 ---
SATELLITE FOR RESIDUAL FILE                         --> :       5 ---
MAX TOLERATED TERM ''OBS-COMP''                     --> :    0.05 m
```

Table 5: Option/Input File of Program CLKEST

After reading the data from one epoch, **CLKEST** removes the geometry and atmosphere terms from the code observations, exactly as outlined in Chapter 3, using the (best available) orbits, station coordinates, and atmosphere models. (Bernese clock, troposphere, and ionosphere files may be used).

There may be outliers in both, code and phase observations. In addition there may

be cycle slips in phase observations. Code analysis is performed in an iterative way: If the *a posteriori RMS error of observation* exceeds the value specified in the *code processing option section* (Table 5), the observation corresponding to the residual with the highest absolute value is removed (provided it exceeds the value specified) and the adjustment is repeated. The new *RMS* is computed. If this new value still exceeds the prescribed value, the process is repeated (unless the maximum number of iteration steps is already reached).

Phase clock-difference estimates are performed relative to the code-established clocks. It is thus clear that the terms "observed-computed" should already be close to zero within boundaries corresponding to the code RMS of observation. This is why the term "O-C" may be used for cleaning the phase observations.

The basic observation of the third analysis is the difference Δi_k^j of the $L4$ observation of one particular satellite j from one receiver k *w.r.t.* the previous epoch. This observable is modeled according to

$$\Delta i^j(\lambda,\beta) = \Delta i_{00}^j + \frac{\partial \Delta i^j}{\partial \lambda}\cdot(\lambda-\lambda_0) + \frac{\partial \Delta i^j}{\partial \beta}\cdot(\beta-\beta_0) \tag{4.1}$$

Δi_{00}^j, $\frac{\partial \Delta i^j}{\partial \lambda}$, and $\frac{\partial \Delta i^j}{\partial \beta}$ are the parameters of the process, if the degree of the model is 1. Only the mean value i_{00} is estimated if the degree is equal to 0. The entire step is skipped, if the degree is set to a negative value. λ_0 and β_0 correspond to the "center of mass" of the array. Let us point out that the analysis only makes sense for regional arrays. The *AGNES* is a good example. The analysis is performed for each satellite separately. A full report is written for the satellite selected in the option file. It is possible either to store the original epoch-specific estimates or the summed-up estimates relative to the inital epoch. A new initial epoch is set after a long gap (of three hours or more).

4.2 Results

Figure 3 shows the RMS values a posteriori of all code observations as a function of time. Values ranging between about 0.5m and 3m are reported. It should be pointed out that only at one epoch the procedure reported a code-problem. It thus seems that the code measurements in the network are of remarkably high quality. The receiver at *Pfänder* is an exception: It happened rather frequently that code was missing at a particular epoch. This seems to have happened rather often (about 300 times) for low elevation angles.

Figure 4 shows the RMS values a posteriori of the observations for clock difference estimates using phases. These values range between about 5mm and 2cm. This would correspond – as promised – to clock difference errors of a few picoseconds.

Figure 5 gives an impression of the excellent performance of the network. Only one code measurement had to be marked (actually corresponding to an observation made at a zenith distance of about 84^o). The figure does, however, not include the missing code observations of the Pfänder receiver. Not too many phase problems were

encountered, either. It should be mentioned that the number of "phase problems" includes the initialization for each satellite pass at each station.

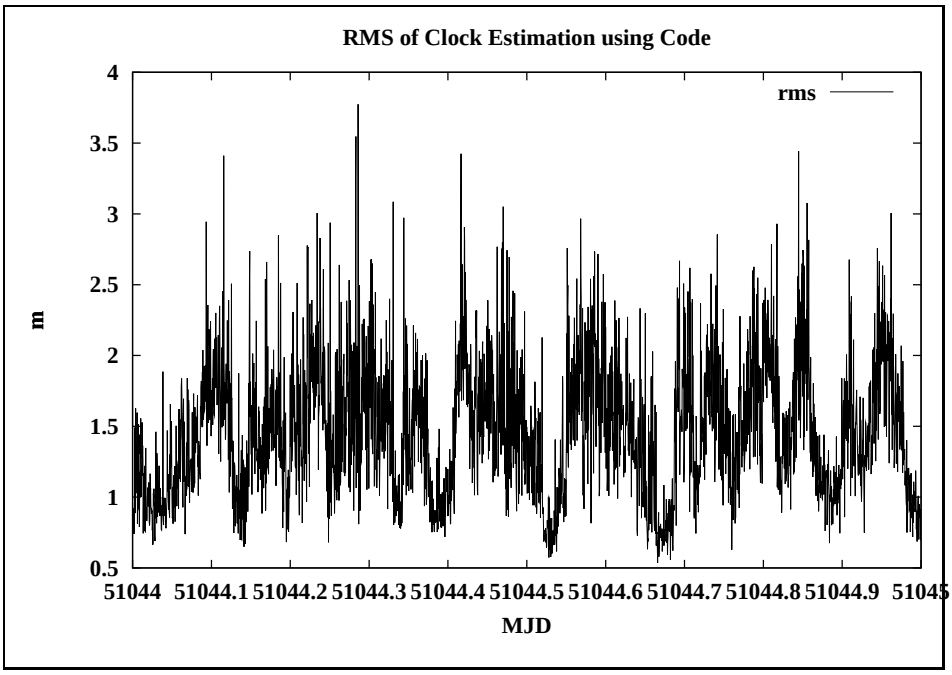

Figure 3: RMS of Clock Epoch-Specific Estimates using Code (1998 08 19)

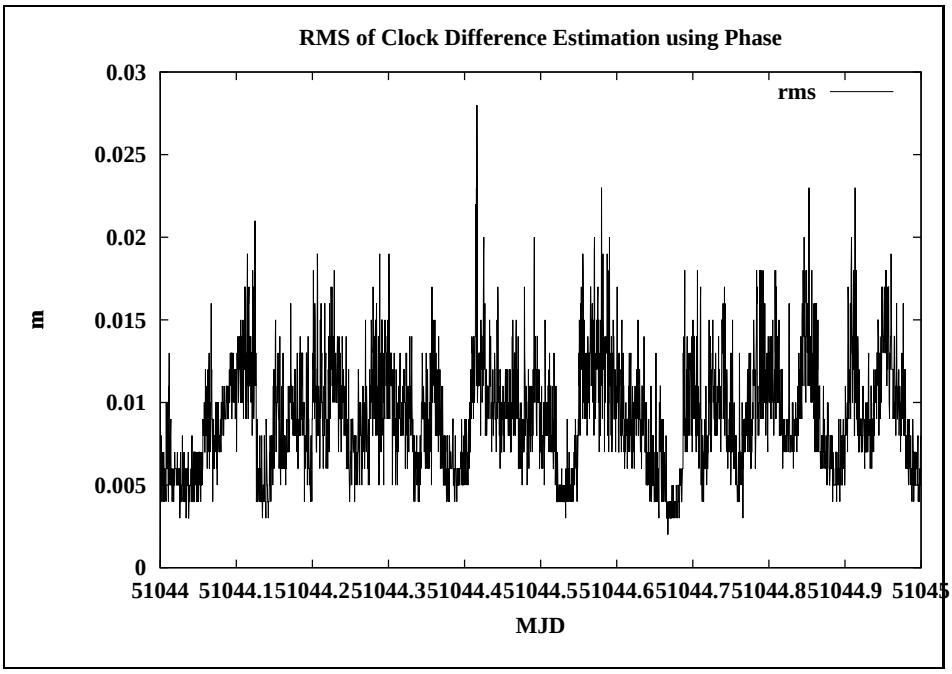

Figure 4: RMS of Clock Difference Estimates using Phase (1998 08 19)

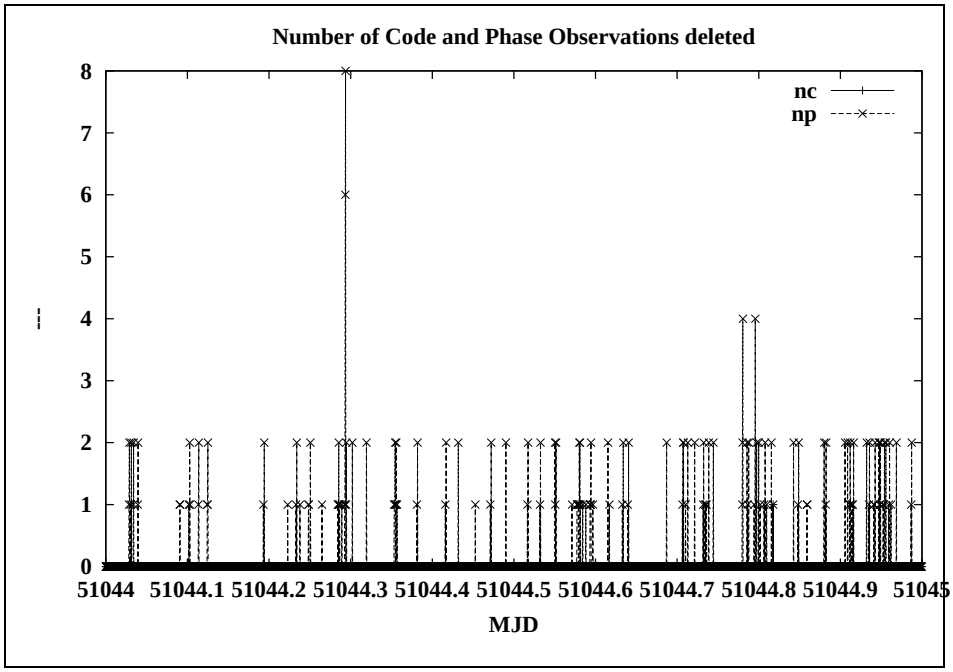

Figure 5: Number of Deleted Code and Phase Observations (1998 08 19)

One easily sees a high degree of correlation between Figures 3 and 4. The structure present in both figures is almost uniquely due to the low elevation data. If a cut-off zenith distance of 70^o is used, the structure disappears almost completely, the RMS error for code drops on the the submeter level, that for phase differences on the few mm-level.

Table 6 also characterizes the excellent performance of the receivers in the network.

Site	# Problems of Type						# observations	
	z	c	f	p	m	x	code	phase
EPFL	0	0	92	1	1	0	24103	24103
SIER	0	0	66	4	1	0	20693	20693
ZIMM	0	0	87	1	0	0	23170	23170
JUJO	0	1	75	2	2	0	22677	22677
FHBB	0	0	88	6	0	0	24293	24293
ETHZ	0	0	86	3	0	0	23567	23567
PFAN	0	0	167	17	216	0	24177	24177
Total	0	0	661	34	220	0	162680	162680

Table 6: Receiver performance in AGNES, August 19, 1998 (z: marked due to zenith distance, c: marked code observation, f: new ambiguity, p: marked phase observation, m: phase, but no code observation available,x: marked phases because # observing stations too small)

As viewed from the code quality, all receivers performed almost perfectly. Using

$RMS < 5$m as a criterion, only one code observation (by the way associated to the Jungfraujoch receiver made at a zenith distance of 84^o) had to be marked.

In view of the fact that 27 satellites were observed and that each satellite had either one or two passes over the region, an average number of $3-4$ ambiguities per satellites is really not too much! The receiver at the Pfänder site is an exception. The problem is caused by the fact that the receiver often has phase, but no code observations. This is not accepted by our program. The situation occurs most of the time at low elevations. If the cut-off zenith distance is set to 70^o, only few events of type "m" would remain in the system.

It is remarkable that only very few (< 10) true cycle slips (events of type "p") are reported for the other receivers (one should be aware of the fact that each cycle slip causes an ambiguity to be set up at the next epoch).

Table 6 demonstrates the power of the approach. We easily recognize that exactly one receiver, the one at the Pfänder site performs significantly worse than all the others. In an operational environment such a receiver should be replaced as soon as possible. If the antenna location is causing the problem, a new location would have to be found. Monitoring programs based on the principles of our program **CLKEST** add value to a network of the AGNES-type.

Figures 6 and 7 show the results of a satellite clock estimation (at each epoch the first satellite in the epoch-specific list was taken as an example) and of a receiver clock estimation, in both cases using the code observations. The clock excursions in Figure 6 are caused by S/A between the five minute intervals at which precise satellite clocks are available.

Figure 7 shows the typical clock performance of a Trimble receiver. The clock is reset to GPS-time if the synchronization is getting worse than one millisecond.

Figures 8 and 9 show the clock difference improvements (between subsequent epochs) using the phase measurements for the satellite and the receiver clocks. For better understanding the clock corrections are expressed in meters (by multiplication with the speed of light c). The figures show in essence the quality of a clock difference estimation using code only.

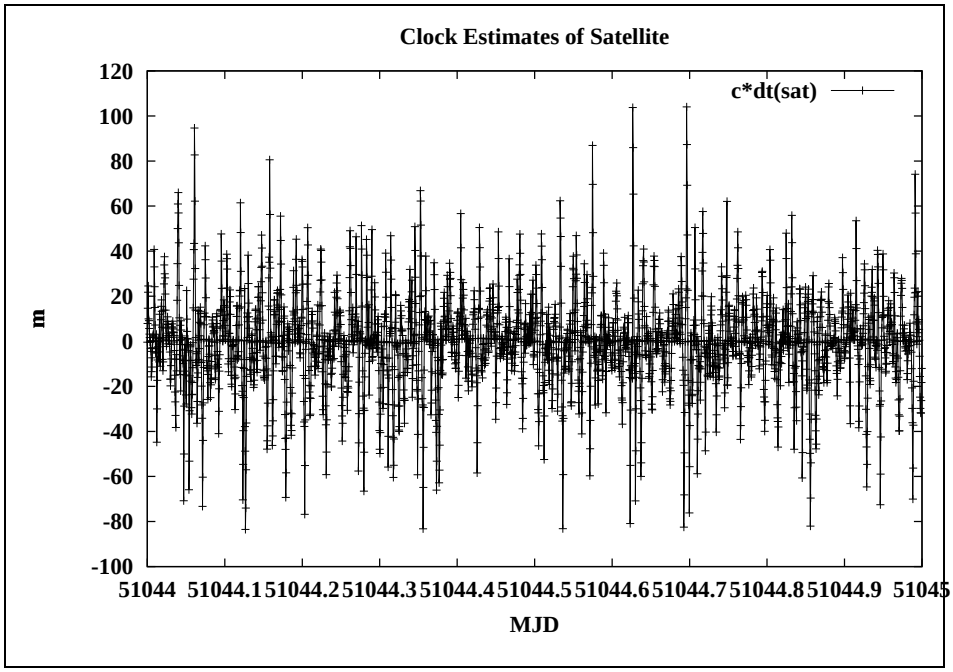

Figure 6: Clock Estimates of one Satellite per Epoch relative to the interpolated Precise Clocks using Code obs. from CODE AC (1998 08 19)

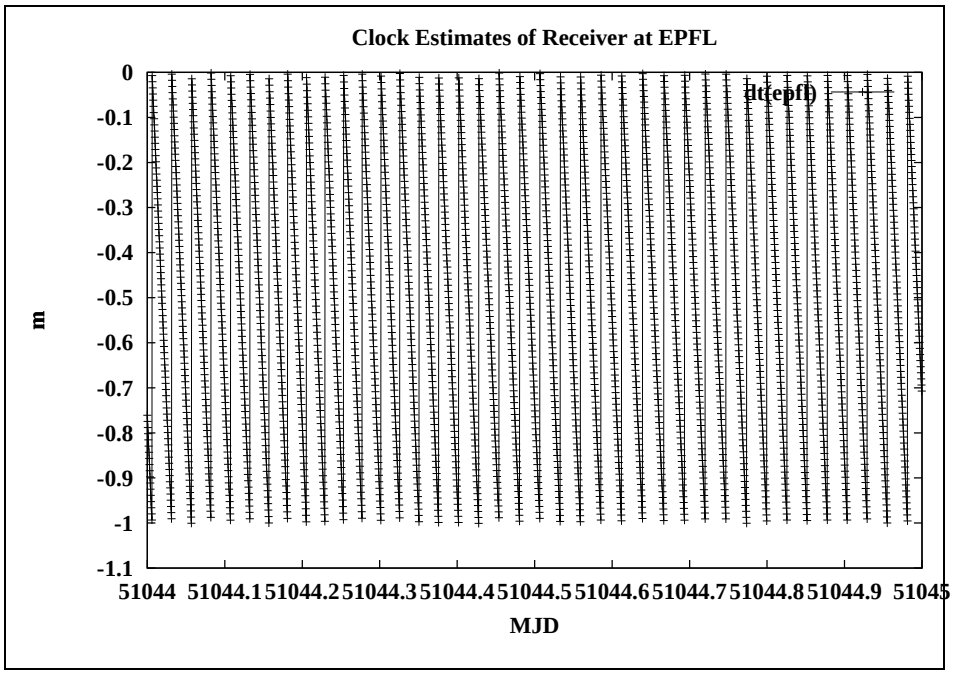

Figure 7: Clock Estimates of Receiver at EPFL using Code observations (1998 08 19)

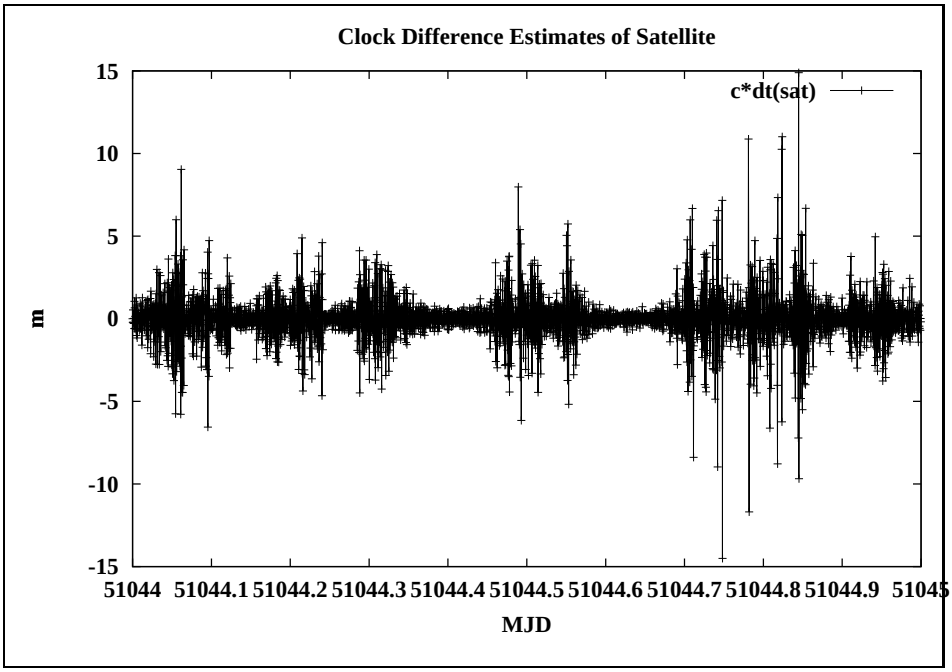

Figure 8: Clock Difference Estimates for one Satellite using Phase (1998 08 19)

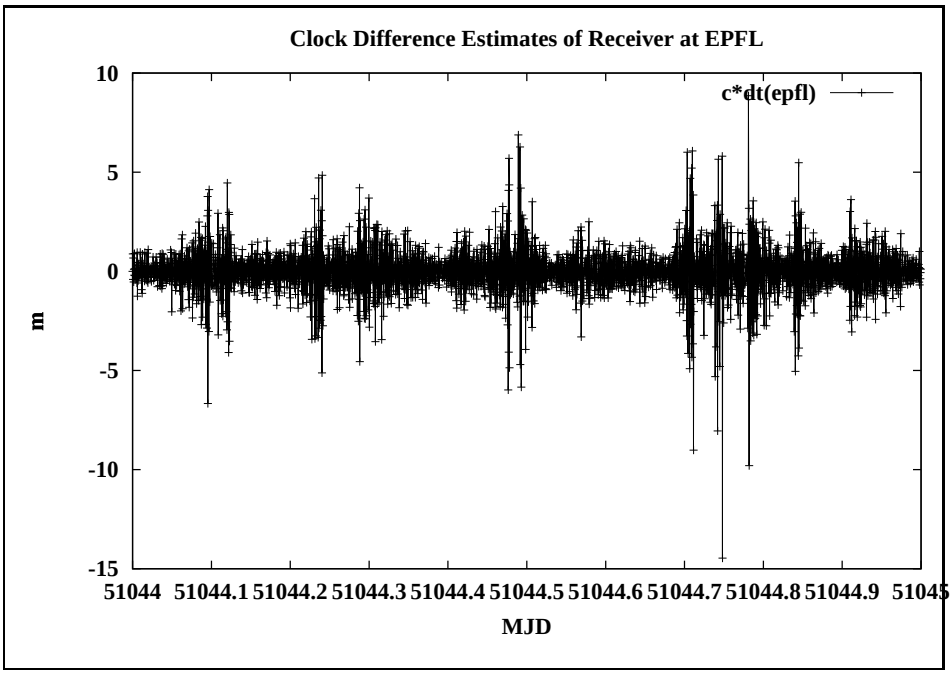

Figure 9: Clock Difference Estimates for Receiver at EPFL using Phase (1998 08 19)

Figures 10 to 38 are related to the ionosphere estimation procedures. As mentioned, all $L4$-differences between subsequent epochs of all AGNES-receivers are analyzed for

each satellite separately. All results refer to the $L4$ observable. A correction factor has to be applied for the effect in the original carriers. The results are stored for one satellite only, at present.

From the entire wealth of data we only discuss the results for $SVNs$ 4 and 5. Two passes may be observed for SVN 4 by the AGNES network (one around midnight, one around noon UT), only one (around midnight) for SVN 5. We may inspect the *change of the total ionosphere content per epoch (term* i^j_{00}*)* and the *changes in the gradients in the North and in the East directions*. Units are meters for the term i^j_{00} and meters/100 km for the gradient terms.

Although only the ionosphere changes per epoch difference are computed, we may also create figures for ionosphere changes relative to the initial epoch by summing up the actual epoch estimates. After a long gap (of the order of 2 hours), the summing-up process is initialized by introducing a new initial epoch.

We may subtract an a priori ionosphere model (established using the procedures developed by [*Schaer*, 1999]). We will always mention whether or not an a priori model was subtracted prior to the analysis.

The first series of results was produced without an a priori ionosphere model. Figure 10 shows the estimated i^j_{00} terms for all epoch differences for SVN 4. We clearly see that pronounced changes are taking place for the noon satellite pass. The ionosphere first decreases, then increases again. This has to be expected for a satellite tracked from horizon to a minimum zenith distance back to the horizon.

Figure 11 shows the observation RMS error as a function of time. As expected we see a clear zenith distance dependence. We may also (artificially) reduce the ionosphere to the zenith by multiplying the estimates and the associated RMS-errors with $\cos z$, where z is the zenith distance. Even then, we would see a clear, although much less pronounced zenith distance dependence. Be this as it may: Reduced to the zenith, we have a noise of 1-2 mm, only. One cannot expect more. It should be pointed out that the RMS is almost the same when we solve only for the term i_{00} and forget about the gradients.

This latter statement seems to be supported by Figures 12 and 13. Let us point out, however, that at the beginning and the end of a path, two or three estimates should have been removed (which might easily be done by defining appropriate input options). It is clear, on the other hand, that most estimates are very close to the noise level.

Figures 14 to 17 give exactly the same information as Figures 10 to 13, but replacing the time argument by an epoch number, leaving out the epochs where the satellite was not tracked. These new Figures give a much better resolution. We even recognize some structure in the gradient estimates.

Figure 18 to 20 show the ionosphere estimates *w.r.t.* an a priori ionosphere model. Comparing Figure 18 to Figure 10, we indeed see that the a priori model takes out a good portion of the ionosphere signal. A similar statement does not hold for the gradient estimates.

Figures 21 to 26 show the estimated values in their summed up version. The first three of these figures use time, the second three the epoch numbers as an argument.

No a priori model is subtracted. We clearly see the changing total ionosphere content (between -2 m to +3.5 m) in Figure 21, and we see a very clear structure of the gradient estimates. The latitude gradient shows changes of up to ±15 cm per 100 km. A signal of this kind actually might be taken out when generating observations for a virtual reference receiver.

Figures 27 to 29 again show the ionosphere changes relative to the initial epoch of the satellites pass, but this time relative to an a priori ionosphere model (we use the epoch number as an argument). If we compare Figure 27 with Figure 24 we see that the a priori model is indeed of good quality, but that it has its limitations, as well. The a priori model is not important for the gradient estimates.

The (difficult) question remains what percentage of the ionosphere remains unmodeled.

This question may – to some extent – be addressed by performing the same analysis once using the full (available) AGNES network, once by leaving out some of the stations. Figures 30 to 32 show the superposition of two estimations, once using the entire network, once using the entire network except the Pfänder receiver. We do not see a difference for estimates of the total ionosphere content, but we see rather pronounced differences for the gradients (Figures 31 and 32). In view of the shape of the network (Figure 1) it seems plausible that the East-West component suffers much more than the North-South gradient the Pfänder site is left out. Let us also mention that the general trend and even some of the "fine structure" remain unchanged in the two analyses. This allows us to be rather optimistic that actually a good percentage of the ionosphere fluctuations might be modeled over an area like Switzerland.

Figures 33 - 38 give the same information as discussed above for yet another satellite, SVN 5. Let us confine ourselves to the remark, that rather pronounced ionosphere gradients may also occur during night time. Apart from this observation, a similar behaviour is observed as for satellite SNV 4.

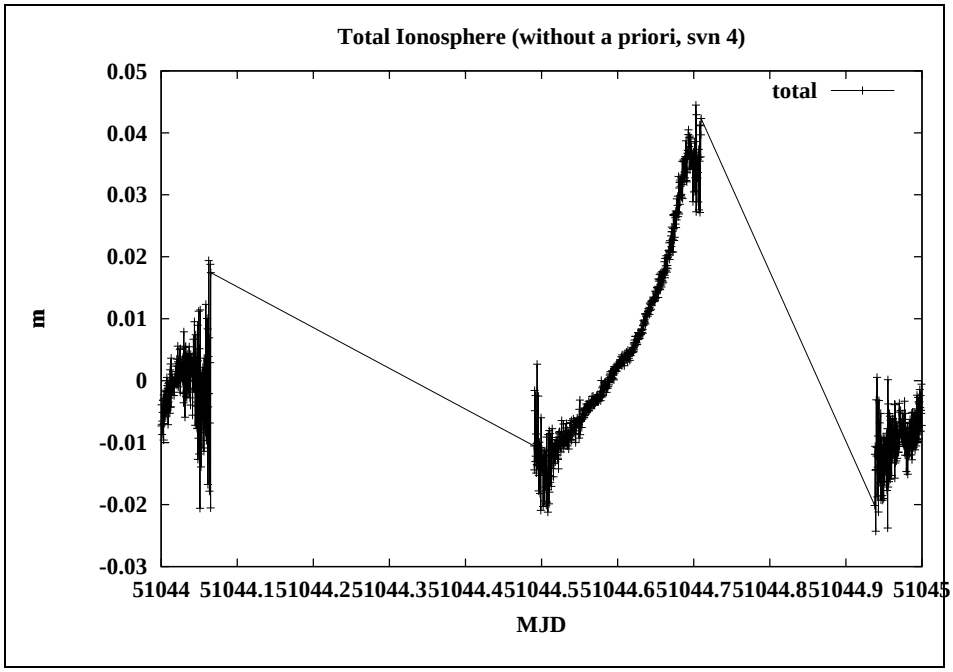

Figure 10: Total Ionosphere Difference relative to previous epoch (SVN 4) no a priori model

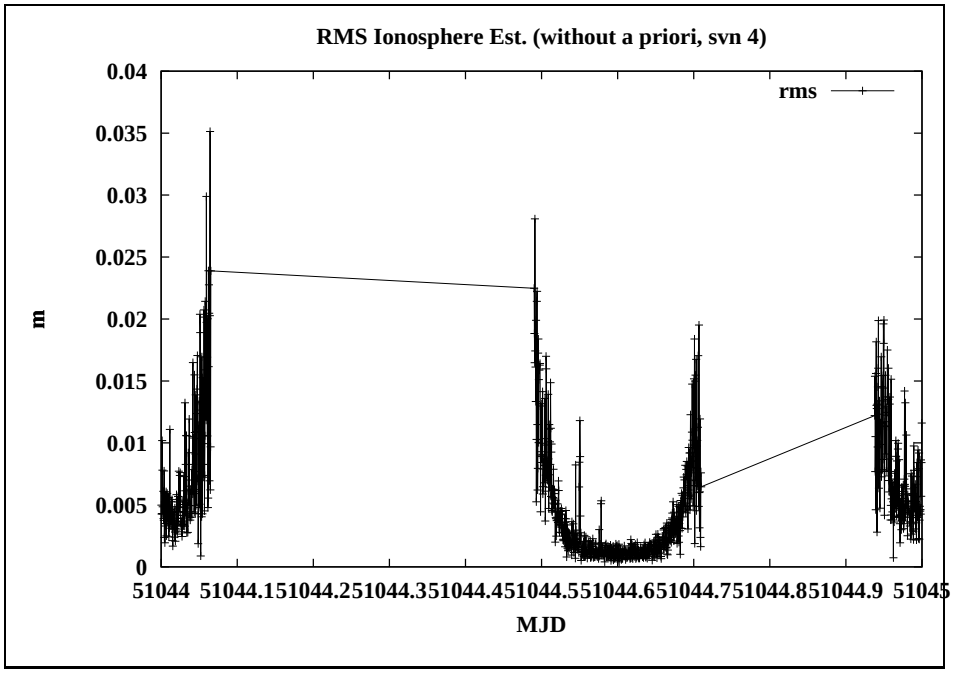

Figure 11: RMS of Ionosphere Difference Estimation (SVN 4)

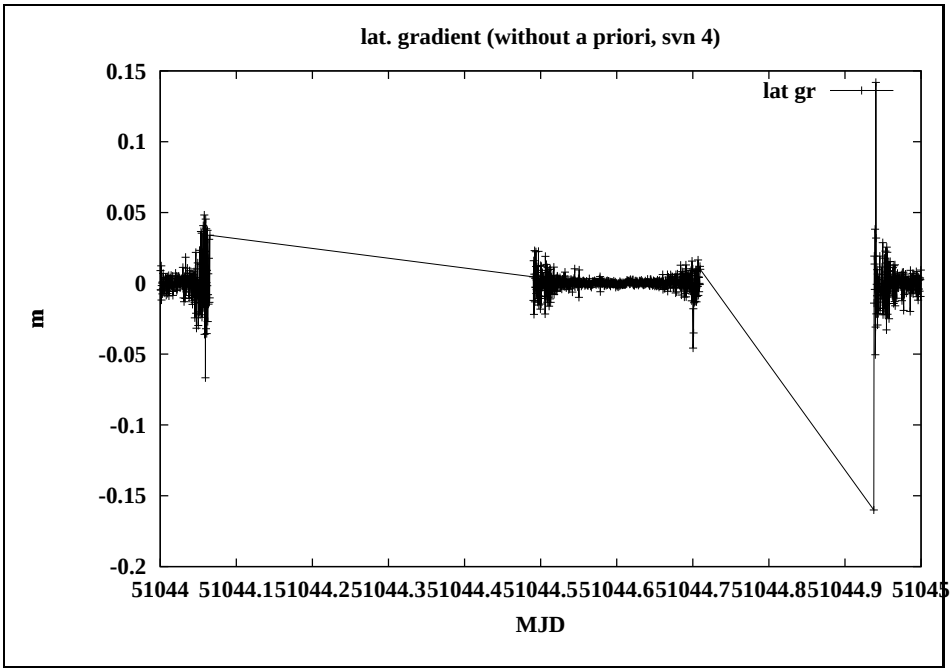

Figure 12: Estimated latitude gradient (SVN 4)

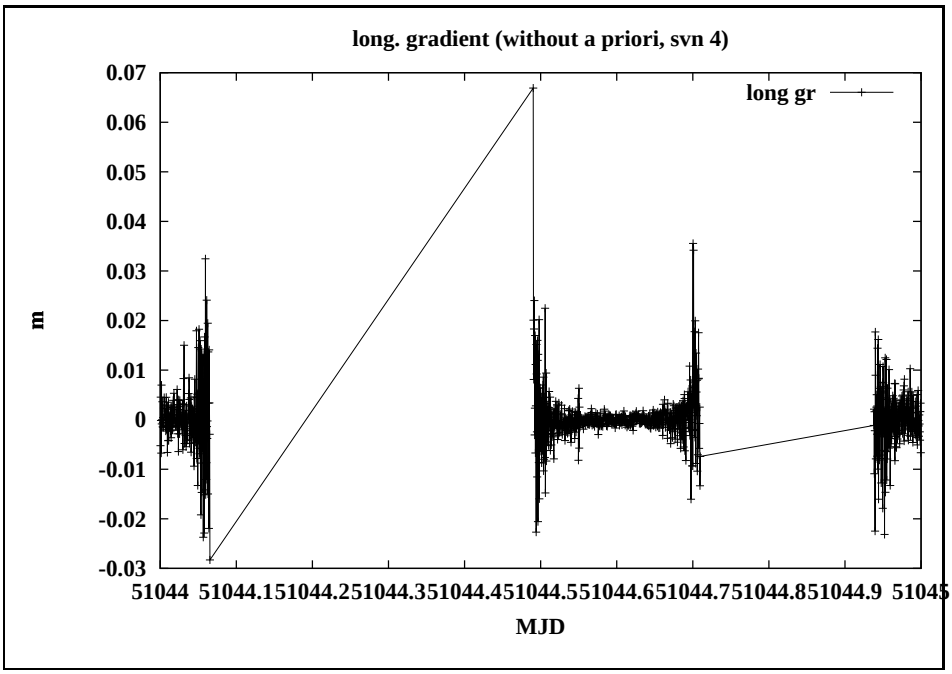

Figure 13: Estimated longitude Gradient (SVN 4)

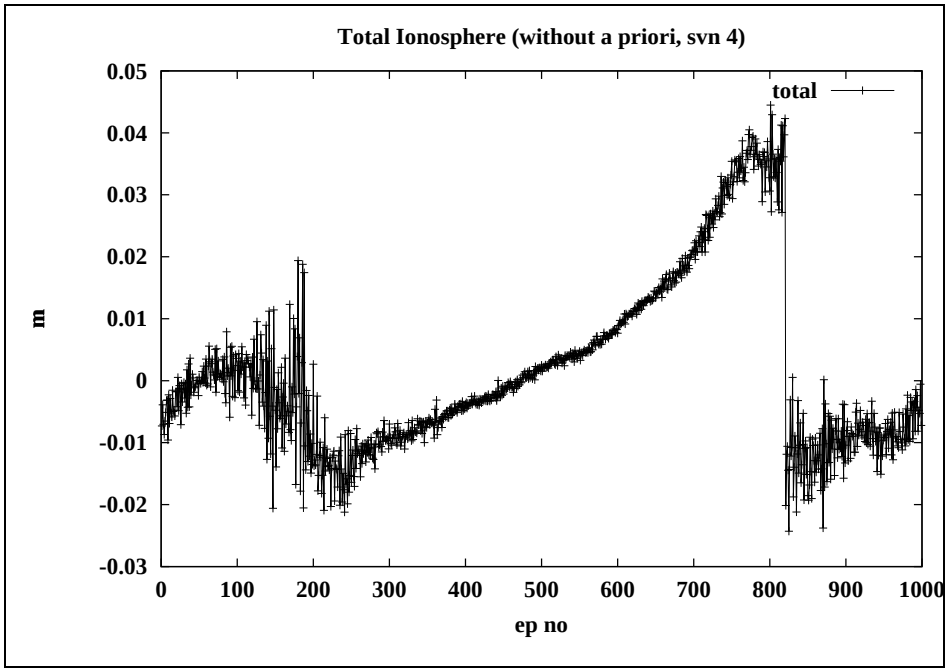

Figure 14: Total Ionosphere Difference relative to previous epoch, SVN 4, fct. of epoch no, no a priori model

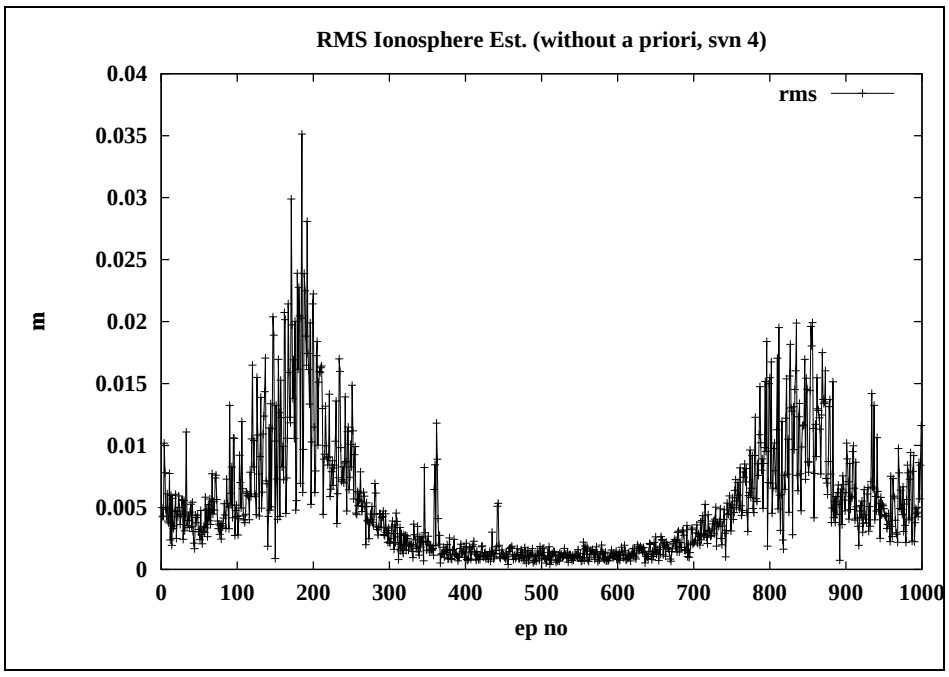

Figure 15: RMS of Ionosphere Difference Estimation, SVN 4, fct. of epoch no)

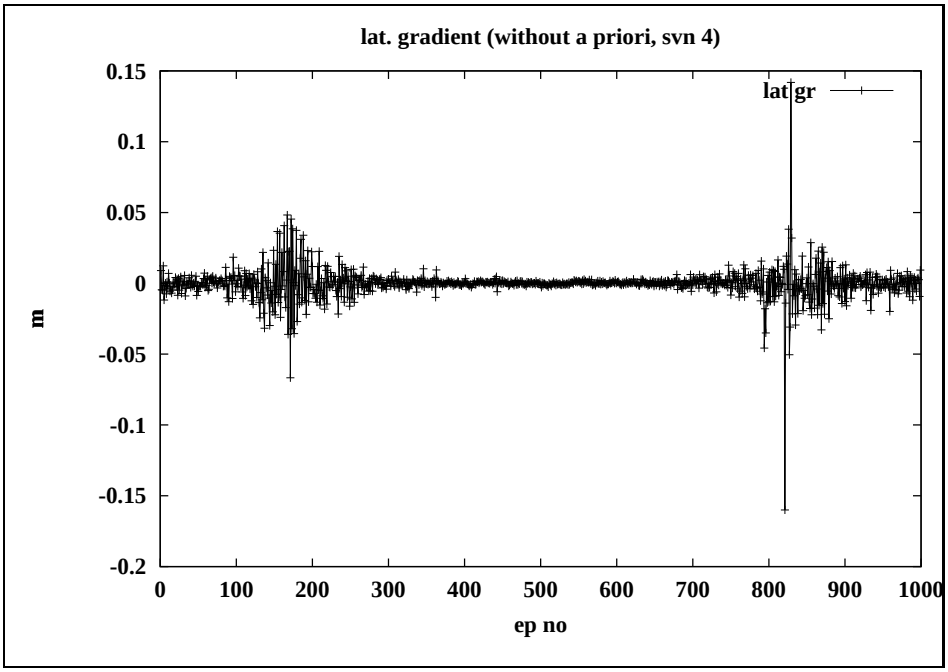

Figure 16: Estimated Latitude Gradient, SVN 4, fct. of epoch no

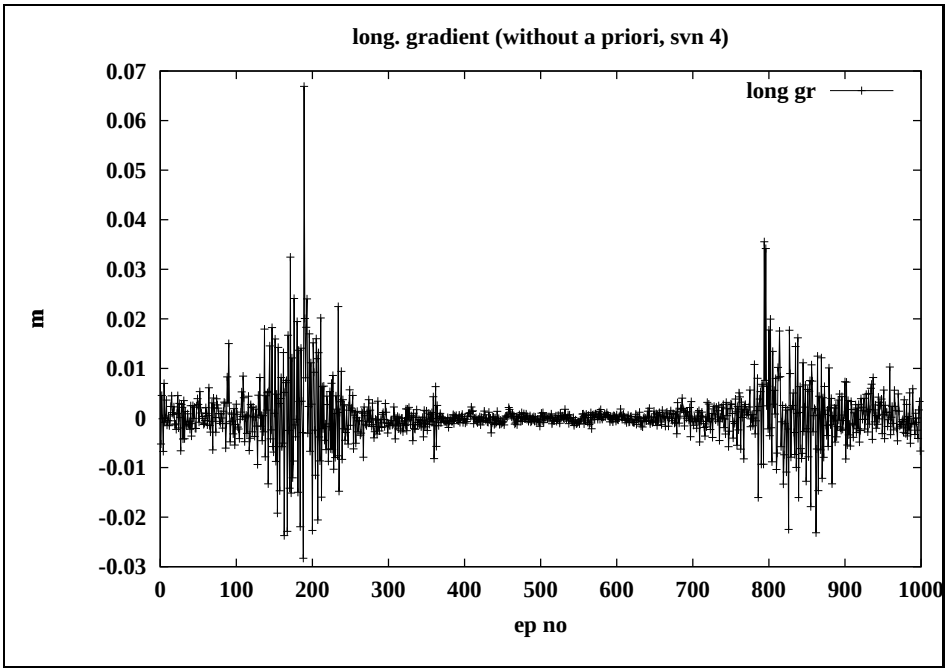

Figure 17: Estimated Longitude Gradient, SVN 4, fct. of epoch no

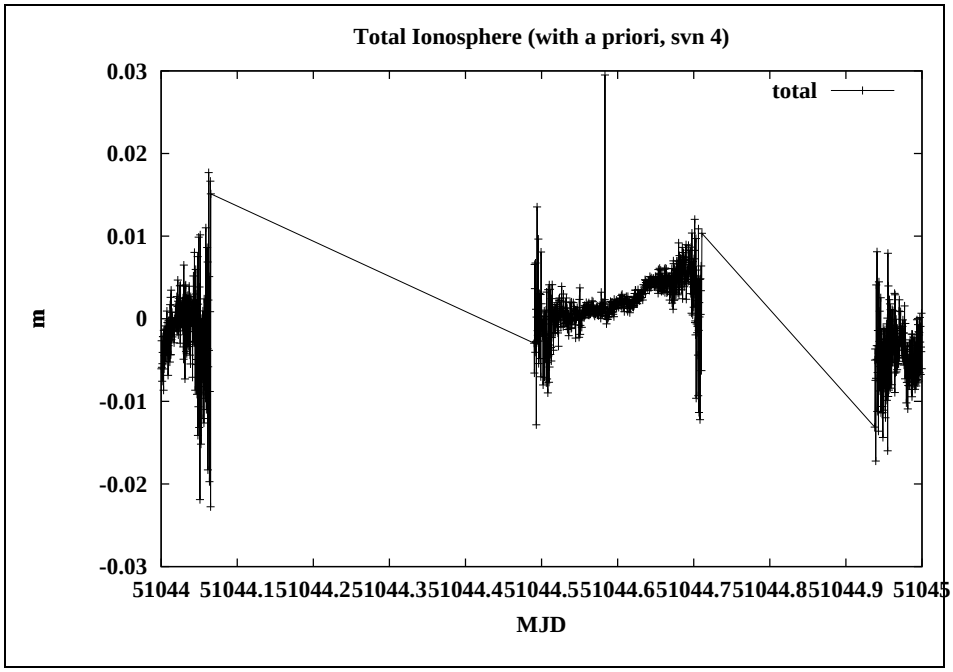

Figure 18: Total Ionosphere Difference relative to Previous Epoch, SVN 4, with a priori model

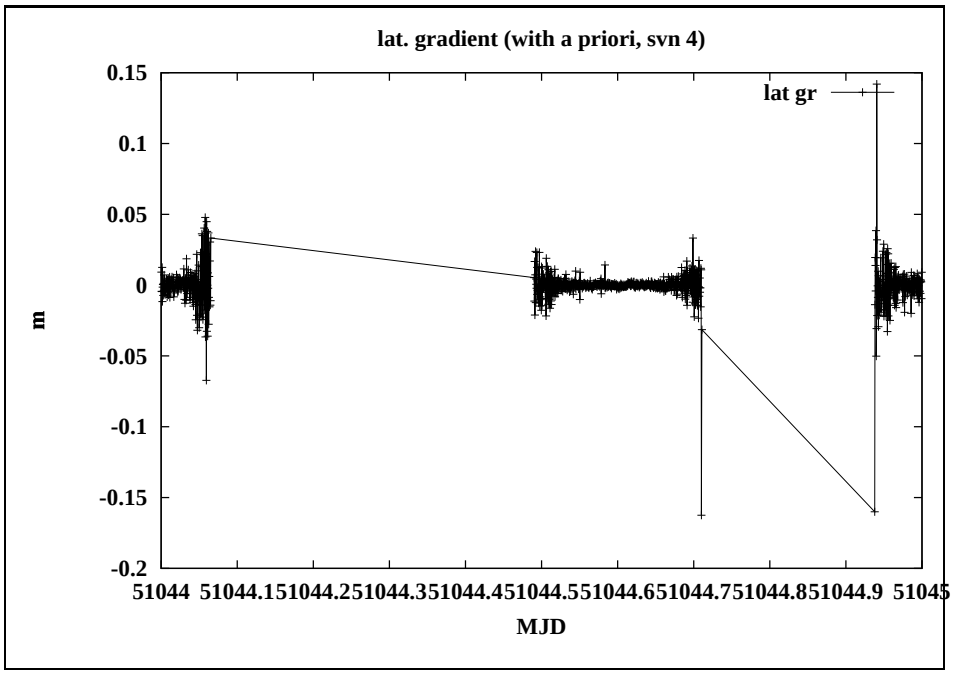

Figure 19: Estimated Latitude Gradient, SVN 4, with a priori model

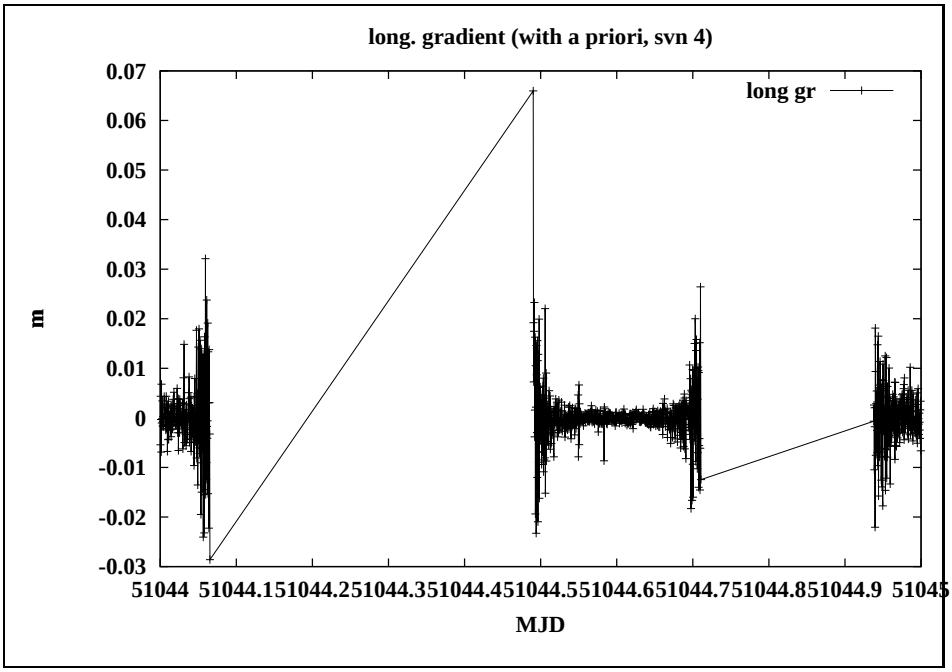

Figure 20: Estimated Longitude Gradient, SVN 4, with a priori model

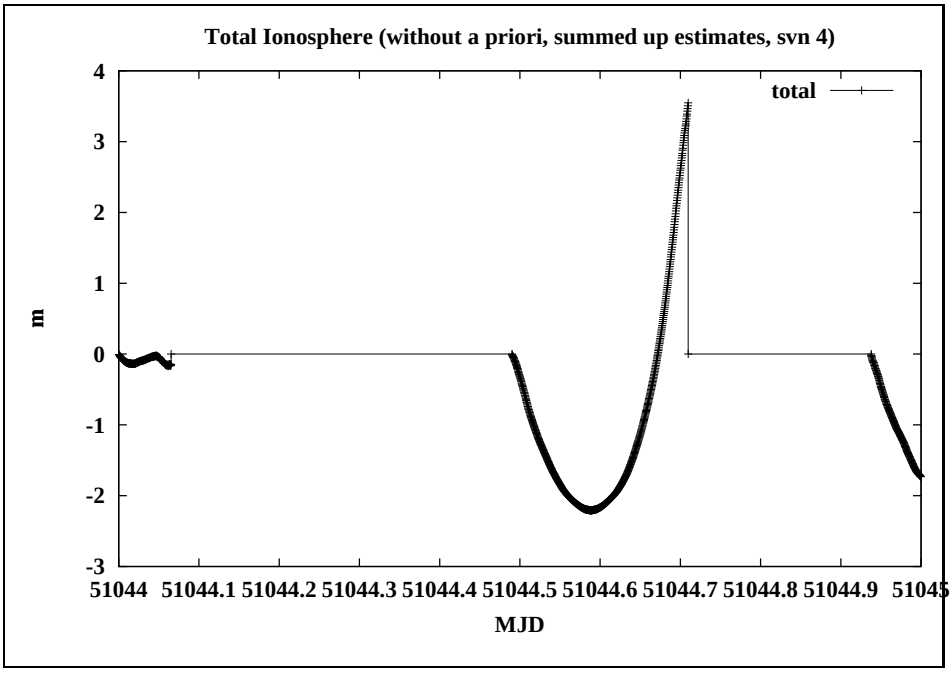

Figure 21: Total Ionosphere Difference relative to first epoch, SVN 4, without a priori model

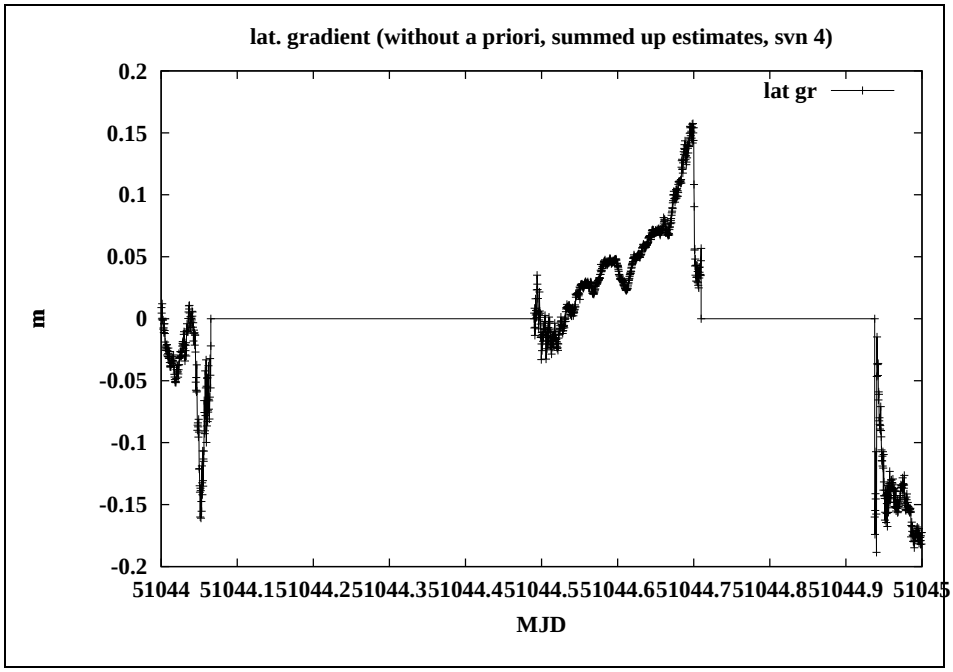

Figure 22: Estimated Latitude Gradient relative to first epoch, SVN 4, without a priori model

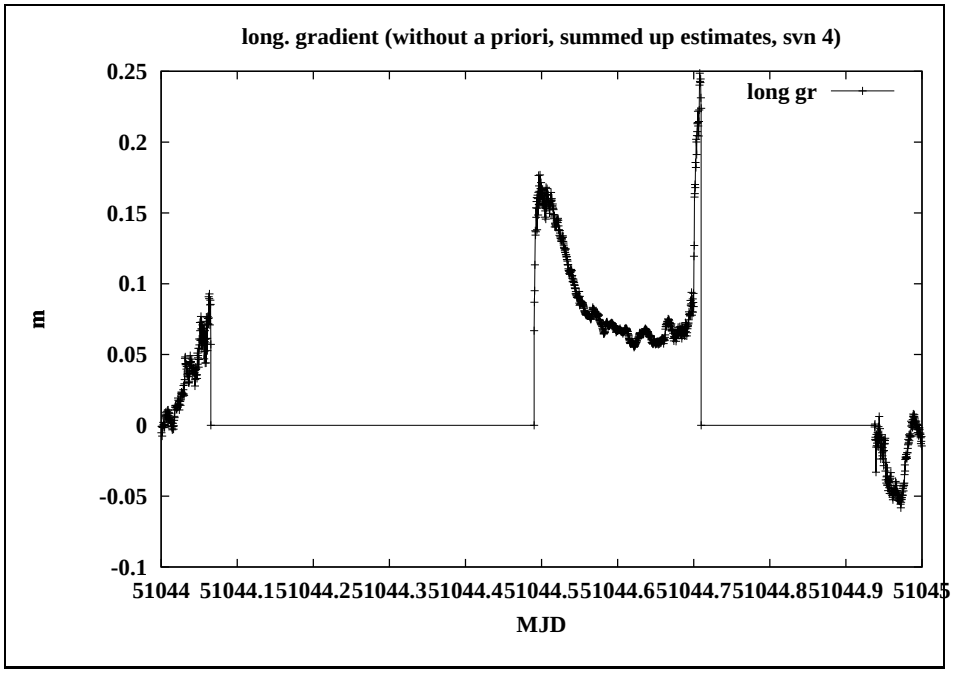

Figure 23: Estimated Longitude Gradient relative to first epoch, SVN 4, without a priori model

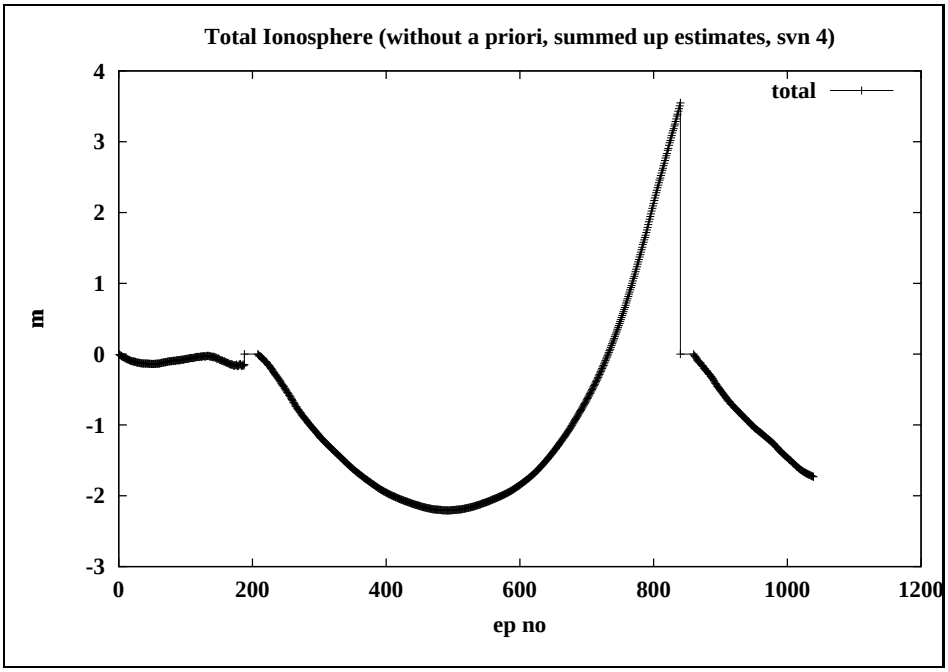

Figure 24: Total Ionosphere Difference relative to first epoch, SVN 4, fct. of epoch no, without a priori model

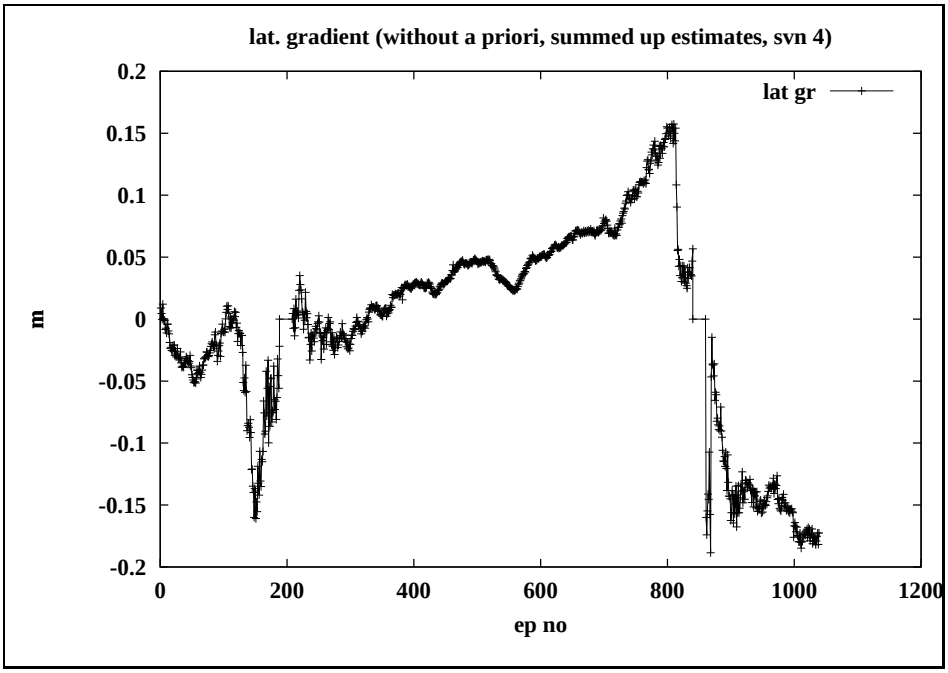

Figure 25: Estimated Latitude Gradient relative to first epoch, SVN 4, fct. of epoch no, without a priori model

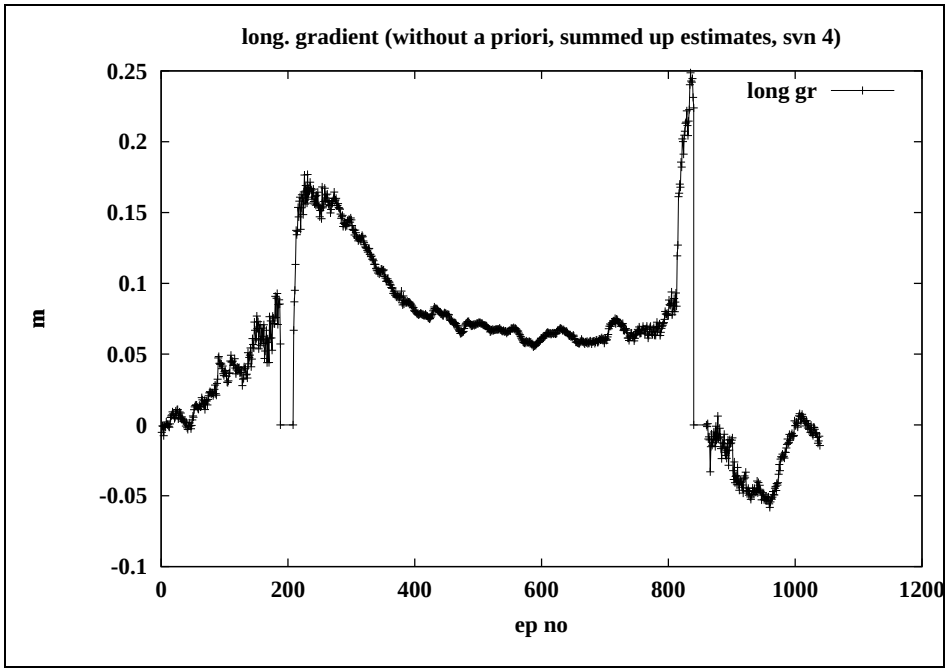

Figure 26: Estimated Longitude Gradient relative to first epoch, SVN 4, fct. of epoch no, without a priori model

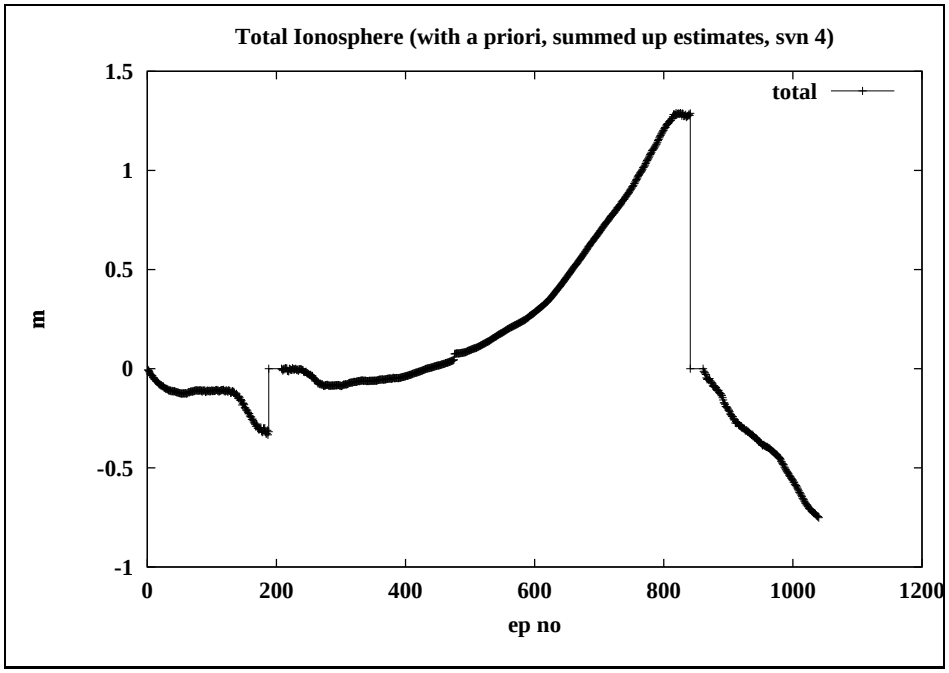

Figure 27: Total Ionosphere Difference relative to first epoch, SVN 4, fct. of epoch no, with a priori model

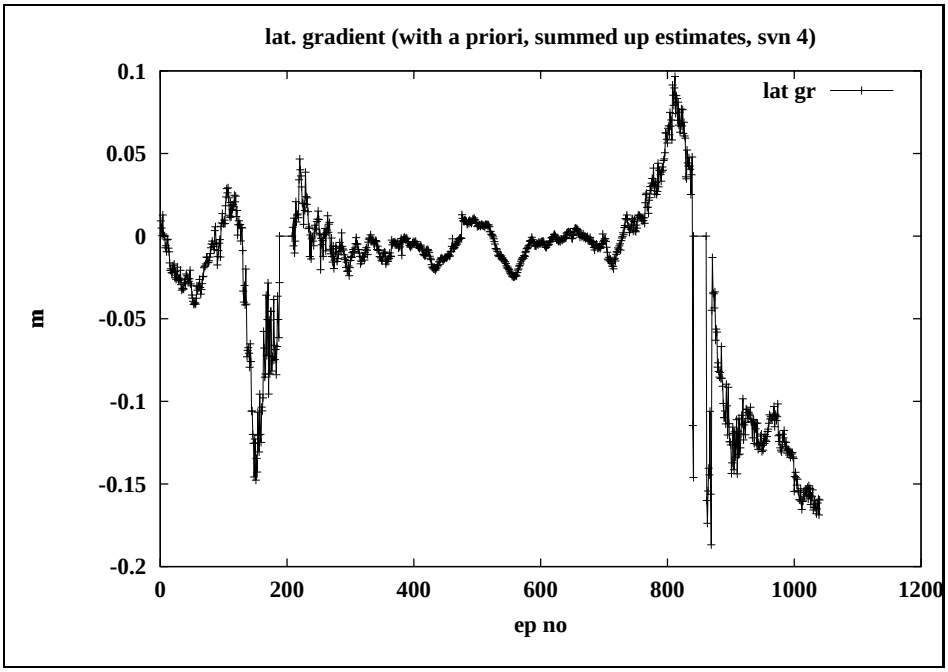

Figure 28: Estimated Latitude Gradient relative to first epoch, SVN 4, fct. of epoch no, with a priori model

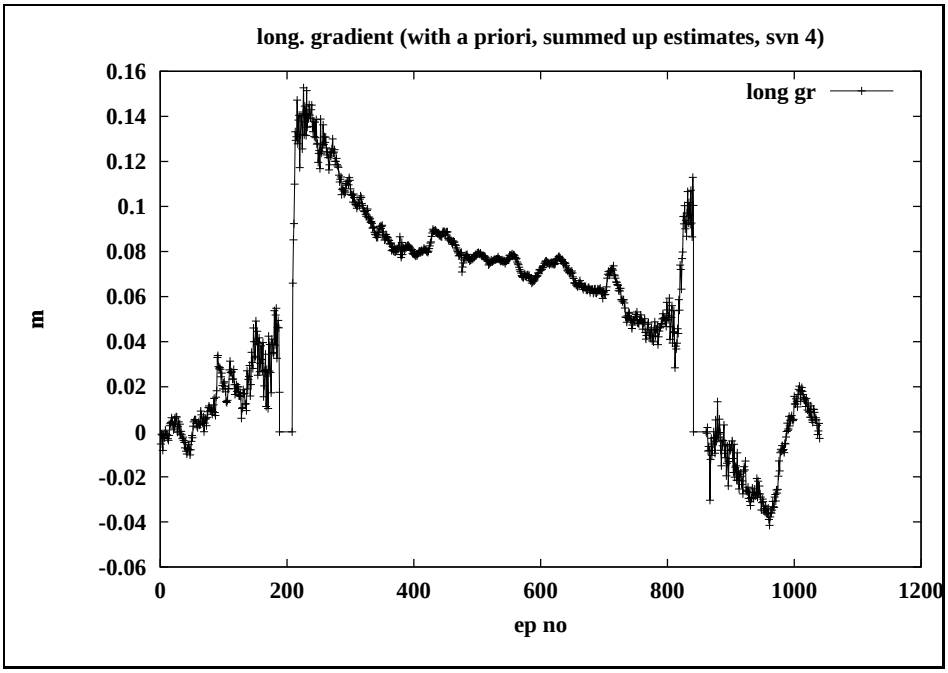

Figure 29: Estimated Longitude Gradient relative to first epoch, SVN 4, fct. of epoch no, without a priori model

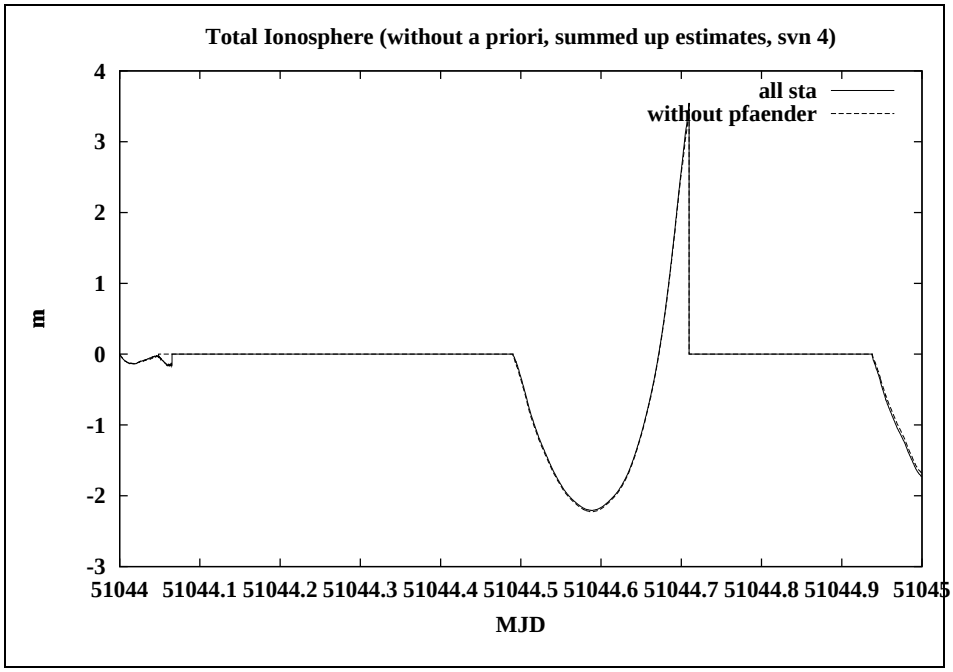

Figure 30: Total Ionosphere Difference relative to first epoch, SVN 4, no a priori model, with/without Pfänder)

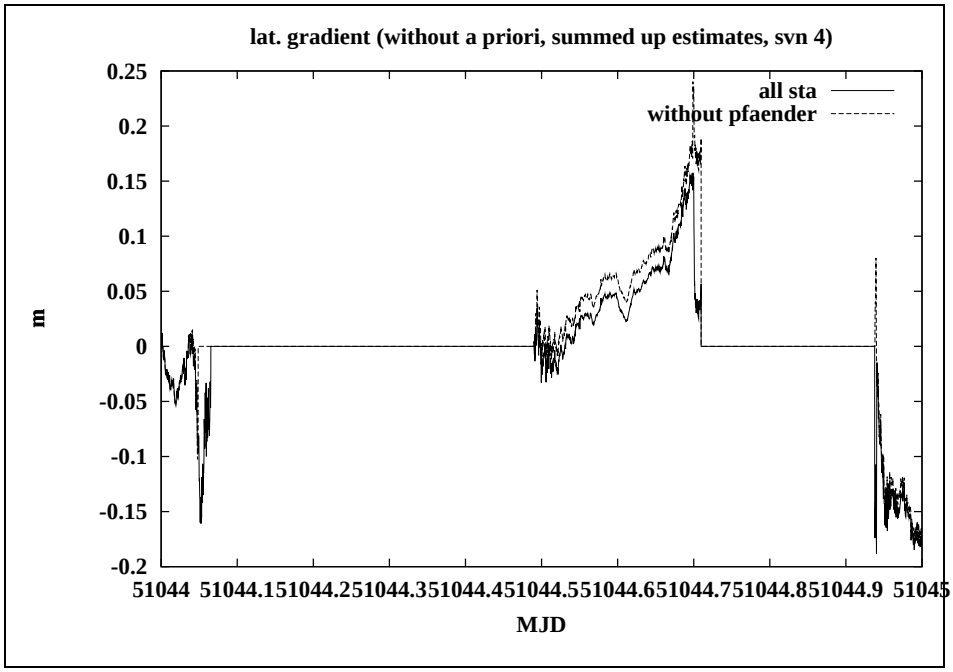

Figure 31: Estimated Latitude Gradient relative to first epoch, SVN 4, no a priori model, with/without Pfänder)

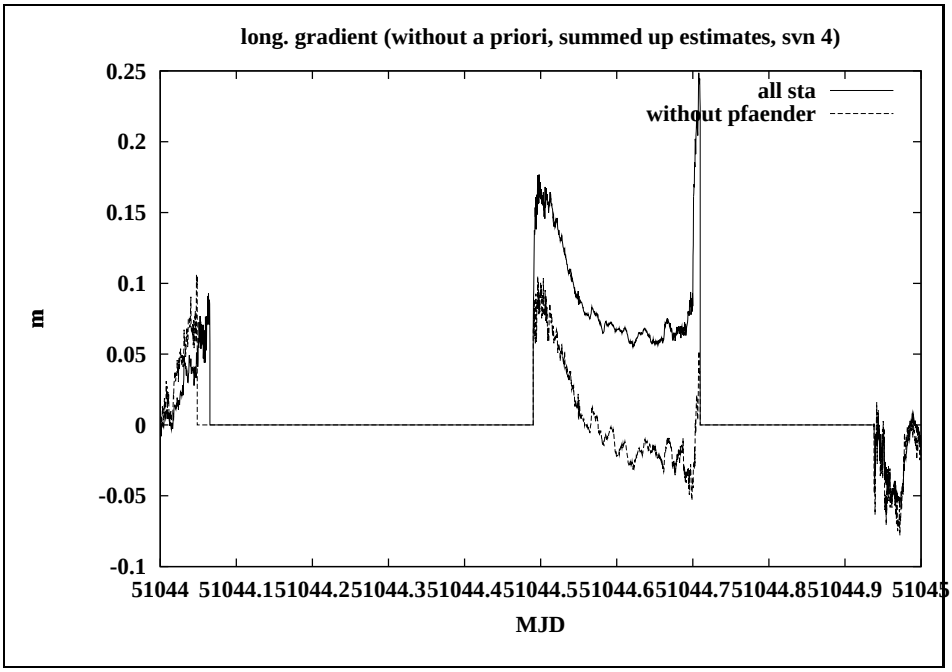

Figure 32: Estimated Longitude Gradient relative to first epoch, SVN 4, no a priori model, with/without Pfänder)

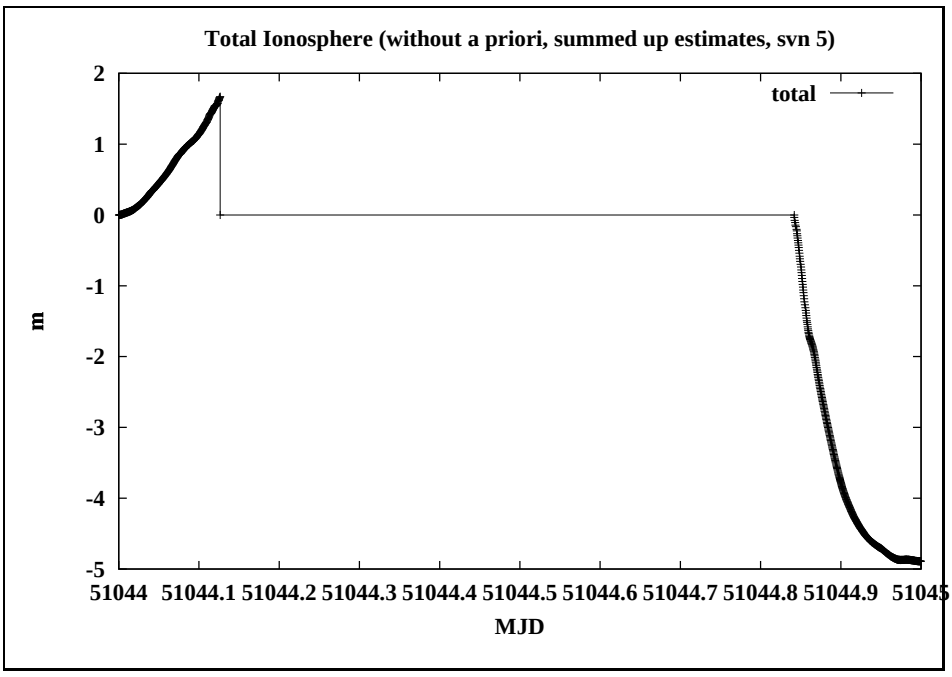

Figure 33: Total Ionosphere Difference relative to first epoch, SVN 5, no a priori model

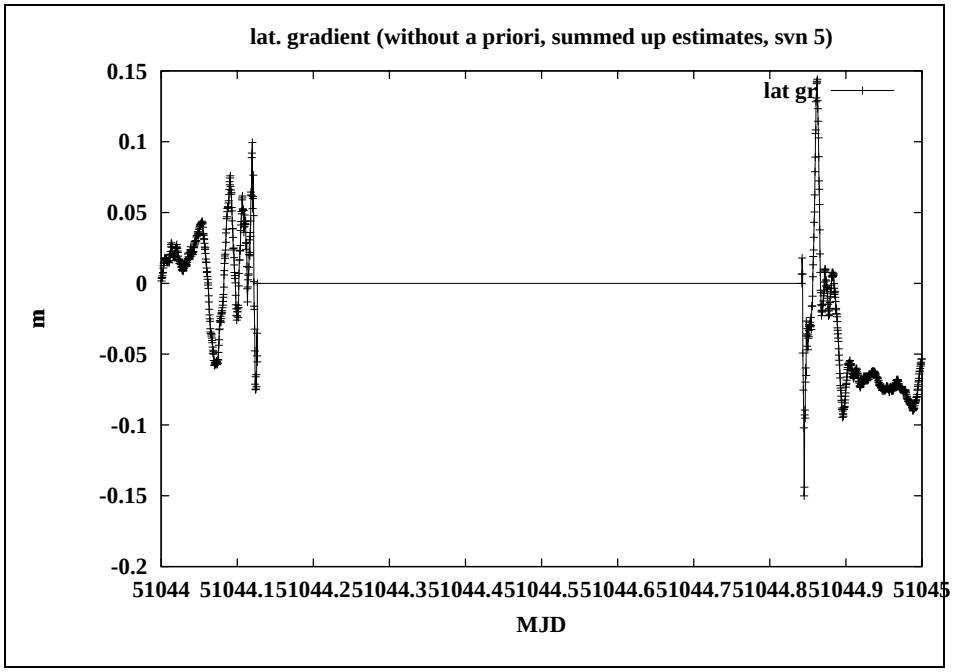

Figure 34: Estimated Latitude Gradient rel. to first epoch, SVN 5, no a priori model

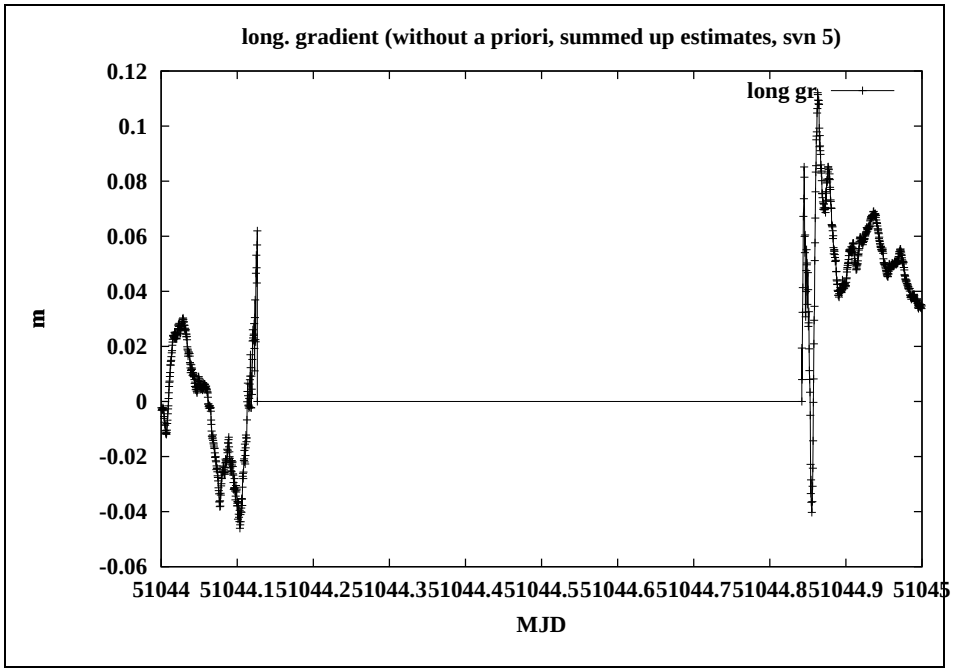

Figure 35: Estimated Longitude Gradient rel. to first epoch, SVN 5, no a priori model

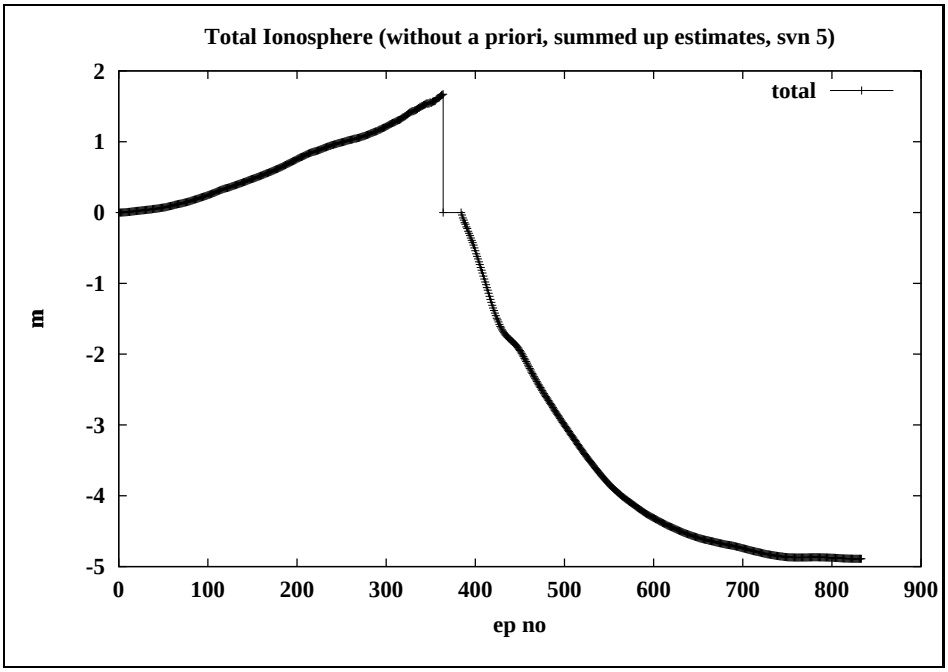

Figure 36: Total Ionosphere Difference relative to first epoch, SVN 5, no a priori model, fct. of epoch no

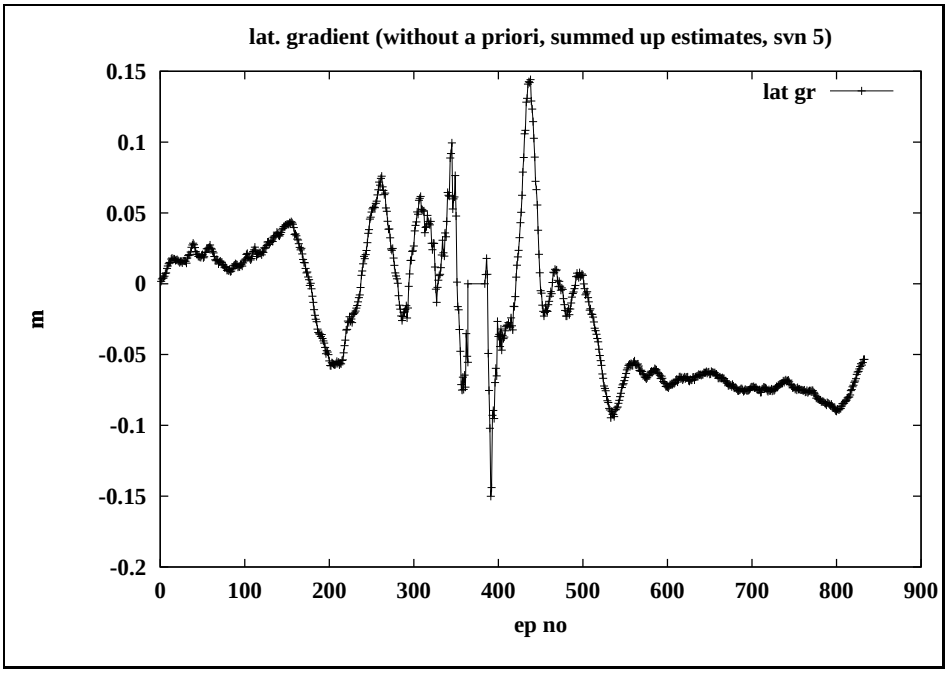

Figure 37: Estimated Latitude Gradient rel. to first epoch, SVN 5, no a priori model, fct. of epoch no

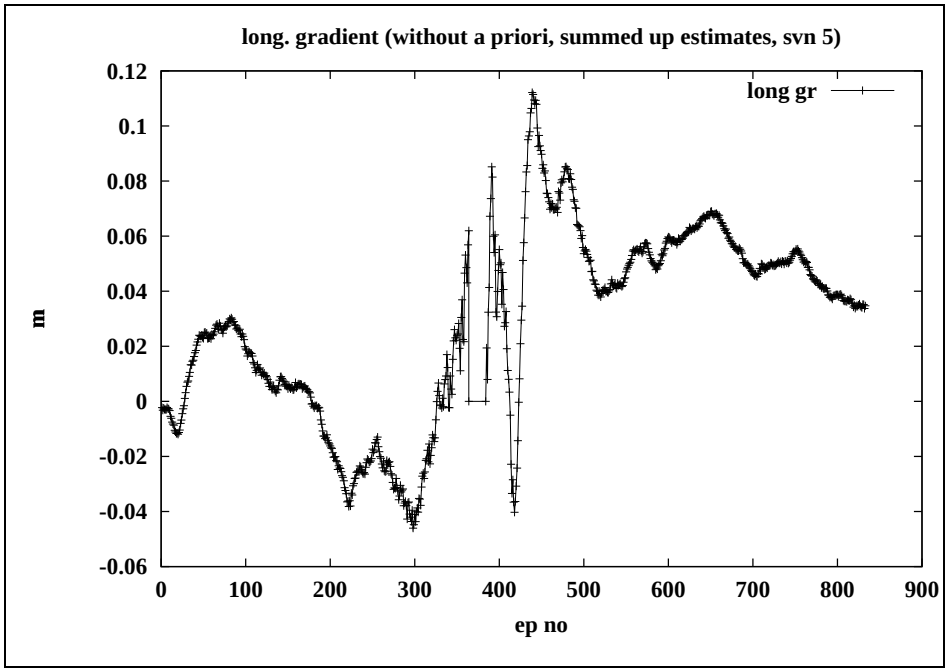

Figure 38: Estimated Longitude Gradient rel. to first epoch, SVN 5, no a priori model, fct. of epoch no

4.3 Summary of Experiences

Program **CLKEST** demonstrates in an impressive way the power of a centrally controlled network. As opposed to a pure baseline-oriented processing the following options are enabled:

- Quality control is possible in an unprecedented way. Table 6 shows that problems of individual receivers may be easily located. It seems quite clear that the Pfänder site has a significant problem.
- Problems like outliers, cycle slips, missing observations, *etc.* may be easily located. It should be possible to produce *clean zero difference files for phase and code for each station.* It may not be possible to repair a detected cycle slip (no attempts were made to repair the $L1$ and $L2$ carriers). It is easily possible, however, to flag the observations.
- Preprocessing is done using the $L3$ linear combinations of phase and code. This avoids the very noisy Melbourne-Wübbena linear combination.
- *It is possible* to extract systematic effects in the network. This is in particular true for the ionosphere, where epoch- and satellite-specific gradients promise to reduce the unmodeled part of the ionosphere.
- **CLKEST** is *not well suited* to model residual tropospheric refraction because only the first time derivative of the phase observable is analyzed. We refer to

the experiments using the Bernese troposphere estimates to model tropospheric refraction as a function of the network geometry.

- **CLKEST** might be generalized to generate data for a *virtual reference receiver* "free" from systematic effects (different receiver types, ionosphere gradients, troposphere gradients) by using the original observations of only one reference receiver, *e.g.*, the Zimmerwald receiver or the receiver closest to the user. One would artificially remove the geometry and atmosphere part of this receiver and add the geometry and atmosphere part corresponding to the user area. This would remove the detected systematic contributions. The result consists of data of a *virtual receiver* with the characteristics of the reference receiver (containing in particular all the receiver related biases of the selected reference), but freed from undesired systematic effects. We view this as a *trivial version* of a virtual reference receiver.

- The unpleasant aspect of this procedure has to be seen in the fact that one transmits all receiver-specific problems, (*e.g.*), unrepaired cycle slips, to the user of the data. (Problems may of course be flagged; it is, however, an open question whether the user software will be able to accept these flags).

- The theoretical discussion in chapter 3 seems to indicate that it is possible to combine the data of all receivers to reduce the noise. The procedure is rather straight forward for code observations. Even the production of phase-smoothed code does not pose a problem.

In summary we strongly recommend to develop a monitoring program along the lines of **CLKEST** in order to make full use of the AGNES. The limited data set we analyzed in our study clearly indicates that the network is capable of generating excellent information for geodetic and atmospheric use.

Programs of this type will have to be developed for all upcoming permanent GPS networks.

5. GPS Campaigns Analyzed and Standard Static Analysis

5.1 The Network and the Data Analyzed

Two data sets were made available to us by the Swiss Federal Office of Topography, one stemming from the year 1998, one from 1999. The first covered one entire week (seven days), the second "only" two days.

Whereas only official AGNES-sites were included in the first data set, three sites (DACH, THUN, WICH) from campaigns or from other experiments were available as well in the second data set.

All AGNES sites were tracking all satellites in view on a permanent basis. The three additional sites in the 1999 campaign were taking data (in essence) from noon to noon of two subsequent days.

The two data sets may be characterized as follows:

- **1998 Data Set:** doy 228-234, 16-22 August, 30 sec data from 7 stations (EPFL, ETHZ, FHBB, JUJO, PFAN, SIER, ZIMM)
- **1999 Data Set:** doy 98-99, 8-9 April, 9 stations (DACH, DAVO, EPFL, ETHZ, FHBB, JUJO, THUN, WICH, ZIMM), 5 sec data used (some stations even had 1 sec-data). The non-Agnes sites DACH, THUN, WICH are observed only from noon-noon.

5.2 Ionosphere Models

Deterministic ionosphere models (using a spherical harmonics representation up to degree 12 and order 8) are being established for each day in the years 1995-"∞" by the CODE Analysis Center of the IGS using the IGS network of about 100 stations. These products were used for our study. The ionosphere models are well suited to remove the general trend of ionospheric refraction.

Figure 39 is based on the CODE ionosphere models. It shows the development of the daily mean electron content in TECUs (total electron content units) since January 1, 1995. We see in essence a protocol of the most recent minimum of solar activity, when the mean TEC was of the order of about 10 TECUs only. We have already registered a clear increase in 1998, the trend is continued in 1999. The next maximum is expected in 2001. The dots in Figure 39 are the actual measurements, the lines represent a fit of the data. The smooth line contains only the eleven year, the annual, and the semiannual components. The "busy" line contains in addition the 27-days terms attributed to solar rotation. The amplitudes of the 27-days signals are increasing very much. They are caused by the (dis)appearing of sunspot groups from the field of view of an observer on Earth due to solar rotation.

Figure 39 shows that a much more pronounced ionosphere has to be expected for the years to come. It should also be pointed out that the conditions may vary strongly from day to day in the next few years.

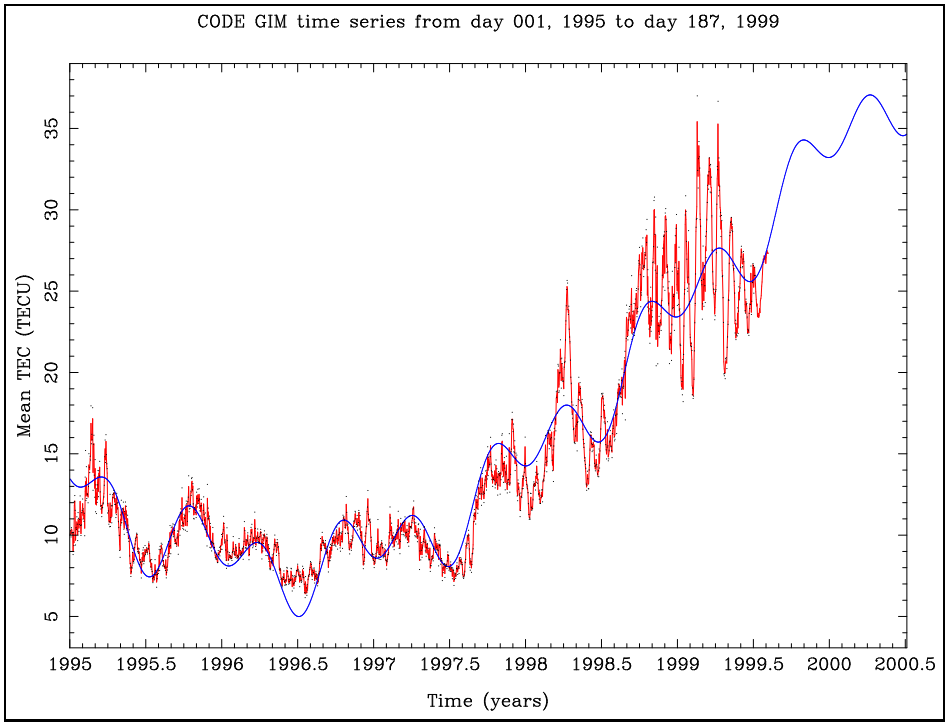

Figure 39: Development of Mean TEC from 1995 till Mid 1999

Figure 40 shows the TEC above the Zimmerwald site as a function of time for the seven days 16-22 August in 1998. Figure 40 was extracted from the global ionosphere model which is routinely generated by the CODE Analysis Center of the IGS. We recognize the daily pattern (maxima around noon, minima in the early morning hours). In view of the variaitons seen in Figure 39 it is not surprising that the height of the daily maximum TEC values differ considerably from day to day. (Small discontinuities at the day boundaries are caused by the fact that no continuity conditions were imposed at the day boundaries).

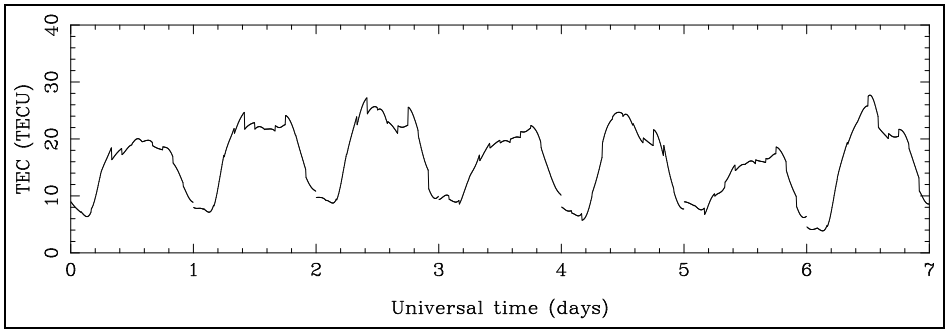

Figure 40: TEC over Zimmerwald 16-22 August 1998

The TEC content over Zimmerwald is representative for the entire AGNES-region.

We see a daily variation of the TEC between about five and twenty-five TECU.

According to [*Beutler et al.*, 1990] the principal effect of an ionospheric layer of uniform density will result in a reduction δl of the baseline length l:

$$\frac{\delta l}{l} = -0.7 \cdot 10^{-17} \cdot E = -0.07 \cdot TEC \tag{5.1}$$

when processing $L1$-data with a minimum elevation angle of 20^o without applying any ionospheric corrections. E is the number of electrons contained in one m^2 of the single ionospheric layer, TEC is the total electron content in TECUs (total electron content units, 1 TECU=10^{16} Electrons/m^2).

In our 1998 data set we thus expect at maximum scale effects of the order of 1.5-2.0 ppm during day time, when processing L1 data with a cut off elevation of 20^o without an ionosphere model. This value was confirmed in the analysis. We will indicate below, when corrections from an ionospheric model were applied.

5.3 Ambiguity Resolution in Reference Network

It was pointed out several times that a correct network solution using the data of the entire reference (AGNES) network has to be performed in near real time when trying to make full use of the network. These network solutions may use long data spans (one hour to several days). Such solutions may be considered as *standard static GPS analyses*.

It is absolutely essential that the double-difference ambiguities are resolved in these solutions. There are different techniques, how to resolve the ambiguities (see, *e.g.*, [*Rothacher and Mervart*, 1996]).

One technique, which would be particularly well suited for our purpose, is the so-called *Melbourne-Wübbena technique*, where the wide-lane ambiguities are resolved using a special linear combination of $L1$ and $L2$ phase and code observations (explained, *e.g.*, in [*Beutler et al.*, 1990] or in [*Rothacher and Mervart*, 1996]) which would eliminate clocks, orbits, troposphere, ionosphere, but not the observation noise and multipath.

It must be viewed as a serious disadvantage of the receivers in the network that this "fool-proof" method could not be used due to the relatively high noise of the code observations. It should also be mentioned that apart from the noise the code was of excellent quality.

Consequently we were obliged to apply ambiguity resolution techniques *without* using code observations. It was decided to use the technique, where the wide-lane ambiguity is resolved first (using the corresponding linear combination of the observations), followed by the resolution of the $L1$ ambiguities using the ionosphere-free linear combination (narrow lane ambiguity resolution). Other techniques, like the *QIF-technique* (see [*Rothacher and Mervart*, 1996]) might have been used as well. We believe, however, that the chosen method gives more insight into the dependence on the error sources.

Let us consider the two steps of ambiguity resolution separately.

5.3.1 Wide Lane Ambiguity Resolution

Figure 41 gives an impression of the wide lane ambiguity resolution. We see a histogram of the fractional parts of the wide-lane ambiguities in the moment they were fixed to integer numbers. The best strategy (which takes over the troposphere estimates from an ambiguities-free network solution and applies the corrections from our global ionosphere model) obviously is represented by the top sub-picture, the second strategy (using an a priori troposphere model) is only marginally worse, the third strategy (not taking into account the ionosphere model), represented by the bottom sub-picture, is significantly worse.

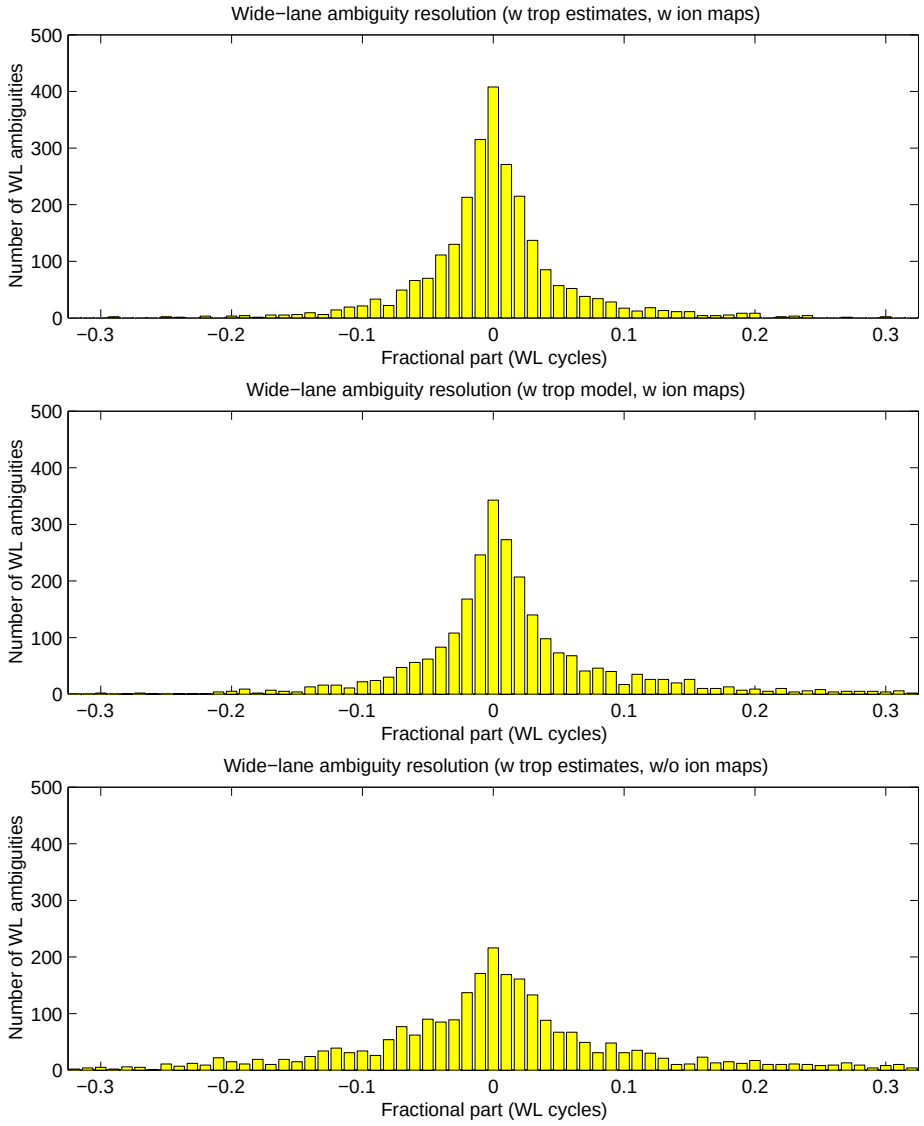

Figure 41: Wide Lane Ambiguity Resolution

The standard deviations for the distribution of the fractional parts of the wide lane ambiguities are $\sigma = 0.056$ cycles, in the first case, $\sigma = 0.075$ cycles in the second case, and $\sigma = 0.101$ cycles in the third case, where the ionosphere remains unmodeled.

Precise orbits were used in all cases, but this was not a crucial issue. The differences of success were smaller than the differences between the top and middle sub-pictures in Figure 41.

In the first case 98.2%, in the second 97.4%, in the third 95.2% of the wide lane ambiguities could be resolved using a cut-off elevation angle of 10^o. The ambiguities that could not be resolved were always associated with low elevations.

In summary it should be stated that wide-lane ambiguity resolution does not pose a serious problem even if the orbit information is not of good quality. Double difference wide-lane ambiguity resolution is in practice and in essence limited by our ability to model the ionosphere — let us say on the 0.2 wide-lane wavelength level ($\approx$ 86 cm/5 $\approx$ 20 cm). With the exception of ionosphere storms this should not pose a serious problem.

Our method used is a post-processing scheme. May it be transferred to real time? One might argue that this is not the case, because in practice we will always have the problem of rising satellites over an area, when we will *have to* make the attempt to resolve ambiguities using short time spans. Whereas this is true, one has to point out that the problem is really limited to exactly one satellite — all other ambiguities (in addition to all receiver positions, orbits, *e.t.c.*) are known with sufficient accuracy to allow for a rapid resolution of the wide-lane ambiguity. The practical consequences, when ambiguity resolution is not possible instantaneously, are limited, as well: it will just not be possible to provide good differential atmosphere corrections to the user shortly after a satellite rise over the area.

5.3.2 Narrow Lane Ambiguity Resolution

After having successfully resolved the wide-lane ambiguities using the wide-lane linear combination, we may now resolve the L1 ambiguities using the ionosphere-free linear combination of $L1$ and $L2$.

In this step we have the advantage that the ionosphere is completely eliminated and cannot bias our solutions. The effective wavelength, however, is now about $\lambda_{narrow} \approx$ 10 cm, which means that other systematic errors become relevant. We have to consider *orbit errors* and *unmodeled tropospheric effects*, in particular.

Figure 42 shows a histogram of the fractional parts of the narrow lane ambiguities in the moment of fixing them to integers. The top sub-picture shows (in our opinion) the best possible solution: Precise orbits are taken over from the CODE/IGS processing *and* the tropospheric parameters, as established by an ambiguities-free solution using the entire network, are introduced as known. In the second sub-picture tropospheric refraction is not estimated, but computed using a standard atmosphere model (Saastamoinen in connection with standard atmosphere). In the third case (bottom sub-picture in Figure 42) broadcast instead of precise CODE orbits were used.

The standard deviations for fractional part of the narrow lane ambiguities are $\sigma =$

0.092 cycles in the first case (top sub-picture), $\sigma = 0.112$ cycles in the second, $\sigma = 0.133$ cycles in the third case, where broadcast orbits are used. In the first case 95.2%, in the second 92.4%, in the third 91.0% of the narrow lane ambiguities could be resolved using a cut-off elevation angle of 10^o.

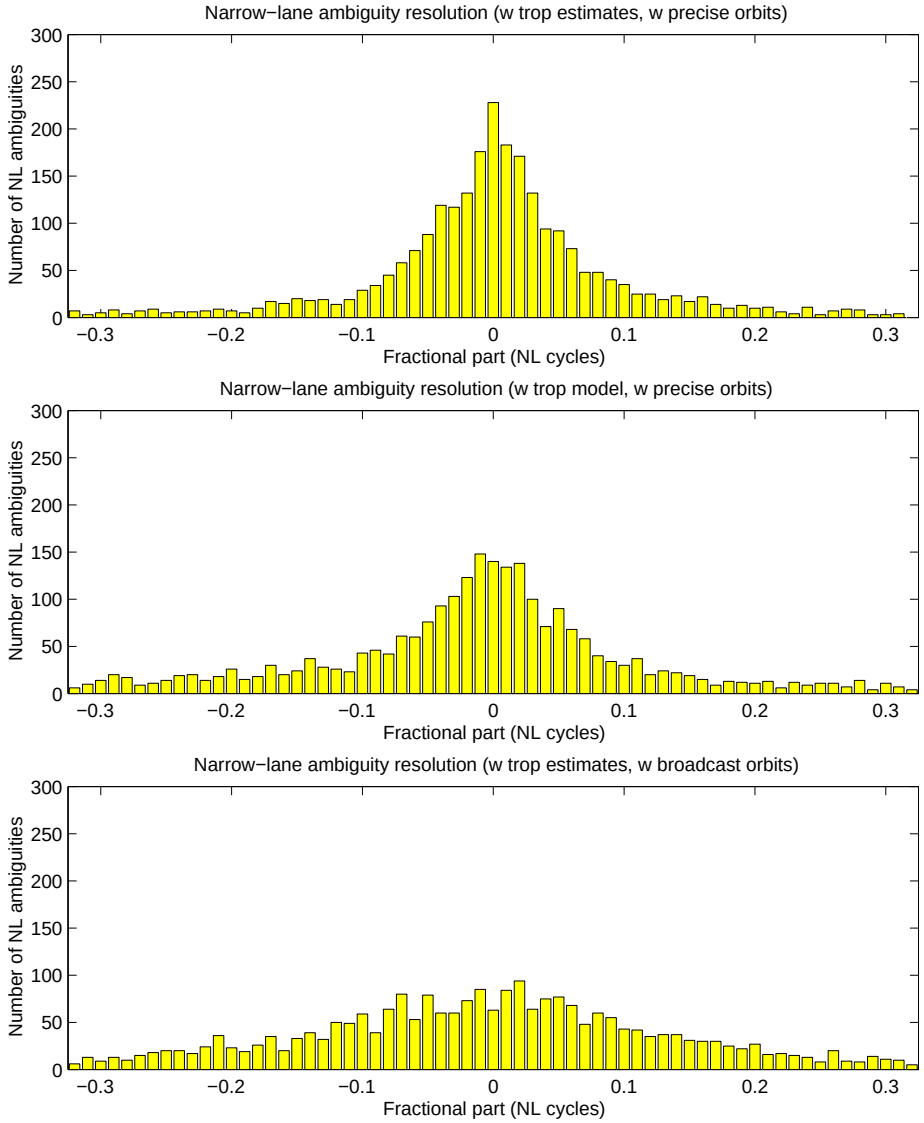

Figure 42: Narrow Lane Ambiguity Resolution

The message is clear: Both, orbits of excellent quality, and a good troposphere parameterization are *mandatory* for a network of the size of AGNES.

It is in particular *crystal-clear* that much better than broadcast orbits are required. [*Wanninger*, 1999] and other authors propose to remove (reduce) the orbit effects by a linear model over the area. We know that this can be done in a much better way

- *either* by

(a) using predicted orbits based on recent data (data with a latency of may be 2-3 hours) stemming from an *IGS* Analysis Center

- *or* by

  (b) invoking a constrained orbit improvement process (maybe solving for along-track errors, argument of latitude u_0 in the Bernese software) using data of the AGNES sites (almost) up to the present epoch.

Both approaches are feasible in practice. We strongly recommend the first one, because the orbits may be established in a safer way when data from a world-wide (or at least a continent-wide) network are available.

Let us get one aspect straight: Orbits, as established by CODE or other IGS Analysis Centers, based on a world-wide network may be extrapolated for – let us say 6 hours in such a way that the quality is sufficient to provide results of the type of the top picture in Figure 42.

Even procedure **(b)** mentioned above would be much better than the epoch-wise procedure proposed by [*Wanninger*, 1999] and others: It makes full use of all observations of a satellite available in the time interval of, perhaps, one day.

What about tropospheric refraction? Figure 42 gives a clear answer, as well: For a network of the AGNES-type it is not sufficient to compute the delay due to tropospheric refraction by adopting a standard atmosphere. The aspect is somewhat less dramatic than the orbit aspect, but the impact is clearly visible (compare sub-pictures 2 *resp.* 3 with the top sub-picture in Figure 42), as well.

The *standard corrective action* consists of avoiding the use of a priori models. Two alternatives should be considered:

- The standard atmosphere might be replaced by a model derived from recent meteorological data. One might, *e.g.*, use pressure, temperature, and humidity values (as a function of the receiver coordinates and the time) of a meteorological network, in the case of the AGNES, of the A-Netz.

- Troposphere estimates stemming from a $L3$ network solution (which is produced regularly) may be used.

Probably a combination of both methods would be an optimum. A comparison of the first two sub-pictures in Figure 42 indicates the impact of the second method. Again: we do not see the need to go for an epoch-dependent modeling.

5.4 The "Ground Truth"

After having preprocessed all data sets and after having resolved (almost) all ambiguities (as described above) a combined solution, based on the ionosphere-free linear combination $L3$ and using the data of all stations and all days (separately for the two years), was performed.

The following general options were used: A cut-off angle of 10^o was set and elevation dependent weighting was invoked (weight $\sim \cos^2 z$, z =zenith distance). An $L3$-solution with correct correlation modeling was produced, one troposphere parameter

per hour and site was estimated (except for Zimmerwald, for which the troposphere estimates were taken over from the European solution from the CODE Analysis Center of EUREF).

Two solutions, one without and one with (daily) troposphere gradients were produced. Tables 7 and 8 give an impression of the daily coordinate repeatabilities for the North-, East- and Up- coordinates (relative to the above described ground truth).

STATION	#FIL	C	RMS	1	2	3	4	5	6	7
EPFL	7	N	1.0	1.2	0.1	-0.2	-0.7	1.3	0.0	-1.7
		E	1.2	1.8	-1.7	-0.1	-1.3	0.1	0.0	1.2
		U	3.3	-2.1	-4.2	-1.5	2.0	-1.8	2.1	5.5
ETHZ	7	N	1.9	-2.6	-2.0	-0.2	2.4	-0.4	0.5	2.3
		E	0.8	1.3	-0.1	-0.1	0.1	0.6	-1.1	-0.7
		U	3.5	1.4	0.6	5.3	-1.7	1.2	-0.5	-6.3
FHBB	7	N	1.5	1.1	0.5	1.0	-0.6	-1.2	-2.5	1.8
		E	1.2	-1.5	-0.4	-0.9	1.0	-0.6	1.9	0.5
		U	2.4	-0.1	-1.3	5.1	-1.6	-0.7	-2.0	0.6
JUJO	7	N	0.8	0.0	-0.7	1.3	0.4	0.2	-0.3	-1.0
		E	1.1	-0.6	0.9	0.8	0.8	0.6	-0.4	-2.1
		U	4.3	-2.4	-0.8	-3.6	-1.0	-2.0	0.5	9.3
PFAN	6	N	2.3		-3.5	-0.3	-0.4	-0.9	2.3	2.8
		E	1.9		1.4	0.4	-3.1	0.9	1.8	-1.4
		U	7.4		-12.2	-5.4	4.0	1.4	6.9	5.2
SIER	7	N	0.8	-0.8	0.4	0.1	-1.0	-0.5	0.9	0.9
		E	0.6	-0.3	0.1	0.0	0.3	0.7	0.3	-1.1
		U	3.6	1.4	3.3	0.3	1.5	2.9	-2.4	-7.1
ZIMM	7	N	1.6	1.1	1.7	-2.0	-0.4	0.6	1.3	-2.3
		E	1.3	-0.7	1.1	0.3	-0.9	-1.4	-0.7	2.3
		U	3.0	1.9	2.5	-5.7	0.8	0.5	2.2	-2.1

Table 7: Daily Coordinate Repeatability without Troposphere Gradients

STATION	#FIL	C	RMS	1	2	3	4	5	6	7
EPFL	7	N	1.4	1.5	1.5	-0.6	-0.7	0.8	-0.3	-2.3
		E	0.9	1.4	-1.3	-0.4	-0.8	0.2	0.0	0.9
		U	3.9	-2.8	-5.3	-1.1	1.8	-1.7	2.6	6.6
ETHZ	7	N	0.9	-1.1	-1.2	1.1	0.9	0.2	-0.3	0.5
		E	0.6	-0.6	1.1	-0.5	-0.1	-0.1	-0.3	0.6
		U	3.6	1.3	0.9	5.1	-1.2	1.1	-0.3	-6.8
FHBB	7	N	0.5	-0.9	0.1	0.5	-0.2	0.2	0.3	0.1
		E	0.7	-1.3	-0.1	0.2	0.1	-0.2	1.0	0.2

		U	2.5	0.0	0.3	4.3	-1.9	-1.8	-2.8	1.9
JUJO	7	N	1.1	1.3	-0.6	-0.1	1.4	0.0	-0.1	-1.9
		E	1.0	-0.4	0.1	1.1	0.7	0.2	0.2	-1.9
		U	3.5	-1.5	-0.9	-3.0	-1.1	-1.1	-0.1	7.7
PFAN	6	N	2.2		-2.9	0.3	-1.8	-0.3	1.6	3.1
		E	1.6		-0.4	0.8	-2.5	-0.1	2.2	0.1
		U	7.4		-11.8	-5.0	4.1	0.7	9.0	3.1
SIER	7	N	1.8	-0.5	-0.2	-0.4	-1.2	-1.8	0.4	3.7
		E	0.9	0.9	0.4	-0.5	0.3	0.7	0.0	-1.9
		U	3.3	0.6	2.0	0.9	1.8	3.1	-1.7	-6.7
ZIMM	7	N	0.5	-0.3	0.4	-0.7	-0.2	0.7	0.1	0.1
		E	1.0	-0.1	-0.3	0.1	-0.1	-0.9	-0.8	2.1
		U	3.3	2.5	3.0	-6.2	0.7	0.5	2.1	-2.7

Table 8: Daily Coordinate Repeatability with Troposphere Gradients

The solution represented in Table 8 was used as our *ground truth* for all subsequent tests. One may assume that the coordinates are of 1-2 mm rms in position, and of 3-5 mm rms in height. Observe that the Pfänder site is an exception: Repeatabilities of about 2mm in the horizontal of about 7mm in the vertical coordinates show that the problems we were discussing in Chapter 4 actually have an impact on results.

6. Biases in Processing as Seen by a "User" after Ambiguity Resolution

In this chapter we want to address the question what kind of biases a normal AGNES user has to cope with, *assuming that in one way or another all ambiguities were resolved.*

Let us keep in mind what the minimum, maximum, and optimum services provided by a network of the AGNES-type are:

- **minimum:** The user downloads the data of the nearest reference station and performs a baseline solution.
- **maximum:** The user sends his observations to the AGNES-center and has them processed in the network mode by the AGNES operators.
- **optimum:** The user downloads data corresponding to one of the AGNES-sites or corresponding to a so-called virtual site, which, however, were corrected for cycle slips (to the extent possible) and for systematic effects (orbits, atmosphere, multipath) to make the user believe that the site is actually nearby *or* that the atmosphere is very smooth and regular between his site and the reference site and that the orbits are of excellent quality, as well.

Let us point out once more that, from the quality point of view, the optimum service may approach the maximum service, *provided* the systematic errors may be interpolated in the region of the network with sufficient accuracy.

6.1 Baseline *vs.* Network-specific Processing

Let us assume that there are no systematic errors in the analysis. Let us assume furthermore that we are producing the best possible, *i.e.*, the network solution with n reference and one user receiver. The situation with $n = 6$ reference receivers is given in Figure 43. One may easily show that the rms-error σ_{new} of the user position may be computed in the following way as a function of the rms of observation σ_{obs}:

$$\sigma_{new} \sim \sigma_{obs} \cdot \sqrt{\frac{n+1}{n}} \tag{6.1}$$

The case $n = 1$ corresponds to a baseline-specific processing, "$n = \infty$" corresponds to a network with an infinite number of receivers. One should therefore note that the best case is only better by factor of $\sqrt{2}$ when compared to the baseline-specific case! This "poor" gain function is easily explained by the fact that all errors of the AGNES are reduced (in the best case!) by the $\sqrt{n}$-law, but that the user-errors cannot be reduced (in an essential way)!

These considerations may look academic but they indicate, that one should not expect miracles from the above mentioned maximum or optimum services, as opposed to the minimum service.

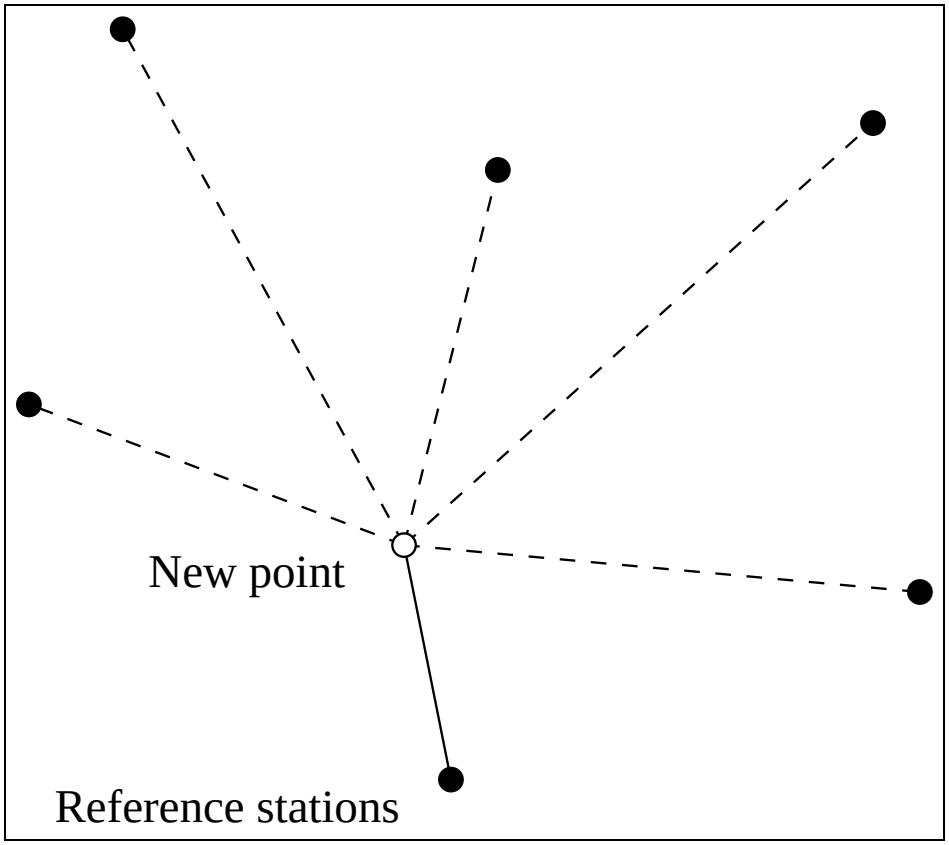

Figure 43: Estimating a New Receiver Position in a Permanent Network (of $n = 6$ Receivers)

6.2 Quality of Solutions based on Short Data Spans

Table 9 gives an impression of the quality a user may expect in different processing modes with short data spans, *provided* the (wide- and narrow-lane) ambiguities could be resolved.

In all subsequent solutions *Zimmerwald* was considered as the user site, the coordinates of which had to be estimated. When processing the data in the *network mode*, all other sites were considered to be normal AGNES reference sites. When processing the data in the *baseline mode*, the AGNES-site *FHBB*, at a distance of 74 km from Zimmerwald, was considered as reference site with known coordinates.

The repeatabilities (rms value) given in Table 9 are based on processing all possible *n-minute intervals* contained in day 231 of the year 1998. There are 288 5-minute intervals, 1440 1-minute intervals, and 2880 1-epoch "intervals".

Line	Span	Orbit	Mode	Trop	Iono	Cut Off (deg)	Wgt	Repeatability (mm) North	East	Up
1	5m	prec	bl	inp	L3	10	ele	7.2	5.3	15.0
2	5m	prec	nw	inp	L3	10	ele	6.1	4.7	11.7

3	5m	brd	bl	inp	L3	10	ele	11.3	8.1	20.9	
4	5m	pred	bl	inp	L3	10	ele	14.1	7.8	21.4	
5	5m	prec	bl	inp	L3	15	ele	6.9	5.5	16.3	
6	5m	prec	bl	inp	L3	15	---	7.8	5.7	17.7	
7	5m	prec	bl	apr	L3	10	ele	8.8	5.7	37.8	1)
8	5m	prec	nw	apr	L3	10	ele	7.9	5.5	26.7	2)
9	15m	prec	bl	inp	L3	10	ele	6.4	4.8	13.4	
10	1m	prec	bl	inp	L3	10	ele	8.1	5.9	16.6	
11	1epo	prec	bl	inp	L3	10	ele	8.9	6.3	18.3	
12	15m	prec	bl	est	L3	10	ele	8.1	5.4	35.4	3)
13	5m	brd	nw	inp	L3	10	ele	8.3	7.7	16.4	
14	5m	pred	nw	inp	L3	10	ele	10.6	8.5	22.1	
15	5m	prec	nw	inp	L1w	10	ele	18.4	14.8	31.5	
16	5m	prec	nw	inp	L1wo	10	ele	19.5	19.6	32.7	4)
17	15m	prec	bl	est,nm	L3	10	ele	7.0	5.3	35.5	5)
18	15m	prec	nw	inp	L3	10	ele	5.6	4.4	10.4	
19	1m	prec	nw	inp	L3	10	ele	6.7	5.1	12.8	
20	1epo	prec	nw	inp	L3	10	ele	7.4	5.5	14.3	
21	5m	prec	bl	ipol	L3	10	ele	8.3	5.5	28.4	6)

Table 9: Solution Coordinate Repeatability using Short Data Spans

1) Offset of 57 mm *w.r.t.* ground truth, 2) Offset of 45 mm *w.r.t.* ground truth, 3) Offset of 10 mm *w.r.t.* ground truth, 4) scale error of 30 mm, 5) Offset of 0 mm *w.r.t.* ground truth, 6) Offset of 49 mm *w.r.t.* ground truth.

Most solutions are based on 5 minute intervals, some on 15 minutes, some even on one epoch (kinematic case). Data were either processed in the network (nw) or in the baseline (bl) mode. Tropospheric refraction was either taken over from the L3-solution (assuming that this effect may be perfectly interpolated!), or the a priori atmosphere model was used, or the troposphere was estimated using the short data spans, or tropospheric refraction was interpolated using a scheme discussed in the next chapter. A cut-off angle of 10 degrees was used in most cases. The data were either weighted according to the square of the zenith distance (ele) or the unit weight $w = 1$ (—) in Table 9 was used.

Let us make a few specific remarks concerning Table 9:

- With few exceptions the ionosphere-free linear combination was processed. In view of the network size this is in general the only acceptable solution. Exceptions might be considered for short distances to the nearest AGNES site ($<$ 10 km).
- With few exceptions the rms repeatability is of the order of 5-10 mm for the horizontal coordinates, of the order of 15-30 mm for height. These values would

probably be acceptable in most cases in practice. Let us point out, however, that we assumed successful ambiguity resolution!

- The developments given in the preceding section concerning the number of stations in the network are confirmed by the results in Table 9: When comparing the repeatabilities in the first two lines of Table 9, we would expect an rms-ratio of approximately 1.3. This corresponds very well to the actual values. Other examples (using different processing options) show a similar agreement.

- When comparing, *e.g.*, lines 1, 3, 4, 13, and 14 we see the impact of the orbit quality: clearly the precise orbits are of superior quality. The quality of the predicted orbits is disappointing, at first sight. The bad result is caused by a few satellites which are not well predicted. If the satellite-specific rms-errors, accompanying each set of precise orbits, would have been used to weight the observations, the result would have been much better.

- It is important to note that this prediction problem will be removed in the near future: In fall 1999 IGS rapid orbits with a latency of 12-24 hours only will be available. This measure alone will significantly improve the predictions. In about one year from now IGS orbits with 3-6 hours latency will be available. This implies, that the orbit error will be eliminated from the error budget — even for real time applications. (A parallel development to the post-processing "scene".)

- When comparing lines 1 and 5 we do not see a big difference between using a cut-off angle of 10 degrees and 15 degrees. When comparing lines 5 and 6 we conclude that elevation-dependent weighting is important.

- Many commercially available software packages are not capable of solving for troposphere parameters. It is important to note (compare lines 1 and 7, *resp.* 2 and 8) that this is a problematic simplification of facts. If big height differences between the nearest AGNES and the user site are involved, the effect is even more pronounced. It is important to establish a good troposphere model with a relatively high time resolution for a network of the AGNES type. It is important, that in addition to the increased noise, we have systematic offsets of 6 cm or 4 cm, depending on the bl/nw-processing mode. We will further address the issue in the next chapter.

- Lines 1, 9, 10, 11 and 2, 18, 19, 20 show the impact of the length of the data span. There is a tendency that longer data spans reduce the rms. The issue is not dramatic, however.

- One might conclude from the discussions concerning the troposphere that the user "should be honest" and solve for one troposphere parameter for each of the short time intervals. As usual, honesty has its price, in this case a much worse height repeatability (compare lines 9 and 12). On the other hand honesty has its merits, as well: the height bias is reduced to zero — as opposed to 4-6 cm when

using a priori troposphere values! Line 17 differs only in the mapping function (Neill mapping instead of the $1/\cos z$-mapping) from line 12.

- Lines 15 and 16 are the only tests made using the L1- instead of the L3-observable. We obtain significantly increased values for the repeatabilities in all coordinates. This statement holds independently on whether one is using an ionosphere model or not. (The repeatability, in particular in the East-West direction is slightly better with the model.) It is important to note, that a scale effect of (on the average) 30 mm is completely removed when using the model.

- Let us note, that if we would derive a satellite- and epoch-specific ionosphere model where the number of parameters equals the number of stations, we would obtain a solution corresponding to the ionosphere-free linear combination. We would not be advised, however, to use the estimated parameters for interpolation to a user site!

- Line 21 at last shows the result of a very special experiment: Using the interpolation techniques of the following chapter, tropospheric zenith delays were computed for the Zimmerwald site (using the 3-parameter model) assuming that the troposphere parameters were available for the other six sites. The estimated values were then introduced as known in the subsequent run of program GPSEST. The result must be compared with line 7, where the atmosphere model is used. It is encouraging to see that the height repeatability in line 21 improved by a factor of about 1.33 *w.r.t.* the corresponding value in line 7 and that a slight reduction of the height offset was achieved, as well. The result also documents, however, that we are far from being able to interpolate the entire troposphere signal.

7. Investigations Concerning the Atmosphere, Ambiguity Resolution

7.1 Interpolation of Troposphere Estimates

In this section we analyze the station specific troposphere parameters for the entire campaign (week) in 1998 as they were generated by the network solution where the ground truth was established.

We should keep in mind that we were taking over (and keeping fixed) the one hour tropospheric zenith delay values for the Zimmerwald site from the CODE/EUREF solution and that we were solving for one hour zenith delay parameters for all other sites.

Figure 44 shows the sums "estimates + a priori values", thus the entire tropospheric zenith corrections, for all stations and every hour.

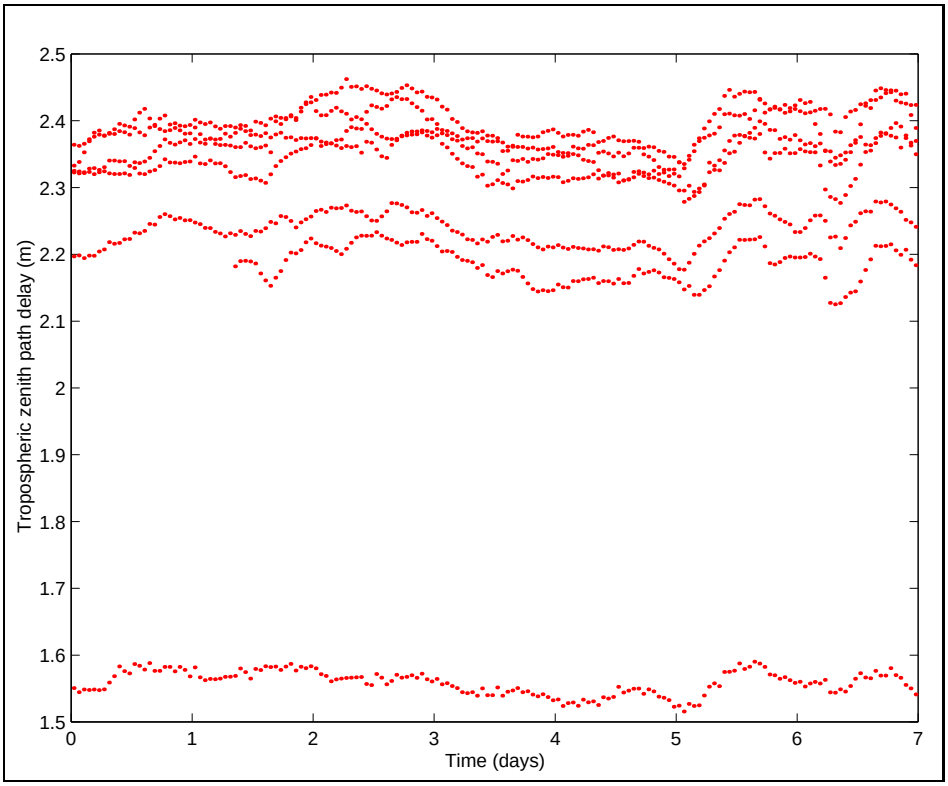

Figure 44: Hourly Tropospheric Zenith Delay Estimates

We recognize seven individual curves in Figure 44 corresponding to the seven AGNES-sites. The offsets of the curves correspond to the height distribution of the sites: The lowest curve corresponds to the highest, the Jungfraujoch site (see Table 4), the highest curve to the lowest site (FHBB). The two curves in the middle correspond to the Zimmerwald and Pfänder sites, the other four curves to the four lower sites in the AGNES (see Table 4).

The curves show a consistent pattern. We see common signals in all curves, we also observe that the Jungfraujoch-curve is significantly smoother than the other curves. This may be explained by two facts:

(1): If the curves were uniquely caused by the dry (pressure) component, and if the atmospheric pressure as a function of height would precisely follow an exponential law of the kind

$$p(h,t) = p_0(t) \cdot e^{-\frac{h-h_0}{H_0}}, \tag{7.1}$$

where h is the station height, h_0 a reference height, $p_0(t)$ the pressure at the reference height at time t, and H_0 a scale parameter,

we would expect each pressure-dependent excursion to be reduced by a factor of $e^{-\frac{\Delta h}{H_0}} \approx 1.5$ for the Jungfraujoch site as compared to the lowest sites in the AGNES.

(2): Similar remarks may be made concerning the wet part of tropospheric refraction. Usually, at high altitudes the temperature is lower than at lower altitudes, which reduces the atmosphere's water vapor content above the higher site. We should point out, however, that we expect less regular variations for the wet component of tropospheric refraction than for the dry part.

Figure 44 documents the difficulty one encounters when trying to interpolate tropospheric zenith corrections as a function of "the geography" in an alpine area.

We have to resolve two issues:

- **Question 1: What are the independent parameters?** Obviously, we should use latitude β, longitude λ, *and* height h. We are sure, however, that we do not have enough stations to model the height dependency in an adequate way. Table 4 also shows that the height distribution is not very nice: we have a cluster of stations roughly between 400 m and 600 m, then two stations around 1000 m, and last but not least one station on 3635 m (the famous Jungfraujoch site, where thousands of tourists are exposed to about 2/3 of the sea level atmospheric pressure).

- **Question 2: What quantity do we try to model as a function of our independent arguments?** There are two candidates:

  - Quantity 1:
  $$q_1(t) \doteq \Delta\rho_{trop}(t) - \Delta\rho_{trop,0}(h) \tag{7.2}$$

  - Quantity 2:
  $$q_2(t) \doteq \frac{\Delta\rho_{trop}(t)}{\Delta\rho_{trop,0}(h)} \tag{7.3}$$

  $\Delta\rho_{trop,0}(h)$ are a priori values either stemming from an atmosphere model (in which case they would be station-specific constants) or from actually measured meteorological values.

Option (7.3) obviously is the right choice if we would only observe the dry part of tropospheric refraction. We might then even reduce the problem to "flat-land geodesy" by

assuming that the height-dependency was already removed by using the exponential decrease of atmospheric density.

Option (7.2) is attractive because we might easily replace $\Delta\rho_{trop,0}(h)$ by values that were derived from actual atmosphere observations (*e.g.*, stemming from the A-Netz). We will use both observables (7.2) and (7.3), and the representation as a function of latitude, longitude, and height will be the following:

$$q_i(t) \doteq c_0 + c_\beta \cdot \Delta\beta + c_\lambda \cdot \Delta\lambda + c_h \cdot \Delta h + c_{h^2} \cdot \Delta h^2 \tag{7.4}$$

(For the sake of simplicity we left out index i on the right hand side).

Figure 45 shows the observations $q_2(t)$ according to the definition (7.3), Figure 46 shows $q_1(t)$ according to definition (7.2). Figure 45 speaks very much in favor of modeling the quantity $q_2(t)$: It is no longer possible to distinguish the curves corresponding to different stations. In Figure 46 we clearly recognize the Jungfraujoch estimate as the smoothest curve.

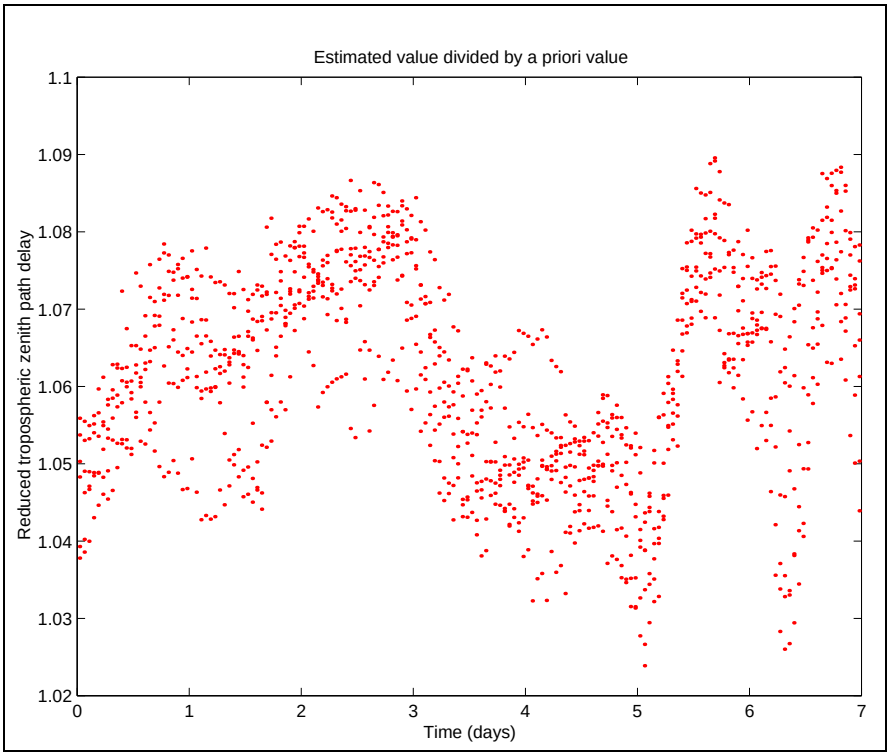

Figure 45: Hourly Tropospheric Zenith Delay Estimates rel. to A Priori Values

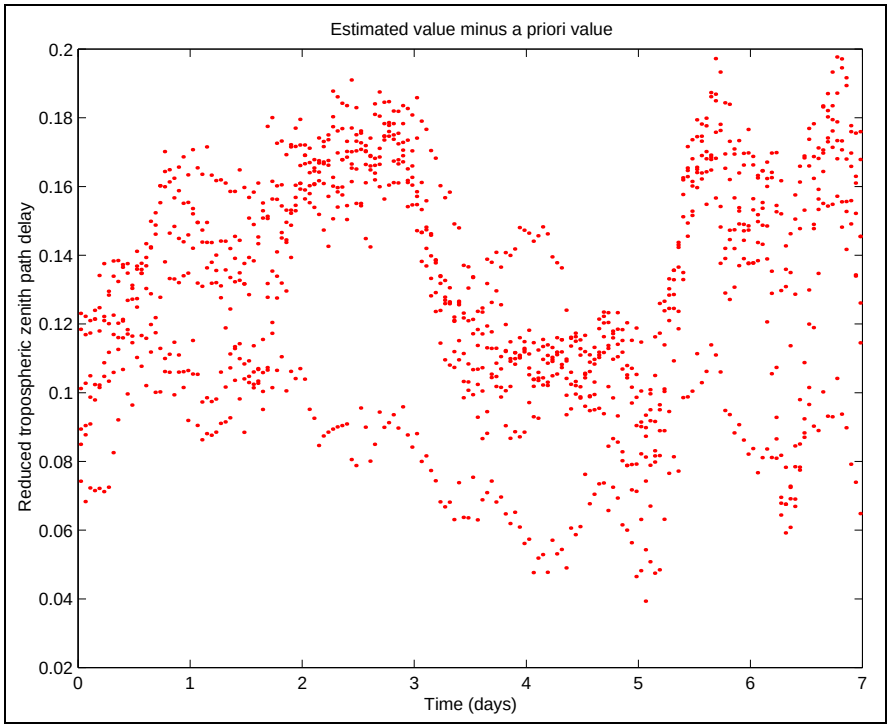

Figure 46: Hourly Tropospheric Zenith Delay Estimates minus A Priori Values

Despite the fact that probably $q_2(t)$ should be used, we produced solutions based on $q_1(t)$ and $q_2(t)$. Table 10 characterizes the solution types.

n_{par}	f	RMS(q_2) (—/mm)	RMS(q_1) mm	Parameters
1	6	.0085/17.8	26.6	c_0
2	5	.0083/17.3	17.7	c_0, c_h
3	4	.0076/15.9	28.6	c_0, c_β, c_λ
4	3	.0056/11.7	11.3	c_0, c_β, c_λ, c_h
5	2	.0041/8.50	9.00	c_0, c_β, c_λ, c_h, c_{h^2}

Table 10: Solution Types to fit the Zenith Delay Estimates

n_{par} is the number of parameters, f the degree of freedom. The RMS when modeling $q_2(t)$ is dimensionless. In order to compare the performance of the two approaches, we multiply the dimensionless RMS values with an average value for $\Delta\rho_0 \approx 2.1$ m. The RMS values in Table 10 are the mean values for the entire week. From Table 10 we conclude that in the present realization phase of AGNES either a model of three or four parameters seems to be an optimum.

The RMS of the fit is around 1 cm for the models with four or five parameters. We would therefore hope that it is possible to interpolate the tropospheric delay (via the quantity $q_2(t)$) within the entire network with an RMS uncertainty of about 1 cm,

as well. This assumption is supported by line 21 in Table 9, where we obtain an RMS repeatability of 2.8 cm in height — which corresponds quite well to a zenith delay error of 1 cm. A comparison of lines 7 and 21 tells us that our interpolation is significantly better than using an a priori atmosphere model. We cannot claim, however, that we have removed the entire troposphere induced effect.

Table 10 clearly speaks in favor the quantity $q_2(t)$. It is important in particular, that we obtain a meaningful fit of $q_2(t)$ as a linear function of latitude and longitude (line 3 of Table 10), whereas we definitely need the height dependency for $q_1(t)$. As soon as the height dependency is taken into account, both models perform in a very similar way.

Let us illustrate the estimation process with the next six figures. Figure 47 sketches one particular estimation process using the model in line 3 of Table 10. The quantity $q_2(t)$ is modeled as a linear function of λ and β. We see the AGNES-sites in the $x-y-$plane, the fit is indicated by a plane in the $x-y-q_2$ space. We also see the residuals of the fit.

Figures 48 to 52 show the estimated parameters (and the associated $\pm$RMS-values) using model 5 (line 5) in Table 10 and analyzing the quantity $q_2(t)$. The units for the parameters are m for the constant term c_0, $m/100\ km$ for the terms c_λ and c_β, $m/100\ m$ for the term c_h, and $m/(100\ m)^2$ for the term c_{h^2}. The figures demonstrate that there are significant signals in all terms which can be removed. The figures also tell us, that it is really not necessary to remove tropospheric effects on the epoch-by-epoch basis.

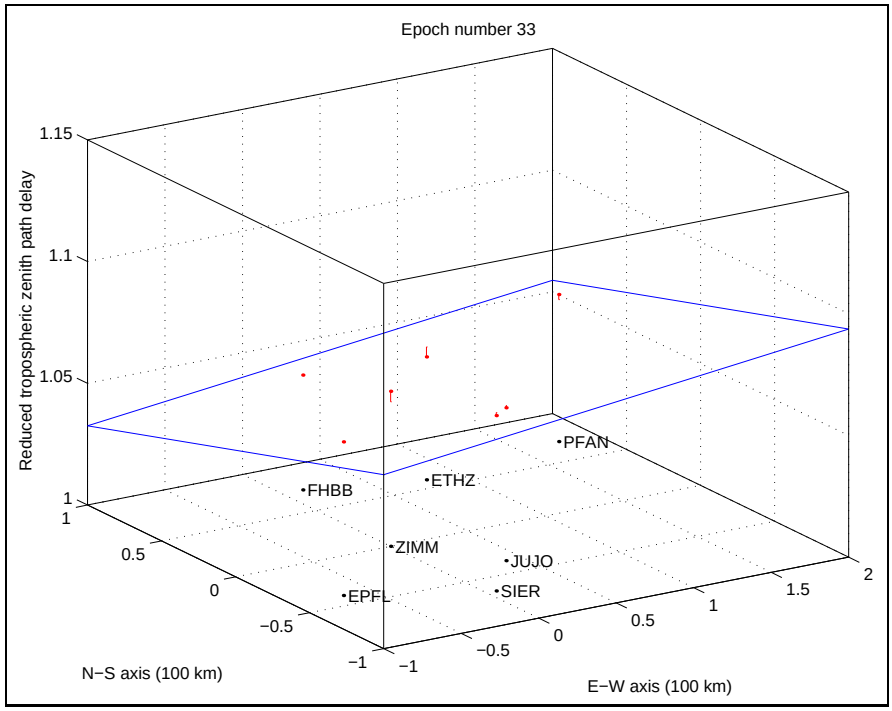

Figure 47: Fit of one Set of 1-hour Tropospheric Zenith Delay Estimates by a Linear Model

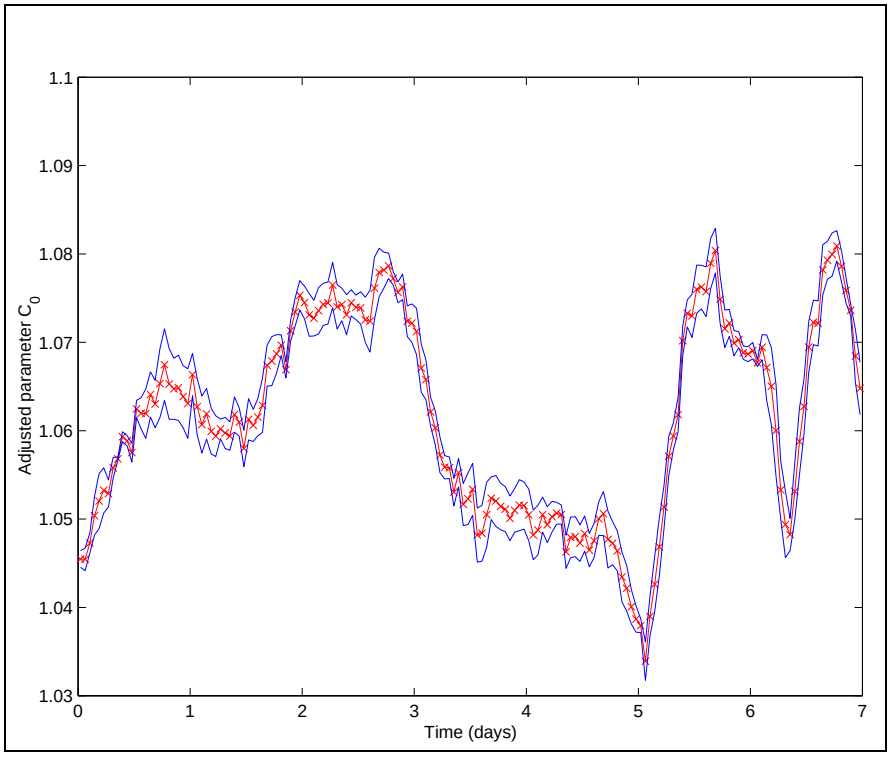

Figure 48: Constant Term

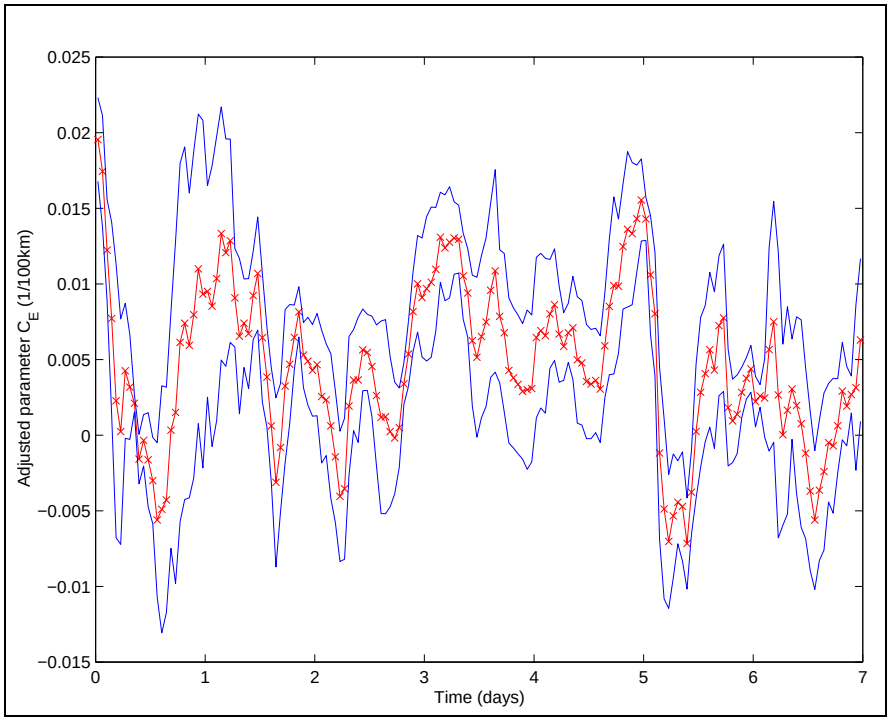

Figure 49: Gradient (East-West)

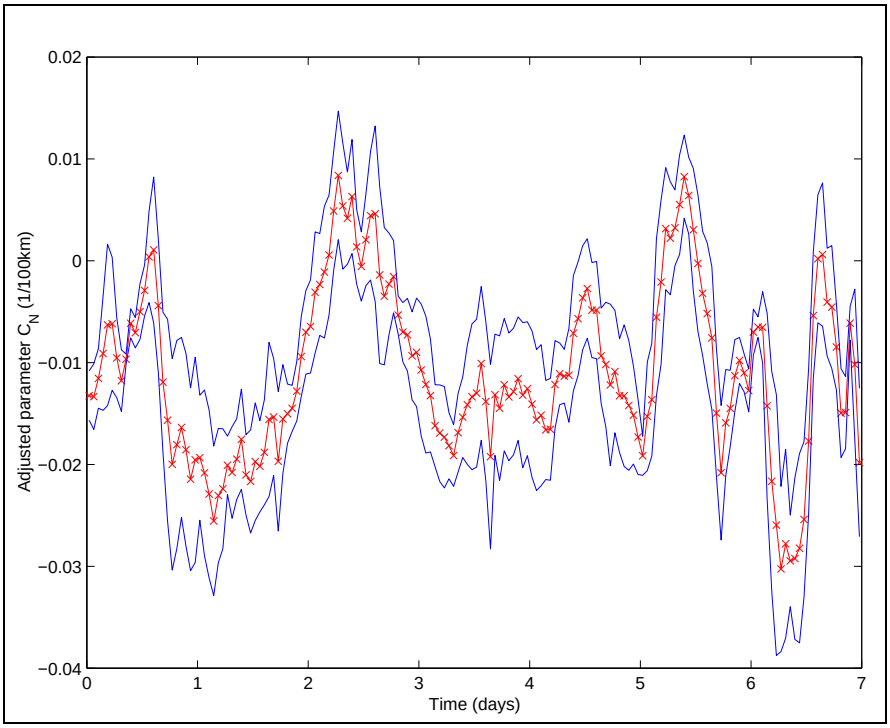

Figure 50: Gradient (North-South)

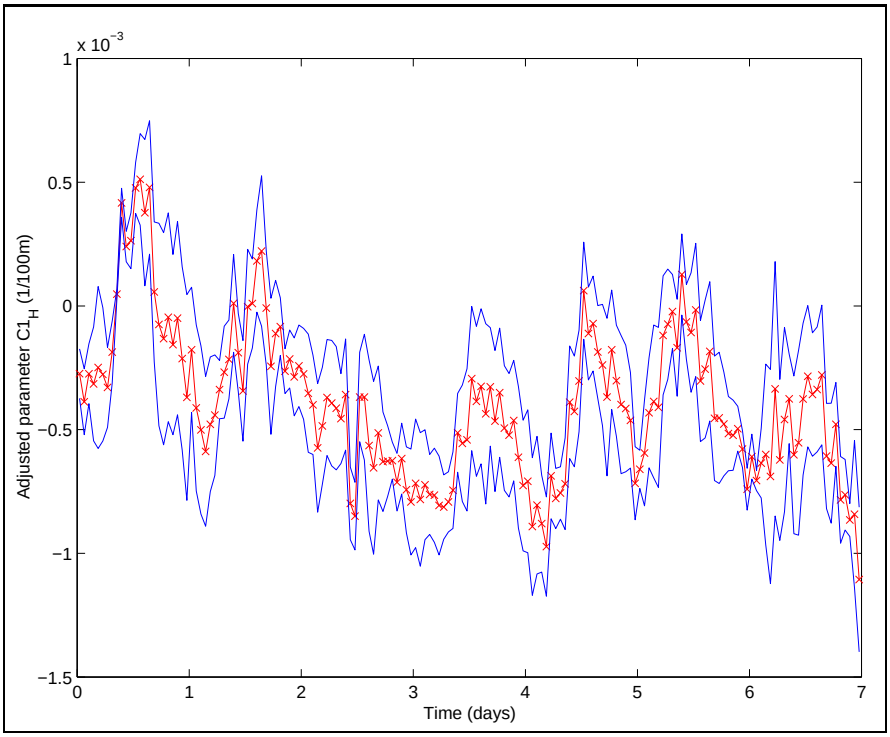

Figure 51: Gradient in Height

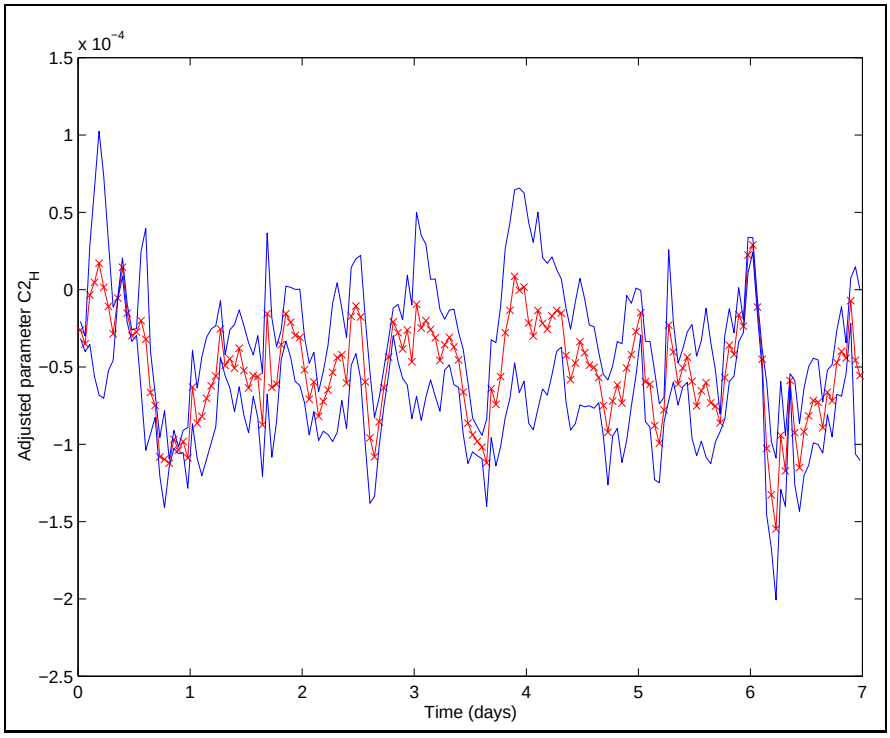

Figure 52: Quadratic Height Term

Our attempts to represent the tropospheric zenith delay estimates by linear or quadratic functions of the site coordinates should be accompanied by a corresponding analysis of a tropospheric zenith delay computed from real meteorological data. In view of the small number of AGNES stations it might well be that better results could be achieved when a tropospheric zenith delay model from the A-Netz would be used. This would assume, of course, that the A-Netz data would be available in near real time (latencies of 1-2 hours would be acceptable).

It would also be highly recommendable to deploy standard meteorological equipment (UNAVCO Clam?) with each AGNES site. It would allow us to remove the dry part of tropospheric refraction and to fit only the wet part (as difficult as this may be). It would be sufficient to retrieve the met-data every (let us say) 30-60 minutes. A requirement that can easily be met, if the GPS-data are transferred every second!

7.2 Ambiguity Resolution using Short Data Spans

For a "normal" user of AGNES it will be absolutely essential to resolve the ambiguities with short data spans (one epoch to fifteen minutes). There are (too) many degrees of freedom "in this game":

- One essential parameter is the baseline length l. We performed tests using the material of the 1999 campaign. The following test baselines were used:
  - Zimmerwald-Wabern (6 km, 300 m height difference)

  - Zimmerwald-Thun (17 km, 300 m height difference)
  - Zimmerwald-FHBB (74 km, 600 m height difference)

- The length of the data span may be varied. We used 5-minute data spans for the two short, 15-minute spans for the long baseline.
- We may vary the minimum elevation. We made tests with 10^o and 15^o.
- We may apply elevation-dependent weighting schemes or not.
- We may use different linear combinations and phase/code combinations. We use phases only and process $L1$ and $L2$ simultaneously (*FARA-method*).
- We may vary the statistical parameters of the method.
- We may or may not introduce epoch- and satellite specific stochastic ionosphere parameters; if we do so, we may vary the a priori σ-values.
- We may introduce an a priori ionosphere model (this is important for long baselines).
- We may use different methods to account for tropospheric refraction (a priori model, use interpolated values, solve for tropospheric zenith-delay parameters, *etc.*).
- We may use different orbit types (broadcast, precise, predicted).
- *etc.*

This list shows that a thorough analysis would contain *an exorbitant number of test runs*. As a matter of fact we performed a substantial number of tests. The results may be summarized as follows:

6 km Baseline Zimmerwald-Wabern

Using 5-minute data spans and a cut-off angle of 15^o, most tests lead to a safe resolution of the L1 and L2 ambiguity parameters. It was not necessary to introduce stochastic ionosphere parameters. Even broadcast orbits were sufficient to resolve the ambiguities. From 132 possible 5-minute intervals 131 could be resolved, one was rejected. A comparison with the true solution showed that the best solution proposed would have been correct.

The result is as expected. If a user is operating at a distance of $<$10 km to a reference site, he is best advised to use the data of this station without any changes.

17 km Baseline Zimmerwald-Thun

Tests without setting up stochastic ionosphere parameters were rather successful, as well: from 143 possible 5 minute intervals only between 5 and 20 could not be resolved. 20 failures were reported, when the global ionosphere model was *not* used. This clearly demonstrates that a good ionosphere model is a prerequisite for successfully resolving ambiguities on baselines longer than 10 km.

All ambiguities could be very safely resolved when epoch and satellite specific stochastic ionosphere parameters were set up. 7 (correct) solutions were rejected when the a priori ionosphere model was *not* used.

Even the least accurate orbits (broadcast) and the most trivial troposphere modeling technique (a priori based on standard atmosphere) proved to be sufficient for the job.

74 km Baseline Zimmerwald-FHBB (Muttenz)

After a few attempts, only tests with 15-minute data spans were made. Ambiguity resolution without introducing stochastic parameters was very problematic: failure rates up to 50% were reported. Although one could fine-tune the parameters to produce good statistics, we would not recommend the average GPS user to play such games.

The situation changes when stochastic ionosphere parameters are introduced: Success-rates of well over 90% — even when the a priori model for tropospheric refraction was used — let us believe that this technique is very promising in the context of AGNES. It is encouraging that today commercially available software packages allow the use of stochastic parameters.

It is interesting to note that [*Wanninger*, 1999] concludes that procedures including the estimation of (what we call) stochastic ionosphere parameters (and what he calls ambiguity resolution strategies for long baselines) have to be recommended even when using corrected RINEX files (corresponding to a virtual reference station). We come to similar conclusions (without using virtual reference station data): For ambiguity resolution on baselines longer than 20 km this option seems to be almost mandatory.

It is an open question whether the methods to produce (the ionospheric part of) the observations for the virtual reference site are not rendered unnecessary, when stochastic ionosphere parameters are set up. The only advantage (we can see) correcting the ionosphere would reside in the possibility to constrain the stochastic parameters more tightly when the ionosphere is modeled — an issue that might be of minor importance.

8. Summary and Recommendations

This report deals with aspects of wide-area differential GPS (*WADGPS*) using data of the *AGNES* (Automated GPS Network Switzerland). The report consists of

- the introductory Chapter 1, where the scope for this work is set,
- an overview of existing work in Chapter 2,
- theoretical developments in Chapter 3,
- a description and results of program *CLKEST* in Chapter 4, a general data validation and receiver and clock estimation tool, developed for use in permanent networks (from local to global size),
- a fair portion of *standard analysis* of AGNES data (seven day in 1998, two days in 1999) using the Bernese GPS Software in Chapter 5,
- an analysis of biases in processing as seen by a "user" after successful ambiguity resolution in Chapter 6,
- investigations concerning the impact of the atmosphere, in particular on ambiguity resolution in Chapter 7, and
- the present Chapter 8 summarizing the findings and recommending further work.

Let us point out that some of the findings contained in this report were presented at the XXIInd IUGG General Assembly in Birmingham (Paper on *The Impact of the Atmosphere and of Systematic Errors on Permanent GPS Networks* by S. Schaer, G. Beutler, M. Rothacher, E. Brockmann, U. Wild, and A. Wiget). The paper was meanwhile completed and sent for review to the convenor of the symposium.

Let us summarize the key findings and the open issues in Section 8.1 and recommend further work on specific topics in Section 8.2.

8.1 Essential Results and Open Issues

Theory (Chapter 3)

The distinction was made between

- creating artificial observations from the ensemble of n receivers under the assumption that there are no biases in the observations of the reference receivers, and
- modeling and application of systematic errors (biases) which are usually not dealt with in commercial-type software.

In order to accomplish the first goal, the code and phase observations were reviewed and the principles of how to produce a consistent set of code and phase observations from a set of n permanent receivers were developed. We conclude that *it is possible to create data for a virtual reference receiver which are correct from the mathematical and statistical point of view in an environment containing no unmodeled biases.*

From the point of view of practice, we are not yet satisfied with the theory, however. This is the basis for our recommendation 1 in the next section.

After successful completion of the theory one should perform the necessary theoretical work to create in program CLKEST (eventually in program GPSEST) the observations for a *virtual dual-frequency reference receiver* with properties contained in recommendation 2 (next section).

The remarks made in section 3.4 are considered valid and should be the "philosophical" basis for all subsequent developments.

From the point of view of theory it is clear that a true combination ("Vernetzung") of the receivers of the AGNES type makes sense and is highly desirable.

A good solution for practical applications is not a trivial issue, however. Even the necessary theoretical work is estimated to be of the order of full thirty working days for a GPS specialist.

Analysis using Program CLKEST (Chapter 4)

Program CLKEST analyzes the raw, unprocessed data stemming from the receivers. It is very well suited to monitor the technical performance of the network, and to characterize the statistical behavior of the ionosphere over the AGNES region. The program should be modified to become a routine receiver performance and regional/local ionosphere monitoring tool (see recommendation 3).

Standard Static Analysis (Chapter 5)

The chapter illustrates that interesting results from the CODE analysis center could be taken over for AGNES purposes (AGNES homepage?). Candidates are:

- global ionosphere maps,
- predicted ionosphere maps,
- mean and maximum ionosphere content,
- predicted mean and maximum ionosphere content,
- troposphere zenith delays for Zimmerwald,
- etc.

The chapter also shows that a close to real-time solution must accompany the AGNES network. Such a solution should be set up in close cooperation between L+T and AIUB. It should be based on CODE/IGS products.

It became clear that the IGS 2-day predictions are not good enough for AGNES operations. Best possible use of the CODE rapid products should be made. Selected results should be made available to the AGNES users.

Biases after Ambiguity Resolution (Chapter 6)

It was shown that the maximum accuracy gain by combining the observations of all AGNES sites into a virtual reference receiver is $\leq \sqrt{2}$. This figure was confirmed in practice.

After successful ambiguity resolution short data spans (1-5 minutes) give repeatabilities and coordinate accuracies of about 1 cm in the horizontal and 2-3 cm in the vertical baseline components.

Atmosphere, Ambiguity Resolution (Chapter 7)

Interpolation techniques for tropospheric zenith delays were developed. It became clear that (as expected) height plays an essential role in this respect. It seems feasible that tropospheric refraction may be interpolated with an accuracy of about 1 cm in the AGNES area. This would result in relative height errors of the order of ≤ 3 cm. Much better results could only be expected for a much denser network.

If a priori meteorological information would be used it might be possible to get around the height modeling. We would not expect better results, however.

Ambiguity resolution using short data spans is the crucial issue. Ambiguity resolution using five minute spans was tested on a 6-km and on a 17-km baseline, using 15 minute data spans on a 74-km baseline. Ambiguity resolution was rather successful on the two short baselines using standard procedures. Using the global ionosphere model significantly improved the performance. Setting up stochastic ionosphere parameters made ambiguity resolution a full success on the short two baselines, it improved the performance dramatically on the long baseline.

It is still an an open issue to what extent the latitude and longitude dependent, epoch-specific ionosphere models would improve ambiguity resolution. A special investigation is proposed in recommendation 4.

Summary and Recommendations, (Chapter 8)

The investigations in this report clearly show that it makes sense to develop a special program which generates the observations (code and phase) for a virtual reference receiver. The principles for the development are based on the the results in Chapter 3 of this report and the resulting reports of recommendations 1 and 2 stated below.

The result of such a development might be a milestone for GPS applications in permanent networks. The proposed work is further specified in recommendation 5 below.

8.2 Recommendations

Recommendation 1 (Theory, Chapter 3):
The theory to produce a consistent set of *phase observations* shall be reviewed and simplified. It should be based on the assumption that all double-difference ambiguities $N_{i_1,i_2}^{j_1,j_2}$ are known (either as integers or as real numbers). Starting from the observation equations (3.3) the developments shall be performed in closest analogy to the developments using code observations, using the following decomposition for the ambiguity parameters:

$$N_j^i = N_{j_r}^i + N_{j,j_r}^i = N_{j_r}^i + N_{j,j_r}^{i_r} + N_{j,j_r}^{i,i_r}, \tag{8.1}$$

where j_r characterizes an arbitrarily chosen reference receiver, i_r an arbitrarily chosen reference satellite. The first term of the second right hand side of the above equation is a satellite specific zero difference term, the second a receiver specific single-difference term, and the third the known double-difference term. The first term may be combined with the epoch-specific satellite clock term, the second with the epoch-specific receiver clock term, the third must be incorporated into the phase pseudorange.

After this modification we have — separately for each epoch — modified phase observation equations (3.3) which are identical with the code observation equations (3.2), *except* that the satellite and code clock terms have a slightly different meaning.

The result will be a very simple mechanism to combine phase observations, as a matter of fact almost identical with the corresponding code procedure.

Estimated time for completion: 10 full working days for G. Beutler. This includes a written report.

Recommendation 2 (Theory, Chapter 3):
The procedure to create the observations (one RINEX file) for a virtual reference receiver with the following properties shall be defined in detail:

- The site coordinates for the receiver (in the ITRF) shall be user-defined.
- The L3 linear combinations shall be used to compute the code clock corrections and the phase pseudo-clock corrections for the virtual reference receiver. For the phase pseudo-clocks the double-difference ambiguities from a standard double-difference network solution (integer and real valued) shall be used.
- The tropospheric corrections for the virtual reference receiver shall be based on the Bernese troposphere files as created by a standard double-difference network solution.
- The linear interpolation schemes for ionospheric refraction (as developed in the present report) shall be used to create the ionospheric effects for the virtual receiver.
- As an option it should be possible to use the "geocenter" as a possible site. In this case the site would have *no atmosphere* and only processing of the L3 double-difference observations w.r.t. this site would make sense. This option would be well suited for processing the data of Low Earth Orbiters (LEOs).

- These theoretical developments shall be based on the existing Bernese Software package.

The latter point is somewhat delicate: The Bernese processing strategies *which allow for ambiguity resolution* are based on single-difference files, which do not allow it to easily reconstruct the corresponding zero difference files. This circumstance requires special attention.

Estimated time for completion: 20 full working days for U. Hugentobler and/or G. Beutler. This includes a written report. This estimated time does not contain any developments for computer programs.

Recommendation 3 (Analysis using Program CLKEST, Chapter 4)):
Program CLKEST shall be generalized to become a receiver performance and regional (stochastic) ionosphere monitoring program.

Estimated time for development: 25 working days for G. Beutler, P. Fridez, R. Dach or L. Mervart (estimated time contains everything including, e.g., a menu program).

This does *not* cover (possible) preprocessing capabilities of program CLKEST.

Recommendation 4 (Investigations Concerning the Atmosphere, Ambiguity Resolution, Chapter 7):
A *quick and dirty* investigation concerning the impact of using the epoch-and satellite-dependent ionosphere models shall reveal the impact on ambiguity resolution on the AGNES network. Only short data spans (1-15 minutes shall be used). Material of the already processed AGNES campaign shall be used.

It is necessary to modify program GPSEST for that purpose. First, per epoch and per satellite the three model parameters have to be stored into a file. Second, the corrections have to applied (if required) for the ambiguity resolution step.

Estimated time for development, implementation, testing, and documentation: 15 working days for (either S. Schaer, L. Mervart).

Recommendation 5
A computer program to generate the observations for a virtual reference receiver shall be developed. The development shall be based on the theory in Chapter 3 of this report, the results emerging from recommendations 1 and 2, the result of recommendation 4 shall be taken into account.

The program user shall be allowed to specify the location of the receiver and the atmosphere peculiarities. It must be possible, in particular, to specify the geocenter as reference site, in which case we might have a station observing the entire set of GPS and GLONASS satellites at each epoch. For local and regional networks the program resulting observations should allow it to model the atmosphere in the best possible way with the goal to significantly improve ambiguity resolution.

The program shall use the resolved double-difference ambiguities from standard GPSEST runs and the real valued estimates for the (unresolved) ambiguities. This is a non-trivial task, because the zero- and single-difference files have to be made perfectly coherent. Open issues are, e.g., whether or not it is necessary to have separate phase, L1 and L2 clocks.

Estimated time for development: One man year for a Ph.D. or a diploma candidate (of excellent quality) plus 20% from Urs Hugentobler and Gerhard Beutler). The first result must be well suited well suited for all post-processing applications. Further developments should make the result perfectly suited for real-time applications.

We could very well imagine that this work will cover, all in all, a diploma thesis and a Ph.D. thesis. One of the results might be a true alternative for the single point positioning approach.

References

Beutler, G., W. Gurtner, U. Hugentobler, M. Rothacher, T. Schildknecht, and U. Wild (1989), Ionosphere and GPS Processing Techniques, Internal Documentation, Astronomical Institute, University of Berne.

Beutler, G., W. Gurtner, M. Rothacher, U. Wild, and E. Frei (1990), Relative static positioning with the Global Positioning System: Basic Technical Considerations, in *Global Positioning System: An Overview*, vol. 102, edited by Yehuda Bock and Norman Leppard, pp. 1–23.

Kouba, J., and J. Popelar (1994), Modern Geodetic Reference Frames for Precise Satellite Positioning and Navigation, in *Proceedings of the KIS94 International Symposium on Kinematic Systems in Geodesy*.

Marel, H. van der, and C.D. de Jong (1999), Active GPS Reference System for the Netherlands, *Allgemeine Vermessungs Nachrichten*, *in press*, 1–6.

Rothacher, M., and L. Mervart (1996), Bernese GPS Software, Version 4.0, Printing Office of the University of Berne.

Schaer, St. (1999), Mapping and Predicting the Earth's Ionosphere Using the Global Positioning System, Ph.D. Theses Series, Astronomical Institute, University of Berne.

Wanninger, L. (1995), Enhancing differential GPS using regional ionospheric error models, *BG*, *69*, 283–291.

Wanninger, L. (1996), Präzise GPS-Positionierung in regionalen Netzen permanenter Referenzstationen, *Zeitschrift für Vermessungswesen*, *9*(1), 441–454.

Wanninger, L. (1997), Real-time differential GPS error modeling in regional reference station networks, in *IAG Symposia*, vol. 118, edited by F. Brunner, Springer Verlag Berlin, London, New York, September 1997.

Wanninger, L. (1999), Der Einfluss ionosphärischer Störungen auf die präzise GPS-Positionierung mit Hilfe virtueller Referenzstationen, *Zeitschrift für Vermessungswesen*, *N.N.*(N.N.), in preparation.

Wanninger, L., and J. Böhme (1998), Verwendung virtueller Referenzstationen in regionalen GPS-Netzen, *Allgemeine Vermessungs Nachrichten*, *41*, 113–118.

Wübbena, A.B., G. Seeber, V. Böder, and P. Hankemeier (1996), Reducing Distance Dependent Errors for Real-Time Precise DGPS Applications by Establishing Reference Station Networks, in *ION GPS-96*, The Institute of Navigation, September 1996.